Natural convective heat transfer in insulated structures

Bankvall, Claes

1972

DIVISION OF BUILDING TECHNOLOGY
LUND INSTITUTE OF TECHNOLOGY

NATURAL CONVECTIVE HEAT TRANSFER IN INSULATED STRUCTURES

CLAES G BANKVALL

REPORT 38
LUND – SWEDEN – 1972

NATURAL CONVECTIVE HEAT TRANSFER IN INSULATED STRUCTURES

CLAES G BANKVALL

CONTENTS

FOREWORD

The present work, investigating the natural convective heat transfer in insulated structures, is part of a larger research program concerning the heat transfer in permeable materials and their behaviour as insulations in a structure. The first part of this work, which dealt with the basic mechanisms of heat transfer in a fibrous material, has already been reported on.

The natural convective heat transfer in insulations and insulated structures has been the subject of many speculations. A thorough theory on the heat transfer in this case has hereto been lacking and relevant influencing factors have frequently been ignored, while peculiarities in the measuring results have been attributed to natural convection. It is therefore hoped that this work will clearly show the important factors and their influence on the natural convective heat transfer in the insulation. Explicit expressions give the qualitative influence from these factors and diagrams show their quantitative influence.

I am greatly indebted to those who have given their assistance to this project: professor Lars Erik Nevander, the head of the department, who initiated and made the research work possible, Miss Gunvor Hällnor, Mr. Thord Lundgren And Mr. Lars Olsson, who helped with the measurements, Mr. Alf Hansson, who erected the test wall and especially to Mrs. Mary Lindqvist, who patiently typed the manuscript and Mrs. Lilian Johansson, who drew the figures for the report. I also wish to thank my colleagues and friends, who have shown interest in my work and given me helpful advice.

The work presented here have in part been supported by a grant from the Research Fund of the Swedish Counsil for Building Research.

Lund, November, 1972.

Claes Bankvall

SUMMARY

This report investigates the natural convective heat flow in insulated structures. To understand the heat transfer due to convective flow in an insulation the two extreme limits from the point of heat transfer are observed, i.e. the solid structure and the air space. A discussion is made of the natural convection in the air space. This part is largely based on the literature. The factors influencing the convective heat transfer in the vertical and in the horizontal air space are illustrated. A discussion is made of the laws governing fluid flow in porous media and the concept of specific permeability is introduced. This makes it possible to develop a theoretical model for the convective heat flow in the permeable space. A numerical solution to this problem is presented and verified by available experimental results.
The factors influencing the convective heat transfer in the vertical and horizontal insulated structure are calculated and discussed. Experimental investigations are presented to establish the presence of natural convection in insulations in building technological applications. Numerous measurements were made on wall insulations, representing the vertical space and in a guarded hot plate in order to establish the behaviour of the horizontal space. The experiments on the wall structure include a tentative investigation of the influence of small air spaces and openings in the insulation. A discussion is made of the measurements on wall insulations reported in the literature. It is found that the theories are in good agreement with these findings and give a consistent qualitative and quantitative explanation of the natural convective heat transfer in the insulated structure. The conclusions are presented in Section 7.

NOMENCLATURE

b	width of space	m
d	thickness of space	m
D	fiber diameter	m
h	height of space	m
h_b	height of crossbar	m
A	area	m^2
x, y, z	coordinate	m
X, Z	dimensionless coordinate	-
u, v, w	velocity	m/s
ψ	streamfunction	-
t	time	s
T	temperature	K (^oC)
T_C	temperature of the cold side	K (^oC)
T_H	temperature of the hot side	K (^oC)
T_m	mean temperature	K (^oC)
ΔT	temperature difference	K (^oC)
θ	dimensionless temperature	-
λ	thermal conductivity	W/mK
λ_{cv}	thermal conductivity due to convective flow in fluid space	W/mK
λ_o	thermal conductivity in permeable material without convective flow	W/mK
λ_b	thermal conductivity in crossbar	W/mK
a	thermal diffusivity	m^2/s
a_o	thermal diffusivity in permeable space	m^2/s
C_p	specific heat	J/kgK
β	coefficient of cubical expansion	1/K
B_o	specific permeability	m^2
$B_o(\parallel)$, $B_o(\perp)$	specific permeability parallel and at right angle to the fiber planes	m^2
Q	volume flow	m^3/s
p	pressure	N/m^2
η	dynamic viscosity	Ns/m^2
ν	kinematic viscosity	m^2/s
ρ	density	kg/m^3
ε	porosity	-
g	gravitational acceleration	9.81 m/s^2

k	Kozeny constant	
Pr	Prandtl number	-
Ra	Rayleigh number	-
Gr	Grashof number	-
Nu	Nusselt number	-
Ra_o, Gr_o	modified Rayleigh and Grashof numbers	-
C_{air}	coefficient (cf. FIG. 3.6)	-
$C_{air,o}$	coefficient (cf. FIG. 5.6)	-

1 INTRODUCTION

1.1 Introduction

Effective thermal insulations are of considerable importance for many fields of modern technology. The availability and use of liquefied natural gas, the developments of superconductors for the generation and transmission of electricity, the maintenance of low temperatures for diminishing noise in electronic devices, the increasing use of cryogenic fluids in manufacturing processes and in the medical sciences, the expansion of the food preservation industry, the insulation of space-vehicle cryogenic fuel stages, engine components, etc., are examples where the overall efficiency would have been significantly retarded without suitable thermal insulations. This is also the case in the field of building physics, due to increasing requirements of comfort, and the necessity of reducing costs. In order to fulfil the demands of a more effective utilization of the insulating materials, further knowledge of their properties is required. This is especially true for many new types of high-performing thermal insulations with complicated mechanisms of heat transfer. It is not possible to judge the behaviour of an insulation inside a structure without knowledge of the different ways of heat transfer in the material itself.

Most highly insulating materials are porous, i.e. they usually contain large amounts of air or other gas. The pore system can be closed, as in many cellular plastics, or open, as in mineral wool. The mechanisms of heat transfer in a porous material are: conduction in solid phase constituting the insulation, radiation within the material and conduction due to the gas confined in the insulation. In an open-pore material like mineral wool, the transport of heat can be further increased by natural or free convection, i.e. heat transported by a gas-flow due to differences in gas density induced by a temperature-gradient over the material.

Fibrous insulations with open-pore system and complex mechanisms of heat transfer have presented difficulties when evaluating

building structures where these materials have been used for insulation. The influence of dimension, temperature, temperature differences, etc., have not been conclusively evaluated in many investigations. In some cases the reason for this can be attributed to less rigorous measuring techniques. In most cases, however, a thorough theory on the heat transfer in the insulation has been lacking, which has frequently lead to ignoring relevant influencing factors while peculiarities in the measuring results have been attributed to convection. This situation is partly due to insufficient knowledge of the mechanisms of heat transfer in the non-convecting material, and partly due to the difficulties in calculating the convective heat transfer. These calculations require the use of high speed computers with large capacity, often in combination with sophisticated numerical methods. Only in recent years has it been possible to solve some of the relevant problems. It has thus not been possible to draw any decisive conclusions about the importance of free convection for normal building technological applications of the insulation.

1.2 Disposition

The aim of the present work has been to investigate the natural convection in constructions insulated with open-pore material (mineral wool). This research is part of a project intended to give a detailed and consistent explanation of the mechanisms of heat transfer in the insulating material and the performances of such a material in a structure.

The fundamental mechanisms of heat transfer in open-pore insulation have earlier been calculated theoretically and verified by experiments. That investigation was done with no convection present and gave information on the basic physical mechanisms of heat transfer in the material (Bankvall, 1972a, 1972b).

In the present investigation, natural convection has been studied in detail. The theoretical calculations and considerations give a fairly complete treatment of this problem. The experimental investigations, however, have mostly been concerned with the

insulation in applications normal for building physics and building technology, and the experiments therefore include a tentative investigation of the influences of small air spaces and openings in the insulation. The problem of forced convection and protection from wind is not taken up in the present study.

In Section 2, the general philosophy behind the present approach to natural convection is outlined and discussed.

Section 3 explains the heat transfer due to convection in an air (fluid) space. The influencing factors and variation of the temperature and velocity fields are discussed. Extensive information can be found in the literature on the natural convection in the fluid space, while this is not the case for the one with insulation. This section is therefore largely based on the theoretical and experimental investigations available.

Section 4 discusses the laws governing fluid flow in porous media. The concept of specific permeability is introduced. Theoretical and experimental evaluations of the permeability are presented for mineral wool materials.

The theoretical treatment of natural convection in a permeable material is given in Section 5. Comparisons are made with the scanty theoretical and experimental information on the subject in the literature. The factors influencing heat transfer, temperature field and velocity field are discussed in detail.

Section 6 presents experimental investigations to establish the presence of natural convection in insulations in building technological applications. Measurements have been made on wall insulations, representing the vertical space and in a guarded hot plate in order to establish the behaviour of the horizontal space. The experimental investigations also include a tentative study of the influences from small air spaces and openings in the insulation. This section is concluded by a discussion of the numerous wall insulation measurements previously presented in the literature.

The final conclusions and a summary of the results and their implications are presented in Section 7.

Details of theoretical calculatory methods and experimental results and procedures are given in the Appendix. The literary references are listed in the appropriate category or at the end of the Bibliography. Frequently-used symbols can be found under the heading Nomenclature. SI-units have been used throughout unless clearly stated otherwise in the context.

2 NATURAL CONVECTION

2.1 Phenomenology

Natural or free convection can be considered as the heat transfer by flow of fluid due to the interaction between the field of gravity and temperature-induced density variations in the fluid. This is a fairly well known phenomenon in the air space and in order to understand the heat transfer due to convection in an insulation it is suitable to observe the two extreme limits from the point of view of heat transfer.

One extreme limit of the porous insulation is the solid structure which is reached as the porosity of the material decreases. The other extreme limit is reached as the porosity increases and is the air space (or uninsulated structure). This is illustrated in FIG. 2.1 on a space of different orientation. In the figure the characteristic air flow patterns inside the space and heat flow variations at the boundaries are shown for constant boundary temperatures. This means that it is of interest to investigate to what extent the thermal performances of the insulated structure are similar to those of the air space or those of the solid structure.

When the basic physical mechanisms of heat transfer are known in a material without convective gas flow, the question is under what circumstances natural convection will be of importance to the total effective thermal conductivity of the insulation, for example when installed in a wall. In order to understand the phenomenology of natural convection,valuable information can be gained from the available knowledge of the behaviour of the air space. This approach was suggested earlier by the author (Bankvall, 1966) and will be used in the following.

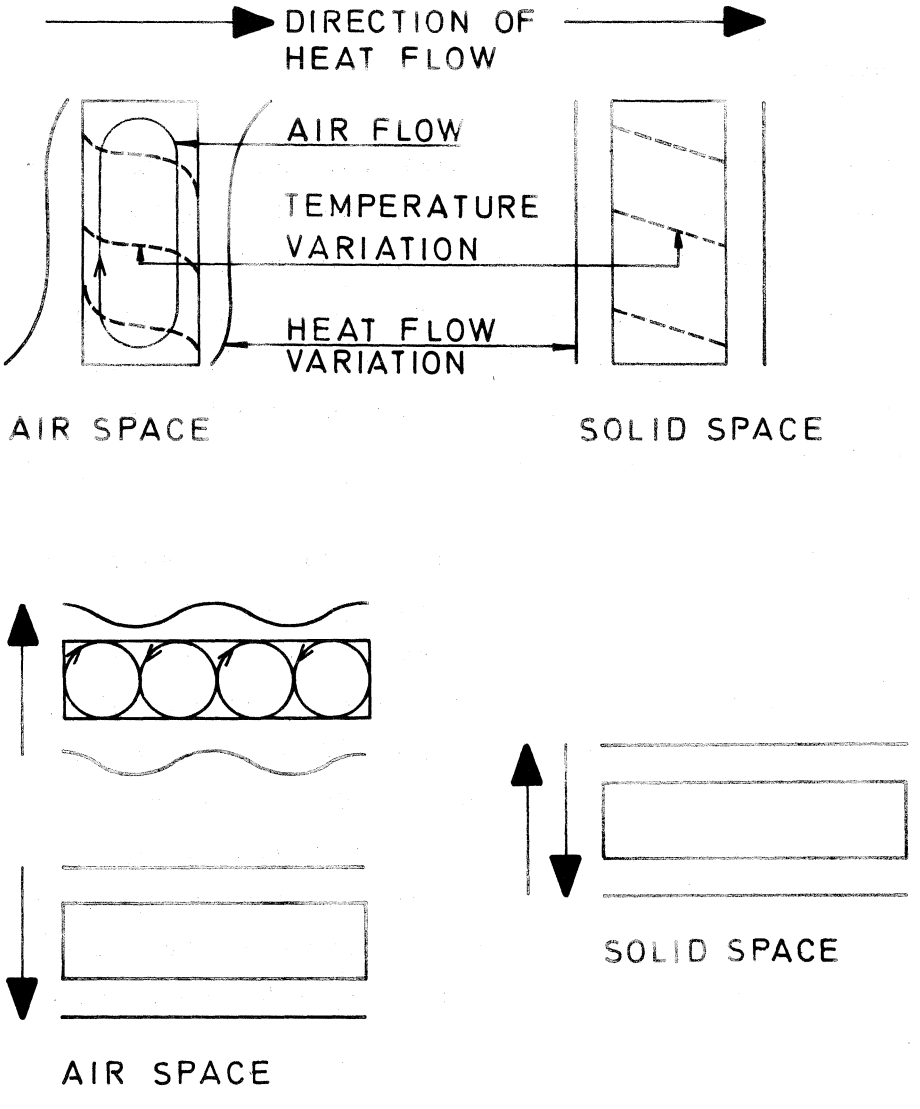

FIG. 2.1. Air flow patterns and heat flow variations for spaces with different insulation and orientation.

3 NATURAL CONVECTION IN AIR (FLUID) SPACE

3.1 Introduction

The heat transfer in a fluid (gaseous or liquid) space has been investigated by several research workers. The transfer by radiation has in most cases given few difficulties, and the main interest has been directed towards the different convective phenomena in the space. Earlier investigations of natural convection or heat transfer in a fluid space have been of experimental character, sometimes with a limited dimensional analysis as the theoretical background. The complete equations governing the heat and mass flow in the system have eventually been given. Their complicated nature has, however, made analytical solutions difficult, and, in most cases, impossible. Only the recent development of large, high-speed computers has enabled the numerical solution of some of the problems. This situation invariably leads to difficulties in evaluating some of the earlier experiments because relevant influencing factors are not given.

In the following, the natural convection in a fluid space will be described, first by establishing the theoretical equations and then by presenting some theoretical and experimental results. This exposition will largely be based on the available literature.

3.2 Vertical space, theoretical background.

The equations governing the natural convection in a vertical fluid space can be developed and discussed with reference to FIG. 3.1. In the figure, h denotes the height, d the depth and b the width of the space. The temperatures of the vertical walls $x = 0$ and $x = d$ are T_C and T_H, respectively. Assume that the variation in temperature is small compared to the absolute temperature, and that pressure differences arising from inertia and gravitational forces are negligible in comparison to absolute pressure. This implies that density variations are significant only in their generation of bouyancy forces and then determined solely by variation of absolute temperature, the so called Boussinesq approximation. Other fluid parameters are

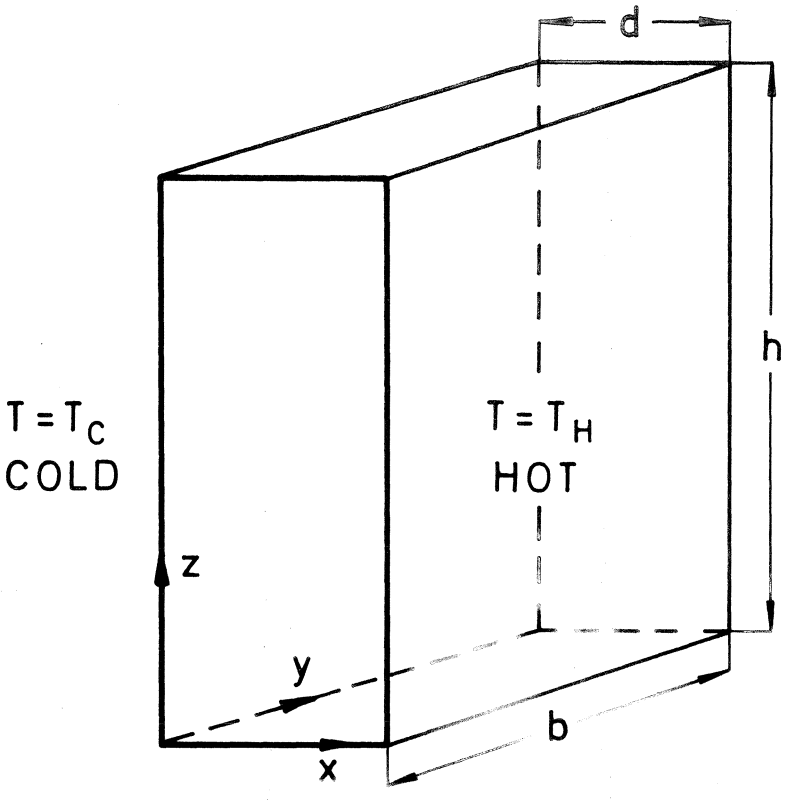

FIG. 3.1. Vertical space notation.

independent of temperature. Assume also that the effects of compressibility and viscous dissipation of energy are negligible. The governing equations can then be expressed in the following form in vector notation.

The continuity equation

$$\operatorname{div} \bar{v} = 0 \tag{3.1}$$

where $\bar{v} = (u, v, w)$ is the local velocity.

The momentum equation

$$\rho \frac{\partial \bar{v}}{\partial t} + \rho(\bar{v} \operatorname{grad}) \bar{v} = - \operatorname{grad} p + \eta \nabla^2 \bar{v} - \rho \beta(T - T_m) \bar{g} \tag{3.2}$$

where t is the time, p and T are local pressure and temperature of the fluid, while ρ, η and β are mean values of density, dynamic viscosity and the coefficient of cubical expansion corresponding to the mean temperature $T_m = (T_H + T_C)/2$. $\bar{g} = (0,0,-g)$ is the gravitational acceleration.

The energy equation

$$\rho C_p \frac{\partial T}{\partial t} + \rho C_p(\bar{v} \operatorname{grad}) T = \lambda \nabla^2 T \tag{3.3}$$

where C_p is the specific heat at constant pressure and λ the thermal conductivity corresponding to the mean temperature T_m.

The governing equations can be derived from the study of a control volume of the fluid (cf. e.g. Chandrasekhar, 1961 or Kays, 1966). The continuity equation expresses that the content of mass in the volume does not change, i.e. the same amount of fluid flows into the volume as flows out of it. The momentum equation states that the change in momentum as the fluid flows through the control volume is equal to all external forces acting on the control surface or volume. The energy equation expresses the change in energy content of the volume, in this case the change in temperature and the heat transported by flow of fluid is

balanced by that due to conduction in the fluid.

If only stationary flow is treated, and if the width of the space is large ($b >> d, h$), then the governing equations for the two-dimensional, stationary case can be formulated:

Continuity,

$$\frac{\partial u}{\partial x} + \frac{\partial w}{\partial z} = 0 \tag{3.4}$$

momentum,

$$u \frac{\partial u}{\partial x} + w \frac{\partial u}{\partial z} = - \frac{1}{\rho} \frac{\partial p}{\partial x} + \nu\left(\frac{\partial^2 u}{\partial x^2} + \frac{\partial^2 u}{\partial z^2}\right) \tag{3.5}$$

$$u \frac{\partial w}{\partial x} + w \frac{\partial w}{\partial z} = - \frac{1}{\rho} \frac{\partial p}{\partial z} + \nu\left(\frac{\partial^2 w}{\partial x^2} + \frac{\partial^2 w}{\partial z^2}\right) + \rho\beta(T - T_m)g \tag{3.6}$$

and energy,

$$u \frac{\partial T}{\partial x} + w \frac{\partial T}{\partial z} = a\left(\frac{\partial^2 T}{\partial x^2} + \frac{\partial^2 T}{\partial z^2}\right) \tag{3.7}$$

$\nu = \eta/\rho$ is the kinematic viscosity and $a = \lambda/(\rho C_p)$ the thermal diffusivity of the fluid at the mean temperature T_m.

In this current case the above equations are solved subjected to certain boundary conditions. At the vertical boundaries these conditions are

$$\begin{aligned} &u = w = 0, \quad T = T_C \quad \text{at} \quad x = 0 \\ &u = w = 0, \quad T = T_H \quad \text{at} \quad x = d \end{aligned} \tag{3.8}$$

At the horizontal boundaries, $z = 0$ and $z = h$, $u = w = 0$ together with some condition on T, e.g. that T varies linearly from the cold to the hot side or that the boundaries are well insulated so that there is no heat flow, i.e. $\frac{\partial T}{\partial z} = 0$. If $h >> d$ the exact conditions for T on the horizontal boundaries are of minor importance.

In order to simplify the previous equations, dimensionless variables are introduced

$$X = \frac{x}{d}$$

$$Z = \frac{z}{d} \qquad (3.9)$$

$$\theta = \frac{T-T_m}{\Delta T}$$

with

$$\Delta T = T_H - T_C$$

$$T_m = (T_H + T_C)/2$$

A dimensionless stream-function ψ is defined by

$$u = \frac{a}{d}\frac{\partial \psi}{\partial Z}$$

$$w = -\frac{a}{d}\frac{\partial \psi}{\partial X} \qquad (3.10)$$

This enables the simplification of equations (3.4) - (3.7).

Equation of energy (by insertion in (3.7))

$$\frac{\partial \theta}{\partial X} \cdot \frac{\partial \psi}{\partial Z} - \frac{\partial \theta}{\partial Z} \cdot \frac{\partial \psi}{\partial X} = \nabla^2 \theta \qquad (3.11)$$

Equation of continuity and momentum (by insertion in (3.5) and (3.6) after derivation, insertion of (3.4) and elimination of p)

$$\frac{\partial \xi}{\partial X} \cdot \frac{\partial \psi}{\partial Z} - \frac{\partial \xi}{\partial Z} \cdot \frac{\partial \psi}{\partial X} = Pr\ Ra \frac{\partial \theta}{\partial X} + Pr\ \nabla^2 \xi \qquad (3.12)$$

where

$$\xi = \nabla^2 \psi \qquad (3.13)$$

$$Pr = \frac{\nu}{a} \qquad (3.14)$$

is the Prandtl number, and

$$Ra = \frac{g \cdot \beta \cdot \Delta T \cdot d^3}{a \cdot \nu} \tag{3.15}$$

the Rayleigh number.

The boundary conditions are

$$\begin{aligned} &\psi = 0 \ , \ \theta = 0 && \text{at} \quad X = 0 \\ &\psi = 0 \ , \ \theta = 1 && \text{at} \quad X = 1 \\ &\psi = 0 \ , \ \theta = X \ \text{ or e.g. } \frac{\partial \theta}{\partial Z} = 0 && \text{at} \quad Z = 0 \ \text{ and } \ Z = \frac{h}{d} \end{aligned} \tag{3.16}$$

By introducing dimensionless variables of an adequate choice and elimination between the original equations, it has been possible to reduce the problem to two equations and the appropriate boundary conditions. This means that the temperature and stream functions, θ and ψ, are uniquely determined by the Prandtl number Pr, the Rayleigh number Ra (sometimes the Grashof number Gr = Ra/Pr is used instead), and the aspect ratio h/d. It should be pointed out that, depending, upon the boundary conditions additional factors may influence the governing equations.

The convective heat transfer through the space can be expressed dimensionlessly as the ratio between the thermal conductivity with convective flow in the space, λ_{cv} and the conductivity in the stagnant fluid, λ.

$$\frac{\lambda_{cv}}{\lambda} = Nu = \frac{d}{h} \int_0^{h/d} \left(\frac{\partial \theta}{\partial X}\right)_{X=0} dZ \tag{3.17}$$

When no convective flow is present the Nusselt number Nu, will be equal to one.

The general conclusion (which can be deduced from a simple analysis of dimensions as well) is

$$Nu = f\,(Pr, Ra, h/d) \tag{3.18}$$

In an air space $Pr = 0.7$ and the interesting variables are h/d and Ra. Instead of Ra, Gr can be used.

Attempts have been made to solve the above equations analytically. In recent years, however, some numerical solutions on computer have been more successful. The governing equations for two-dimensional convective motion in a long vertical space were discussed by Batchelor (1954) in a theoretical study of cavities used for thermal insulation of buildings. This analysis was essentially asymptotic, discussing the behaviour of the space for small Ra, large h/d and large Ra, respectively. Poots (1957) developed numerical approximations for the solution of the partial differential equations. These were solved for $h/d = 1$ and Ra-values between $5 \cdot 10^2$ and 10^4. Emery and Chu (1965) assumed that the convective heat transfer was a result of two boundary layers formed on the vertical surfaces. They calculated a Nusselt number-relationship for $Ra < 10^7$. Similar, somewhat more elaborate evaluations have been made by Gill (1966) and Nagendra and Tirunarayanan (1971), among others.

A numerical procedure involving simple difference formulae for solving the governing equations was presented by de Vahl Davis and Kettleborough (1965). Their finite-difference solution was performed for $h/d = 1.875$ and $Ra \leq 5 \cdot 10^4$. With some modifications, this procedure was used by de Vahl Davis (1968) to investigate the convective flow for $Ra \leq 2 \cdot 10^5$ and h/d in the range 1 - 5. Wilkes and Churchill (1966) treated the problem of a fluid initially at rest in an isothermal space. This space was then subjected to the relevant thermal boundary conditions. They gave some solutions for $Ra < 7.5 \cdot 10^4$ and $h/d = 1$, 2 or 3. A similar problem was treated by MacGregor and Emery (1969). Details of the convective flow were given for $Ra \leq 10^6$ and from 1 to large values of the aspect ratio h/d. In recent years Szekely and Todd (1971) have made an analysis of transient laminar natural convection in a rectangular space containing either one fluid or two immiscible liquids.

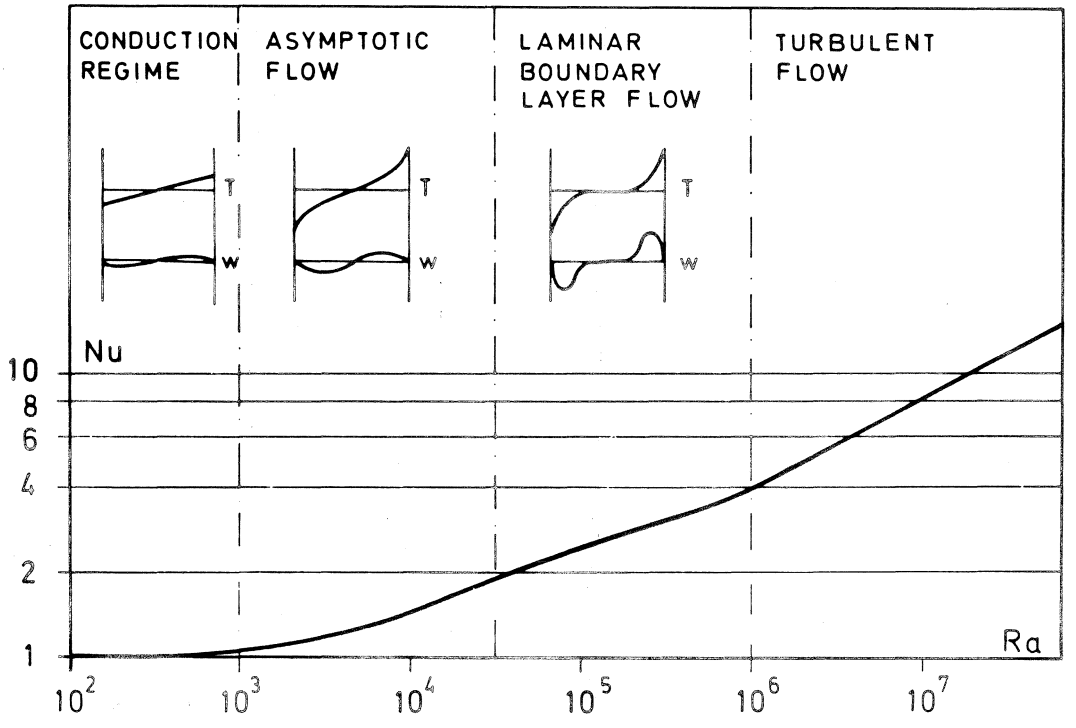

FIG. 3.2. Schematic temperature and flow fields in natural convective heat transfer in a vertical fluid space ($h/d \simeq 10$).

3.3 Characteristics of natural convection, vertical space.

In the preceding section it was found that the interesting characteristics for the natural convection in the vertical air space were the Rayleigh number Ra, the aspect ratio h/d and the boundary conditions. A discussion of these influencing factors will now be made, on the basis of the extensive literature available.

In order to understand the convective heat transfer in the air space it is suitable to study the temperature and velocity fields in the space. FIG. 3.2 shows the different types of flow at different values of Ra, at a h/d value of approximately 10.

The first regime ($Ra < 10^3$), the conduction regime, is characterized by a linear temperature variation from the cold to the hot side of the space. The flow of air that may occur is insignificant and the heat is transfered through the space by conduction in the air i.e. Nu = 1. Under these conditions no influence from Ra or h/d can be expected.

As Ra increases ($10^3 < Ra < 3 \cdot 10^4$), a more noticeable flow will develop all over the space. The flow is directed upwards at the warm side and downwards at the cold side. This so-called asymptotic flow leads to deformations in the temperature field. The temperature gradients at the boundary surfaces are changed and this gives as a whole an increased heat transfer through the space. The heat is transferred simultaneously by conduction in and flow of the air, i.e. by convection. In this case, the heat is transferred roughly equally over the height of the space with the exception of the top and the bottom, where the flow of air especially influences the heat transfer. In these end-regions the addition of heat to the air is somewhat greater at the bottom of the warm side, and the loss of heat correspondingly larger at the top of the cold side than is the case for the side-surfaces as a whole. This is due to the warming and cooling, respectively, of the air as it flows along the surfaces and at top and bottom passes from one side to the other. In this case, a certain influence of h/d can be expected. In a space with a large aspect ratio,

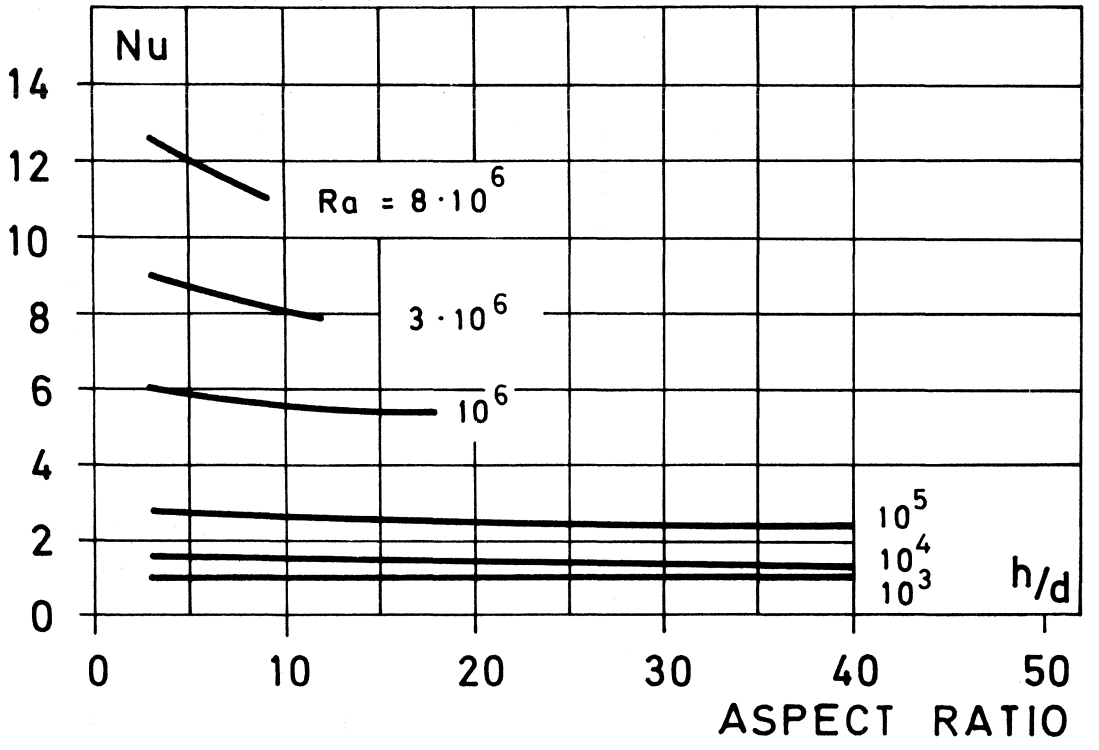

FIG: 3.3. The influence of aspect ratio and Rayleigh number upon the convective heat transfer in a vertical air space (after measurements made by Mull and Reiher, 1930).

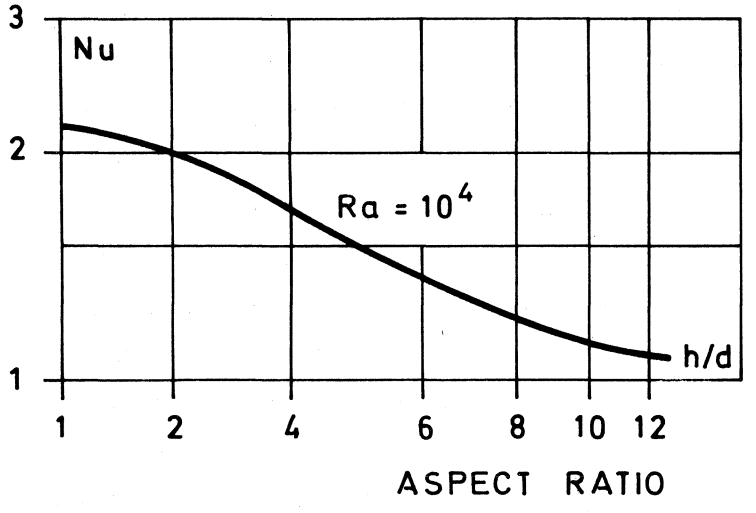

FIG. 3.4. The variation of Nu-value with aspect ratio in a vertical space (from calculations made by MacGregor and Emery, 1969).

the heat transfer in the end-region will influence a relatively smaller part of the space. This influence will be more marked as Ra, i.e. the flow in the space, increases.

Further increase of Ra ($3 \cdot 10^4 < Ra < 10^6$) gives a more noticeable flow along the vertical boundaries. Eventually, a boundary layer flow is developed, where the boundary layers are separated. The temperature change occurs in these boundaries in a way similar to that at a free vertical surface. The heat transfer is mainly due to the flow of air at the top and the bottom of the space. In this case a more noticeable dependence on h/d can be expected.

Sufficiently large values of Ra ($Ra > 10^6$) will give turbulent flow in the air space. As long as the turbulence develops within the boundary layer the influence of the aspect ratio h/d is noticeable, if the turbulence encompasses the whole space it is likely that this influence decreases again.

A summary of the influence of h/d and Ra upon the heat transfer in the vertical space can now be made.

An increase of h/d is likely to decrease the total heat flux through the space. Dividing the space horizontally will consequently increase the heat transfer. The extent of the influence of h/d upon the heat transfer will depend upon the condition of flow in the space. This is illustrated in FIG. 3.3 where the measurements of Mull and Reiher (1930) have been used. The figure shows that for high Ra-values the variation in Nu with h/d is more pronounced. It should be pointed out that if the aspect ratio decreases below approximately one, the reverse will be true, since the convective flow will be seriously restricted when h/d < 1. FIG. 3.4 from the calculations of MacGregor and Emery (1969) shows some indication of this. In these latter cases, the horizontal boundary conditions will be of importance. The problem of the horizontal boundary conditions will, however, be left for a discussion in connection with the fiber insulated space. All the illustrations in this section refer to the case of insulated horizontal boundaries. To complete the picture of the influence of h/d it should be noted that the

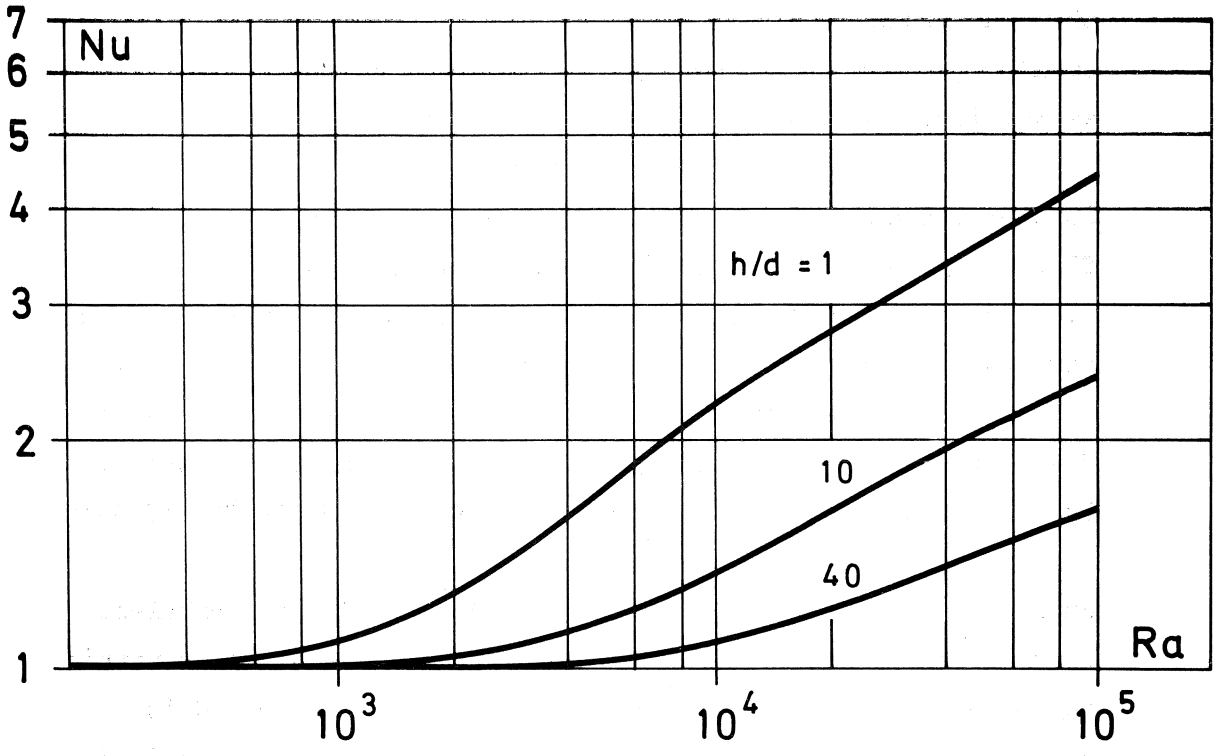

FIG. 3.5. Natural convective heat transfer in vertical air space (from calculations of MacGregor and Emery, 1969).

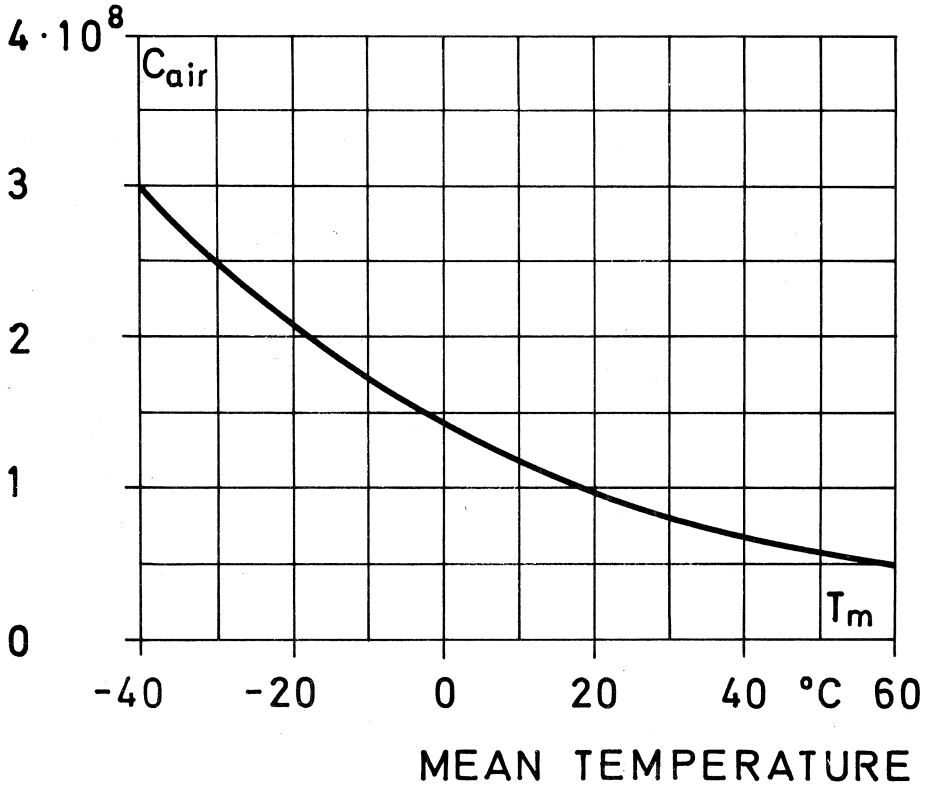

FIG. 3.6. Coefficient for calculation of Ra-value for an air space, $Ra = C_{air} \cdot \Delta T \cdot d^3$.

transition from one type of flow to another, as indicated in FIG. 3.2, generally takes place at a slightly higher Ra value as h/d is increased (cf. Eckert and Carlson, 1961).

FIG. 3.5 shows the general influence of the Ra-value for different aspect ratios upon the convective heat transfer through the vertical space from calculations of MacGregor and Emery (1969). The Rayleigh number is defined by

$$Ra = \frac{g \cdot \beta \cdot \Delta T \cdot d^3}{a \cdot \nu}$$

If the air in the space is treated as an ideal gas, $\beta = 1/T_m$ and

$$Ra = C_{air} \cdot \Delta T \cdot d^3 \qquad (3.19)$$

where

$$C_{air} = \frac{g}{a \cdot \nu \cdot T_m} \qquad (3.20)$$

only depends upon the gas (air) and the temperature. C_{air} for different mean temperatures is shown in FIG. 3.6. It is obvious from the above relationships that for applications in building physics the temperature difference and the space thickness are the most important influencing factors.

3.4 Horizontal space, background.

The heat transfer due to natural convection in a horizontal air (fluid) space heated from below, which is the interesting case, is governed essentially by the same equations that were established for the vertical space. FIG. 3.7 shows the notation in this case. The governing equations should naturally be subjected to the relevant boundary conditions.

When a layer of a fluid is heated from below, a cellular regime of steady convection is established if the Rayleigh number exceeds a critical value. These polygonal, so called Bénard cells (Bénard, 1900) are shown in their hexagonal form in FIG. 3.8. In the cell the warm air will descend in the center and

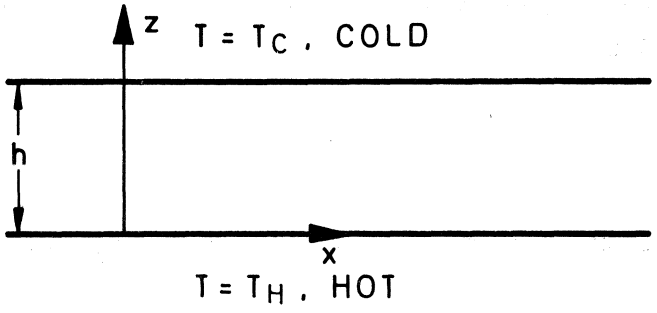

FIG. 3.7. Horizontal fluid space notation.

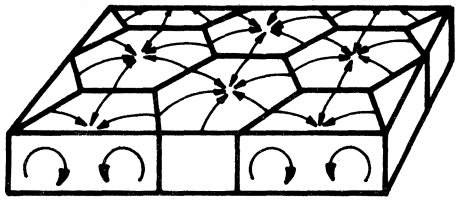

FIG. 3.8. Convection cells in horizontal air space.

the cold air will ascend at the edges of the cell - in the case of a liquid, the reverse will be true. In general when a system changes from an unstable equilibrium it can do so in several principal modes, of interest may then be the mode for which the instability is greatest.

The case of a fluid between two infinite isothermal planes was treated by Rayleigh (1916). He made a linear analysis of the stability criteria for certain boundary conditions. An analysis of the fluid layer was made by Jefferys (1926, 1928) for several different boundary conditions giving the critical Rayleigh-values for stability. Pellew and Southwell (1940) made a thorough treatment of the linear disturbance theory for cells of arbitrary plan form. In an extension of the linearized stability theory Malkus and Veronis (1958) made a study of non-linear processes in cellular convection. This approach was used by Edwards and Catton (1969) to estimate the influence from vertical sidewalls on the convective heat transfer. The natural convection in a horizontal fluid space was treated numerically in two dimensions by Fromm (1965) for different horizontal boundary conditions. Aziz and Hellums (1967) presented a method for numerical finite difference solution of the three dimensional problem.

3.5 Characteristics of natural convection, horizontal space.

The natural convection in the horizontal space is governed by roughly the same factors as the convective flow in the vertical space. These are the Rayleigh number, in this case with h as dimension parameter, the aspect ratio h/d and the boundary conditions. In many cases d >> h and the convection in fluid space is governed by the Rayleigh number

$$Ra = \frac{g \cdot \beta \cdot \Delta T \cdot h^3}{a \cdot \nu} \qquad (3.21)$$

In the preceeding section it was pointed out that when a system becomes unstable it can do so in different principal modes. FIG. 3.9 shows the convective heat transfer due to the independent

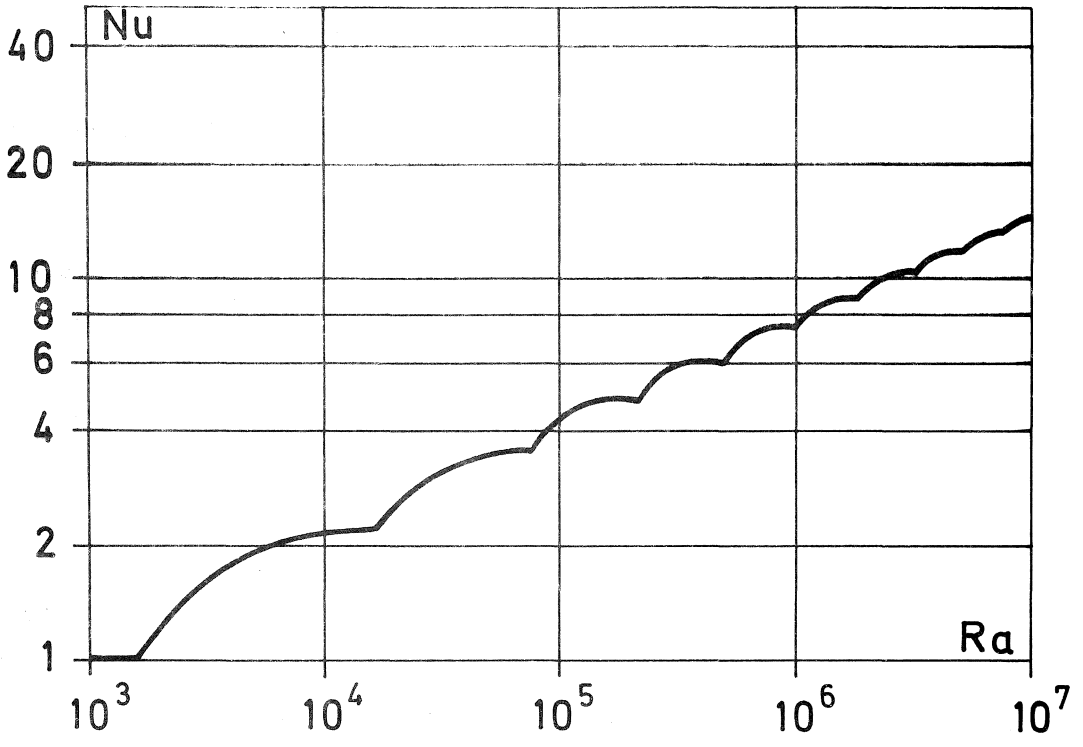

FIG. 3.9. The convective modes of heat transfer in the horizontal fluid space (as calculated by Catton, 1966).

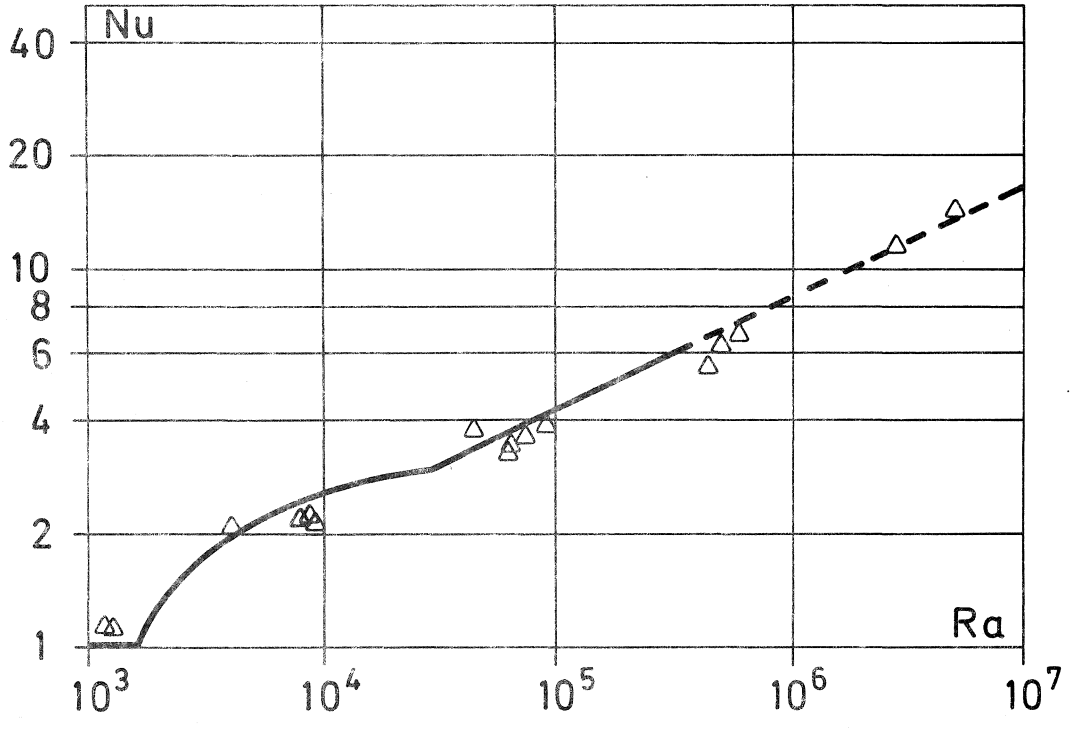

FIG. 3.10. Convective heat transfer in horizontal space (- mean curve for measurements on liquids by Silveston, 1958, Δ measurements on air space by Mull and Reiher, 1930).

growth of the first second and higher Rayleigh - like modes. The calculations were done by Catton (1966) following the relationship given by Malkus and Veronis (1958). The figure shows that the first critical Ra-value is reached at 1700 giving the first convective mode of gas flow; when the Ra value reaches about 17600, the second mode is initiated and adds to the convective heat transfer, etc.. This behaviour has been confirmed by several theoretical and experimental investigations. In FIG. 3.10 results from experiments on liquids by Silveston (1958) and on air by Mull and Reiher (1930) are shown. The results agree favourably with FIG. 3.9. It should be pointed out that for very thin gaseous spaces, h < 10 mm, the critical value is smaller due to another type of convective flow. If the upper surface of the fluid layer is free the critical value is about 1100, Pellew and Southwell (1940).

The above figures are valid when the aspect ratio $h/d \lesssim 0.2$, for higher values of h/d the convective motion sets in at a higher Ra-value and the boundary conditions on the vertical sides can be of importance. This influence of the aspect ratio was investigated experimentally and theoretically by Catton and Edwards (Catton & Edwards, 1967 and Edwards & Catton, 1969). FIG. 3.11 shows the influence from h/d on the convective heat transfer according to these investigations.

The criterion for natural convective flow in a horizontal air space is given by

$$Ra \gtrsim 1700 \qquad (3.22)$$

where

$$Ra = \frac{g \cdot \Delta T \cdot h^3}{a \cdot \nu \cdot T_m} = C_{air} \cdot T \cdot h^3 \qquad (3.23)$$

The coefficient C_{air} depends upon the gas (air) and the temperature. C_{air} is given in FIG. 3.6. It is evident that in applications in building physics the temperature difference over the space and its height are the most important influencing factors.

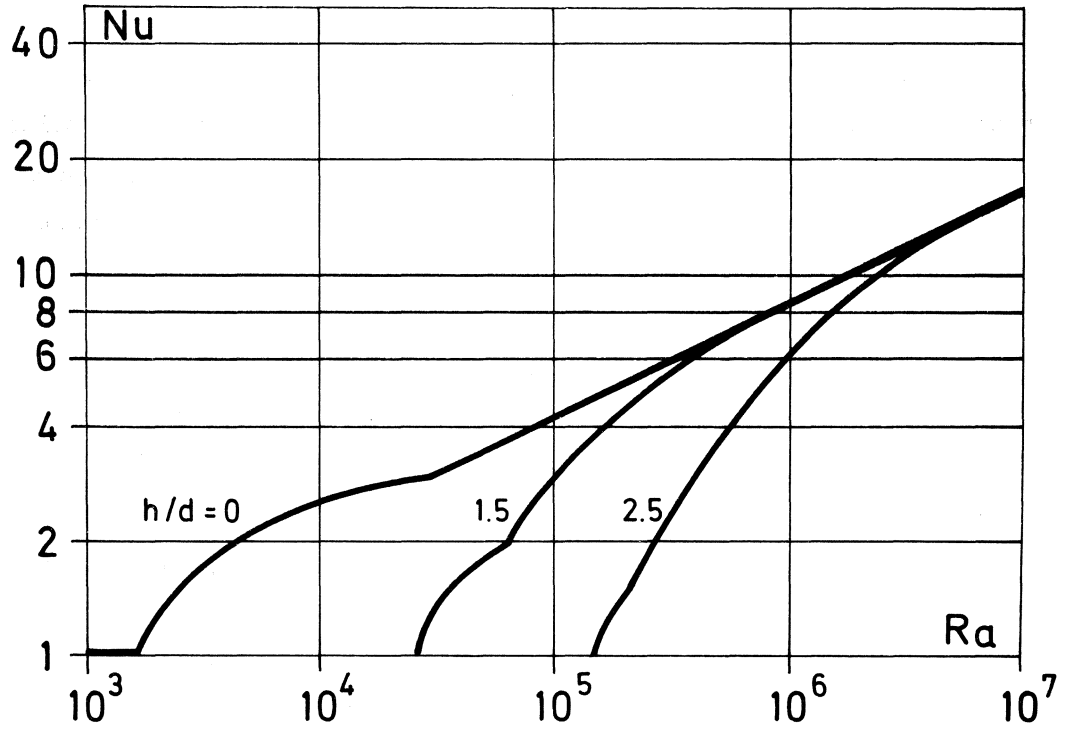

FIG. 3.11. The influence of vertical walls and aspect ratio upon the convective heat transfer in a horizontal fluid space (cf. Catton & Edwards, 1967, and Edwards & Catton, 1969).

4 FLOW IN POROUS MATERIAL

4.1 The governing equation

In order to correctly evaluate convection in an open-pore material it is necessary to know the equation governing the gas flow through the material. It is then possible to treat the heat transfer in the insulated space and make comparisons with the air space.

The mechanisms of flow processes through porous media are generally complicated (cf. Carman, 1956, Collin, 1961, and Scheidegger, 1963). Attempts to describe the flow directly by means of basic physical equations have been unsuccessful for long-range prediction of the behavior of the flow. Equations used are therefore generally semi-empirical and the basic equation governing calculations of flow of fluids through porous media is that of Darcy (1856). This empirical law states that the rate of flow is directly proportional to the pressure gradient causing flow, i.e.

$$u = B_1 \frac{\Delta p}{L} \tag{4.1}$$

where u is the apparent linear rate of flow, Δp the total pressure drop across a specimen of length L and B_1 is a permeability coefficient. The apparent linear flow rate u is defined by

$$u = \frac{Q}{A} \tag{4.2}$$

where Q is the volume flow across the cross-sectional area A.

The above proportionality between flow rate and pressure gradient does not always hold, but it can be applied in most cases of viscous streamline or laminar flow. If the decrease in pressure is small, i.e. compressibility can be ignored, the equation can be rewritten in the following form

$$u = - \frac{B_o}{\eta} \frac{\partial p}{\partial x} \tag{4.3}$$

where η is the dynamic viscosity and B_o the specific

permeability coefficient.

Several workers have reformulated the Darcy-law and discussed its applicability (cf. e.g. Hubbert, 1956, Houpeurt, 1959, Whitaker, 1966, in addition to the previous references). The relationship has also been derived more or less stringently and as a special case, from e.g. in recent years, classical continuum mechanics (Fulks et al, 1971) or by statistical models where the randomness is described as inherent in the fluid particles (Liao & Scheidegger, 1970) or ascribed to the medium (Torelli & Scheidegger, 1971).

4.2 The specific permeability.

The specific permeability coefficient is defined by

$$B_o = -\frac{Q}{A} \cdot \frac{\eta}{\text{grad } p} \qquad (4.4)$$

Generally speaking the permeability is the fluid conductivity of the porous material and the value of B_o is determined by the structure of the material. From the defining equation it is seen that B_o has dimensions of length squared (m^2) and it is roughly a measure of the mean square pore diameter of the material. In many branches of applied science other units have been adopted specific to that branch. The permeability coefficient B_1, in the original formulation of the Darcy-law, is rather restricted in its usefulness. This constant is obviously indicative of the permeability of a certain medium to a particular fluid. It depends on the properties of both the medium and the fluid. In the 1930-s, when several research workers pointed out the advantages of a coefficient that separated the influence of the porous media from that of the liquid, the specific permeability B_o was more or less generally accepted. The verification of this concept consists in the innumerable successful determinations of permeability that have been performed with it.

In an unisotropic porous material the permeability will have different values in different directions (cf. Scheidegger, 1954). In such a case three orthogonal principal axes can be assigned to the sample with corresponding permeability coefficients, B_{o1},

B_{o2} and B_{o3} (cf. e.g. Ferrandon, 1948, Scheidegger, 1963). If the coordinate axes are oriented parallel to the principal axes, each component of the linear rate of flow is proportional to the corresponding component of the potential (pressure) gradient with the appropriate permeability coefficient. In the mineral wool insulation the fibers are generally oriented randomly in parallel fiber planes. The permeability coefficient in two directions can therefore be assumed to be the same and the principal directions of interest are B_{ox} and B_{oz} ($B_{oy} = B_{ox}$ or B_{oz}).

Many attempts have been made to relate the structure of the porous material to its permeability. It is, however, intuitively clear that this is a most difficult task simply because a correct description of the structure of the material is exceedingly difficult. In order to find theoretical correlations the porous media are represented by theoretical models that can be treated mathematically. The simplest models are those consisting of capillaries (cf. Scheidegger, 1963). The usefulness and applicability of these models are very restricted. More elaborate models are based on hydraulic radius theories. The most generally accepted theory in this case is that of Kozeny (1927). In this theory the porous material is represented by an assemblage of channels. The Navier-Stokes equations are solved simultaneously for all channels passing through a cross-section normal to the flow in the porous media and the permeability is expressed in terms of the porosity and the specific surface of the medium. The basic treatment by Kozeny has been modified by several research workers. A commonly used modification is the one by Carman (cf. Carman, 1956)

$$B_o = \frac{1}{k \cdot S_o^2} \cdot \frac{\varepsilon^3}{(1 - \varepsilon)^2} \qquad (4.5)$$

where ε is the porosity of the material, k the Kozeny constant and S_o the specific surface of the solid phase. For a cylindrical fiber of diameter D, $S_o = 4/D$. The porosity is defined by

$$\varepsilon = 1 - \rho_t/\rho_s \qquad (4.6)$$

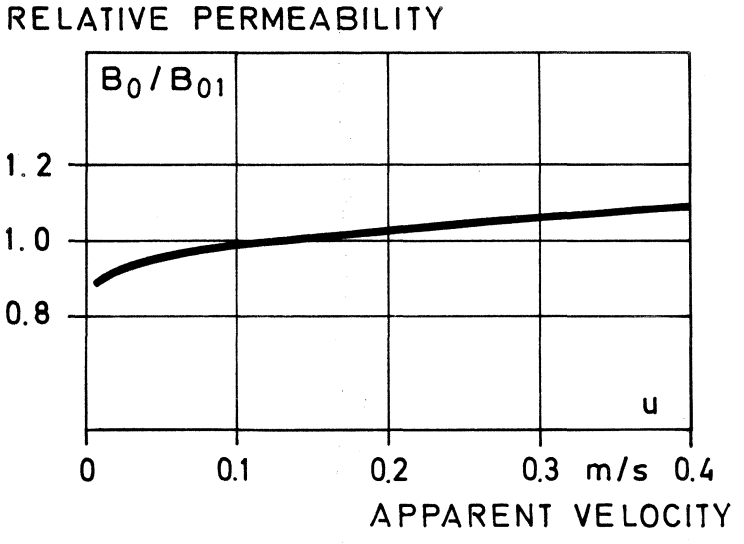

FIG. 4.1. The variation in permeability with flow velocity according to the drag theory, cf. equation (4.7).

where ρ_t is the (bulk) density of the material and ρ_s the density of the solid phase.

Unfortunately the Kozeny theory also fails in many cases, especially for high porosities. This is noticeable from the variation of the Kozeny constant, theoretically given as 2, from experiments chosen as 5 and in the case of high porosity fibrous materials increasing further with increasing porosity (cf. Carman, 1956). A different approach was developed by Emersleben (1927). In this theory the walls of the pores are treated as obstacles to the viscous flow. The drag of the fluid is estimated from the Navier-Stokes equations, and the resistance of the porous media to flow is equal to the sum of all drags. The drag theory is likely to give good results in the case of highly porous media, such as fibers, where the single particles can be regarded as more or less solitary within the fluid. This theory was used by Iberall (1950) in a study of permeability of glass wool and other highly porous media. In the case for the fibrous media

$$B_o = \frac{3}{16} \cdot \frac{\varepsilon D^2}{1 - \varepsilon} \cdot \frac{2 - \ln Re}{4 - \ln Re} \qquad (4.7)$$

where Re is the Reynold number

$$Re = \frac{D \rho u'}{\eta} \qquad (4.8)$$

ρ is the fluid density and u' is the local flow velocity related to the linear rate of flow by

$$u' = u/\varepsilon \qquad (4.9)$$

A significant implication of equation (4.7) is that the permeability varies with the Reynolds number i.e. the velocity of flow. This effect is generally attributed to the fluid inertia. FIG. 4.1 shows the variation in relative permeability as a function of apparent velocity.

The drag theory has been treated in different ways by differnt research workers. In a recent paper by Kyan et. al. (1970)

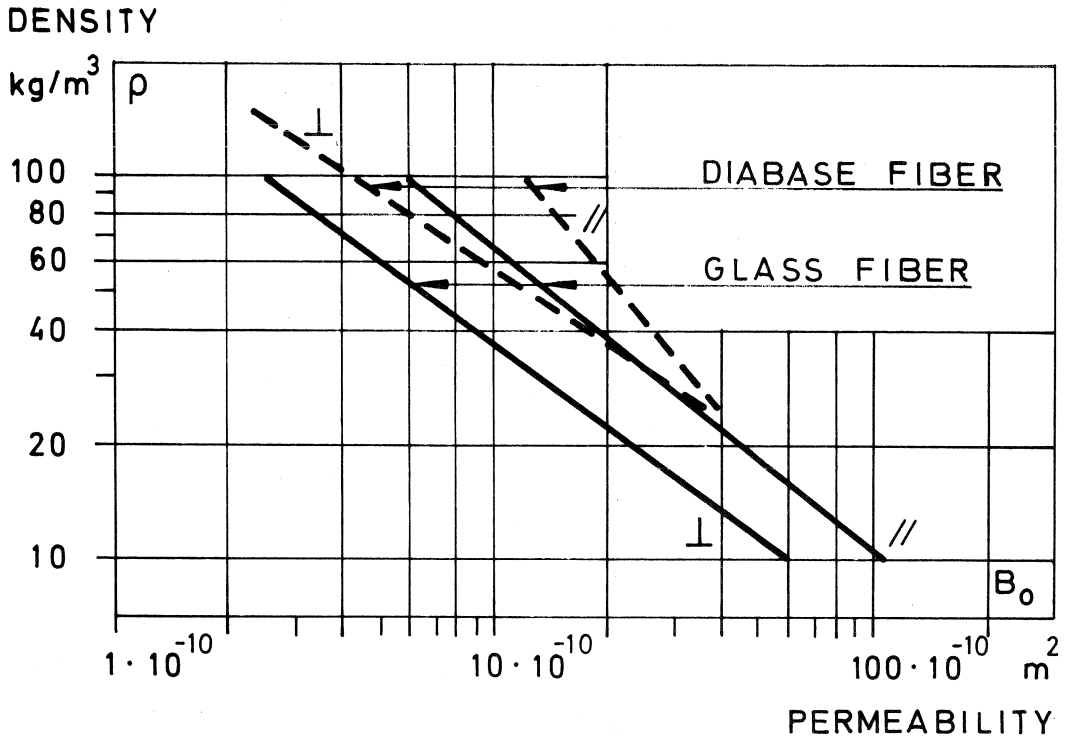

FIG. 4.2. Experimental specific permeability values for different mineral wool densities.

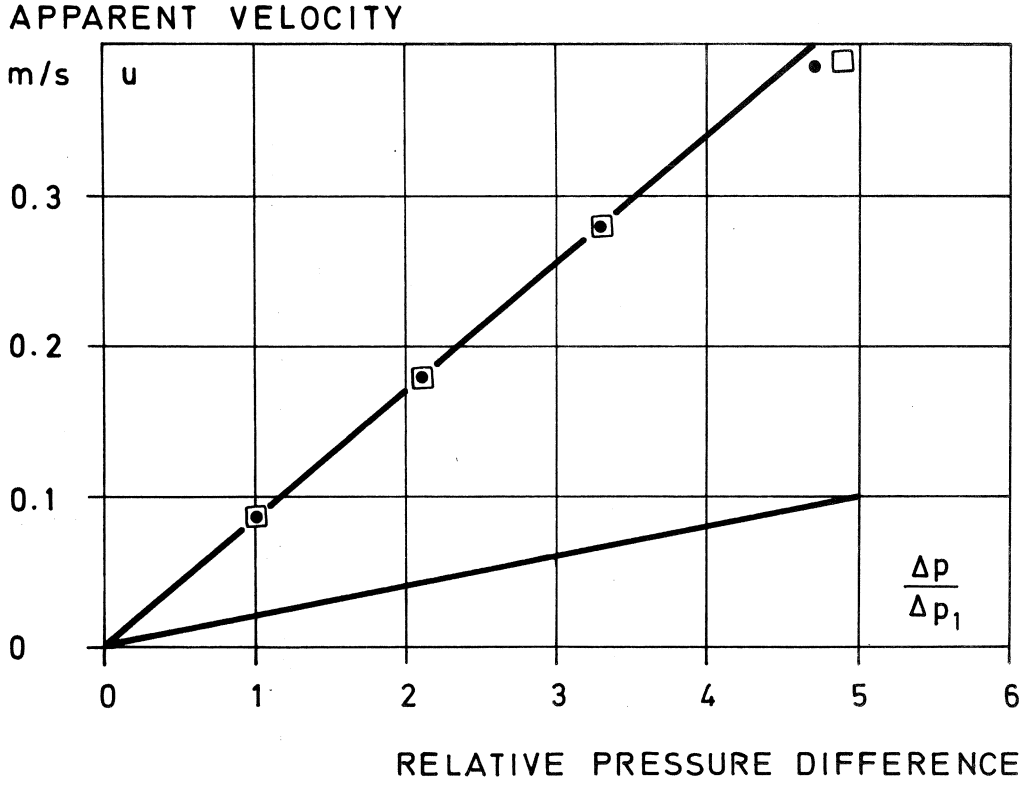

FIG. 4.3. The apparent velocity in the permeability measurements at different relative pressure difference.

the deflection of individual fibers was also considered. A comparison was made with the Kozeny theory.

None of the previous models are, however, complicated enough to represent true porous media. Therefore they describe the permeability of the material with the same insufficiency as many other semi-empirical relations found in the literature. In recent years statistical models of flow through porous material have been tried with some hope of leading to an understanding of the relevant mechanisms.

4.3 Measurements of permeability.

The measurements of permeability are done using the Darcy relationship. This means that for a certain porous system the relevant pressure drop and simultaneous flow are measured. In some cases these methods have been standardized e.g. ASTM (1968) and DIN (1958).

In the present investigation the permeability of two different types of mineral wool insulations (diabase and glass fiber) was measured. The measurements were performed parallel and at right angle to the fiber planes. The different measurement techniques used are described in the Appendix together with the detailed results. The conclusive results of the permeability measurements are shown in FIG. 4.2. Regression lines give the specific permeability depending upon type of fibrous material, orientation and density.

As was pointed out earlier there is some doubt as to what extent the proportionality between the pressure gradient and the apparent rate of flow (or velocity) is true. In order to investigate this, measurements were made with different flow rates. This is illustrated in FIG. 4.3 where the lower line indicates the velocity range in which most of the measurements were performed. No departure from the proportionality relationship could be detected. Two sets of measurements were made at higher velocities as is indicated by the upper line in the figure. In this case a slight deviation from the simple linear relationship was

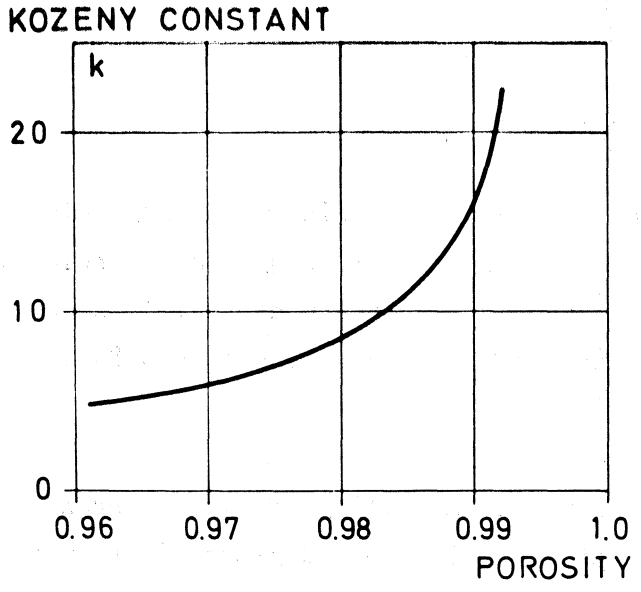

FIG. 4.4. The Kozeny constant calculated from experiments.

detected for $u > 0.3$ m/s. This indicates that in this type of material the Darcy equation is applicable for fairly high velocities. The result does not show any influence from apparent velocity upon the permeability as was indicated by the drag theory in FIG. 4.1.

The Kozeny-Carman equation (4.5) can be used to calculate the Kozeny constant from the permeability measurements in FIG. 4.2. This has been done in FIG. 4.4 for the glass fiber, $B_o(\perp)$. The figure shows the rapid increase in the "constant" and the failure of the theory at high porosities. This phenomenon has been reported by many research workers, e.g. Lord (1955) found values varying from 5 to 25 when ε varied from 0.90 to 0.99. Kyan et al. (1970) made comparisons with the Kozeny theory and calculated values for the Kozeny constant, in a development of the drag theory. In the porosity range 0.90 to 0.99 the constant varied from about 5 to over 20. Other investigations have shown even higher values for the Kozeny constant at high porosities, cf. Carman (1956).

It is obvious that the theoretical considerations contain vague factors and it is likely that they can only render a qualitative description of the phenomena. The measured permeability values for the fiber materials will therefore be used as they are presented in FIG. 4.2. These results are in general confirmed by measurements upon similar materials by Fournier et al. (1967) and Höglund (1963) - though a permeability coefficient depending upon the viscosity of the fluid and its temperature was used (cf. equation (4.1)).

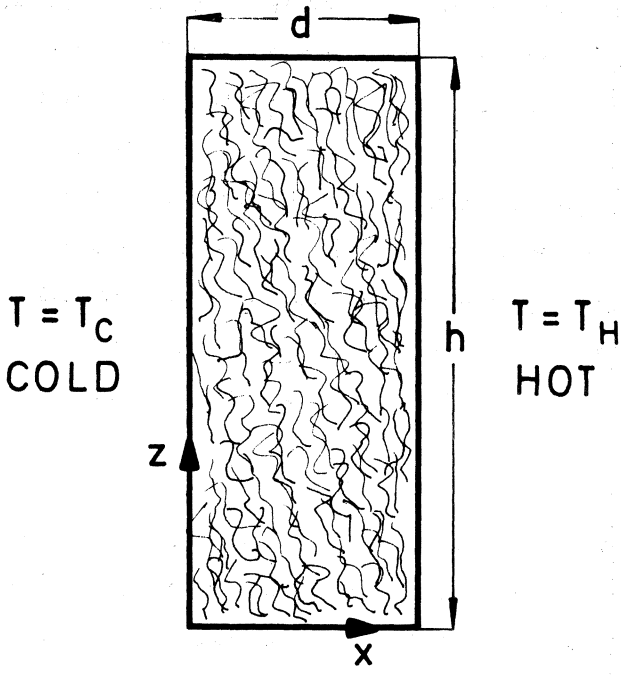

FIG. 5.1. Vertical permeable space notation.

5 NATURAL CONVECTION IN POROUS (FIBROUS) SPACE.

5.1 Introduction.

When a porous material is introduced as insulation in an uninsulated (air) space the resistance to air flow in the space will increase. The deformation of the temperature field due to gas flow will consequently be less pronounced. The behaviour of the space will then shift towards that of the solid structure with linear temperature gradient and constant heat flow at the isothermal boundaries. As was pointed out before, the air space represents one limiting case of the insulated space and the solid structure the other. The natural convection in the permeable insulation will therefore be investigated in much the same way as the air space. Since the research work in this field is considerably less conclusive and elaborate - as will be seen - the study will have to be made throughly, to yield useful results

5.2 Vertical space, theoretical background.

The natural convection in the vertical, insulated space is treated in two dimensions for stationary flow. The problem is defined in FIG. 5.1. The governing equations are with one notable exception largely the same as for the air space. The velocity of flow is governed by the Darcy relationship which leads to a simplification of the momentum equations. This means that to the previous assumptions about the convective flow in the air space is added the assumption that in the permeable space the damping force acting on the flow is of greater magnitude than the viscous force. This is a valid assumption in cases of natural convection where the flow velocity is moderate. The inclusion of the viscous force in the governing equations is quite possible but since this leads to a more laborious solution without increasing the accuracy - as will be shown in the following - there is no reason for doing so in this case.

The governing equations can be formulated as follows

continuity,

$$\frac{\partial u}{\partial x} + \frac{\partial w}{\partial z} = 0 \tag{5.1}$$

momentum,

$$u = -\frac{B_{ox}}{\eta}\frac{\partial p}{\partial x}$$

$$w = -\frac{B_{oz}}{\eta}\left(\frac{\partial p}{\partial z} - \beta\rho(T - T_m)g\right) \tag{5.2}$$

and energy,

$$(\rho C_p)_f\left(u\frac{\partial T}{\partial x} + w\frac{\partial T}{\partial z}\right) = \lambda_o\left(\frac{\partial^2 T}{\partial x^2} + \frac{\partial^2 T}{\partial z^2}\right) \tag{5.3}$$

B_{ox} and B_{oz} are the specific permeabilities of the material in the direction x and z, respectively. These directions correspond to the directions of the principal axis in the material. $(\rho C_p)_f$ denotes the heat capacity of the fluid, and the index f will be omitted in the following. λ_o is the thermal conductivity of the material at stagnant flow, i.e. when no convection is present.

The previous equations have to be combined with the appropriate boundary conditions and can then be simplified and made dimensionless in roughly the same way as for the air space. The following dimensionless entities are introduced

$$X = \frac{x}{d}$$

$$Z = \frac{z}{d} \tag{5.4}$$

the temperature function,

$$\theta = \frac{T - T_m}{\Delta T} \tag{5.5}$$

the stream function is defined by,

$$u = \frac{a_o}{d} \frac{\partial \psi}{\partial Z}$$

$$w = - \frac{a_o}{d} \frac{\partial \psi}{\partial X} \tag{5.6}$$

with

$$a_o = \frac{\lambda_o}{\rho C_p} \tag{5.7}$$

Derivation of the momentum equations and elimination of the pressure,

$$\frac{\eta}{B_{ox}} \frac{\partial u}{\partial z} = \frac{\eta}{B_{oz}} \frac{\partial w}{\partial x} - \rho \beta g \frac{\partial}{\partial x}(T - T_m) \tag{5.8}$$

insertion,

$$\frac{\eta}{B_{ox}} \frac{a_o}{d^2} \frac{\partial^2 \psi}{\partial Z^2} = - \frac{\eta}{B_{oz}} \frac{a_o}{d^2} \frac{\partial^2 \psi}{\partial X^2} - \rho g \beta \Delta T \frac{1}{d} \frac{\partial \theta}{\partial X} \tag{5.9}$$

For the sake of simplicity, it will be assumed that $B_{ox} \simeq B_{oz} = B_o$. The nondimensional momentum equation can now be formulated

$$-Ra_o \cdot \frac{\partial \theta}{\partial X} = \nabla^2 \psi \tag{5.10}$$

with

$$Ra_o = \frac{g \cdot \beta \cdot \Delta T \cdot d \cdot B_o}{\nu \cdot a_o} \tag{5.11}$$

The non-dimensional energy equation can be found directly by insertion

$$\frac{\partial \psi}{\partial Z} \frac{\partial \theta}{\partial X} - \frac{\partial \theta}{\partial Z} \frac{\partial \psi}{\partial X} = \nabla^2 \theta \tag{5.12}$$

Boundary conditions, containing the aspect ratio h/d and perhaps some other influencing factors, have to be added to these equations.

The introduction of appropriate non-dimensional variables has simplified the original equations into two relationships expressing the momentum and energy conservation of the system. Comparisons with the air space show that the greatest differences are to be found between the momentum-equations, as can be expected. The Rayleigh number used in the case of the air space has been modified and expresses the influence of the specific permeability of the material. The temperature field θ and the stream function ψ are thus determined by the modified Rayleigh number Ra_o and the aspect ratio h/d together with the boundary conditions.

The conventional Rayleigh number for the permeable space is - in analogy with the fluid space,

$$Ra = \frac{g\ \beta\ \Delta T\ d^3}{a_o\ \nu} \tag{5.13}$$

It is of interest to compare this with the modified Rayleigh number. This can be done by taking the ratio between them.

$$\frac{Ra_o}{Ra} = \frac{B_o}{d^2} = Da \tag{5.14}$$

Da is the Darcy number and expresses the modification of the Rayleigh number due to the permeability of the material in the space. If the viscous force is of the same magnitude as the damping force it is found that the solution depends upon Da and Ra, but not necessarily simply on the product $Ra \cdot Da = Ra_o$. The present problem, however, will be solved as stated above with the modified Rayleigh number Ra_o.

As in the case of the air space a modified Grashof number can be introduced

$$Gr_o = Ra_o/Pr = \frac{g \cdot \beta \cdot \Delta T \cdot d \cdot B_o}{\nu^2} \tag{5.15}$$

with

$$Pr = \frac{\nu}{a_o} \tag{5.16}$$

The heat transfer through the insulated space can be expressed in the same way as before, i.e.

$$\frac{\lambda_{cv}}{\lambda_o} = Nu = \frac{d}{h} \int_o^{h/d} \left(\frac{\partial\theta}{\partial X}\right)_{X=0} dZ \qquad (5.17)$$

λ_{cv} denotes the effective thermal conductivity of the material with convective flow. When no such flow is present, Nu equals one.

From the above it can generally be observed that

$$Nu = f(Ra_o, h/d) \qquad (5.18)$$

with the addition of the appropriate boundary conditions.

5.3 Vertical space, numerical solution and its verification.

The governing equations for the vertical space were solved primarily for the problem shown in FIG. 5.2. The insulated space is bounded horizontally with cross-bars, and above and below these bars are other insulated spaces. The calculations are made for the marked area in the figure, i.e. for one space and one bar. For known dimensions and known thermal conductivities of the insulation and the bar, the calculations are generally made with the assumption of isothermal vertical boundaries. It is quite possible, of course,to use any other boundary conditions specifying the temperature, heat flow and (or) the thermal conductivity of the surrounding structural parts.

The non-dimensional equations were solved numerically using a finite-differencing technique. The details of this solution and some investigations of its characteristics are given in the Appendix. In the following the numerical solution is used to compare theoretical calculations with earlier experiments. This is, however, a difficult task since in most cases all the relevant influencing factors have not been specified.

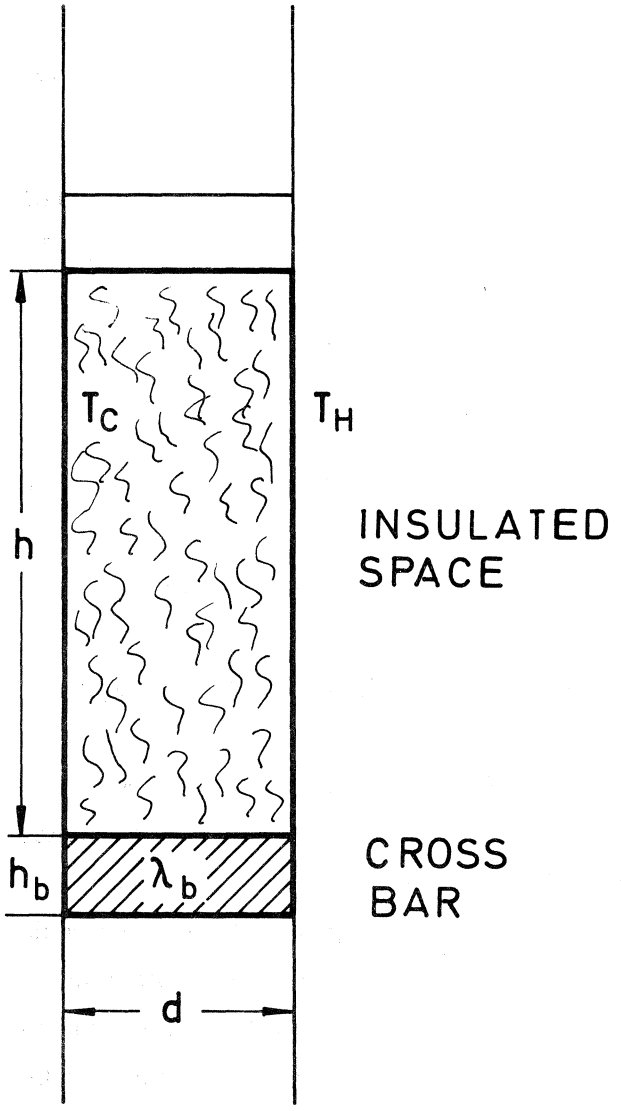

FIG. 5.2. Vertical permeable space, numerical problem.

One of the first and most stringent investigations of the convective heat transfer in the permeable space was that of Schneider (1963). He measured the thermal conductivity of granular materials using glass or steel spheres in water, turpentine, oil and air, respectively. The results were presented as $Nu = f(Ra_o)$ and are shown in FIG. 5.3. The measurements were performed in a guarded hot plate orientated vertically with the aspect ratio for the space 7.5. This information makes it possible to calculate the results theoretically as is indicated by the solid line in the figure.

Mordchelles-Regnier et al.(1969) and Klarsfeld (1970) presented optical studies of the temperature field in a vertical space with chlorobenzene and glass fibers. In FIG. 5.4 measurements by Klarsfeld have been compared to the theoretical calculations. Though there is some doubt as to the horizontal boundary conditions, they have in this case been assumed as insulated. Klarsfeld also presents a semi-empirical relationship between Nu and Ra_o and h/d. This relationship does not agree with the present theoretical solution.

The above indicates that the theoretical calculations agree well with the dependable experiments performed. This is further substantiated by the numerical investigation by Chan, Ivey and Barry (1970). Their calculations included viscous force and they discussed their solution in terms of Ra and Da values (cf. section 5.2). They solved the insulated horizontal boundary case and this solution agrees well with the simpler numerical solution presented here - this also is an indication that the viscous force can be neglected in the present study. The theoretical and the numerical model developed will therefore be used to describe the behaviour of the vertical permeable space.

5.4 Characteristics of natural convection, vertical space.

When a permeable insulation is introduced into an air space the convective flow in the space experiences a damping force from the material. It is therefore natural to expect a relation be-

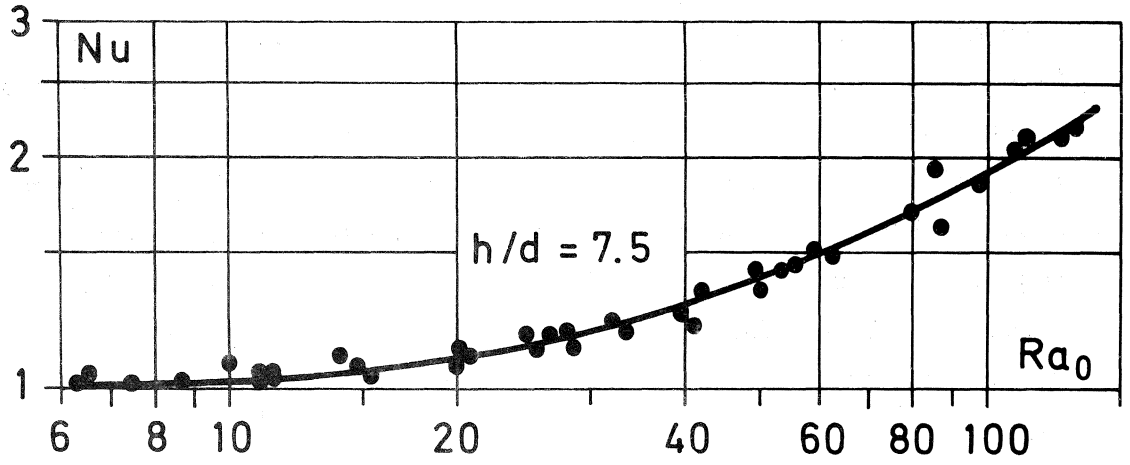

FIG. 5.3. Comparison between theoretical calculation and values measured by Schneider (1963).

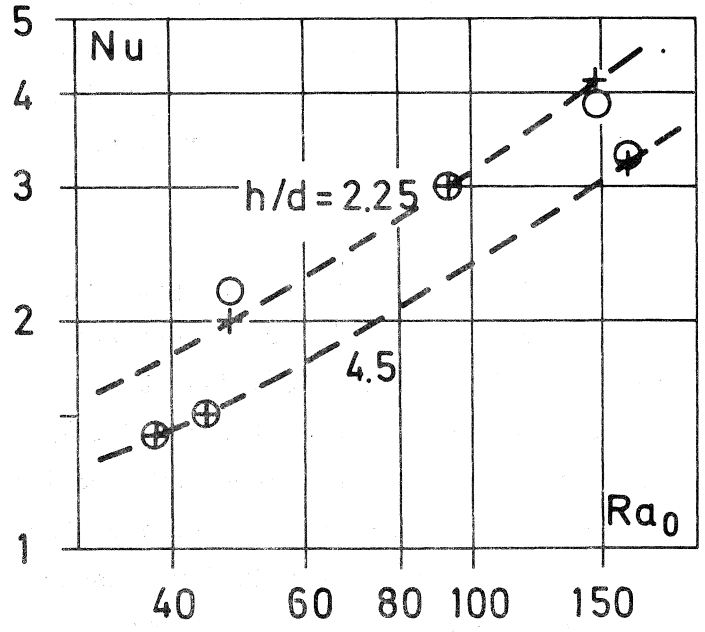

FIG:5.4. Comparison between theoretically calculated values (+) and values measured (o) by Klarsfeld (1970).

tween Nu and Ra_o in this space similar to that between Nu and Ra in the air space. This situation is roughly illustrated in FIG. 5.5 ($h/d \simeq 10$). The boundaries between the different types of flow are marked only tentatively. As for the air space the value of Ra_o, when one type of flow transforms into another type depends upon the aspect ratio. An increase of h/d generally leads to flow transformation at a higher value of Ra_o.

The factors influencing the natural convection in the vertical permeable space are the modified Rayleigh number, Ra_o, the aspect ratio h/d and the boundary conditions. These will be discussed for $Ra_o \lesssim 200$ since this value is well above the values found in applications in building physics.

The modified Rayleigh number Ra_o is defined by

$$Ra_o = \frac{g \cdot \beta \cdot \Delta T \cdot d \cdot B_o}{\nu \cdot a_o} \tag{5.19}$$

and in the case of an ideal gas (air) with $\beta = 1/T_m$

$$Ra_o = C_{air,o} \frac{d \cdot \Delta T \cdot B_o}{\lambda_o} \tag{5.20}$$

where

$$C_{air,o} = \frac{g \cdot \rho \cdot C_p}{\nu} \tag{5.21}$$

The coefficient $C_{air,o}$ depends solely upon the air, and varies with the mean temperature, as is shown in FIG. 5.6. From the standpoint of building physics it is obvious that the largest variations in the Ra_o-value are due to changes in ΔT, d or the choice of material, B_o and λ_o. In the same way as for the air space the air flow in the insulated space deforms the temperature field and for this reason alters the heat flow patterns at the vertical isothermal boundaries. The changes in the velocity, temperature and heat flow fields with increasing Ra_o-value are illustrated in FIG. 5.7-5.8. In these figures results from the computer are reproduced showing θ (indicated by T) varying from 0 to 1, ψ varying from 0 to about 10 and $10000 \cdot d\theta/dX$ (indicated by DT/DX). The Ra_o-values are 1 and 100, respectively, and the aspect ratio

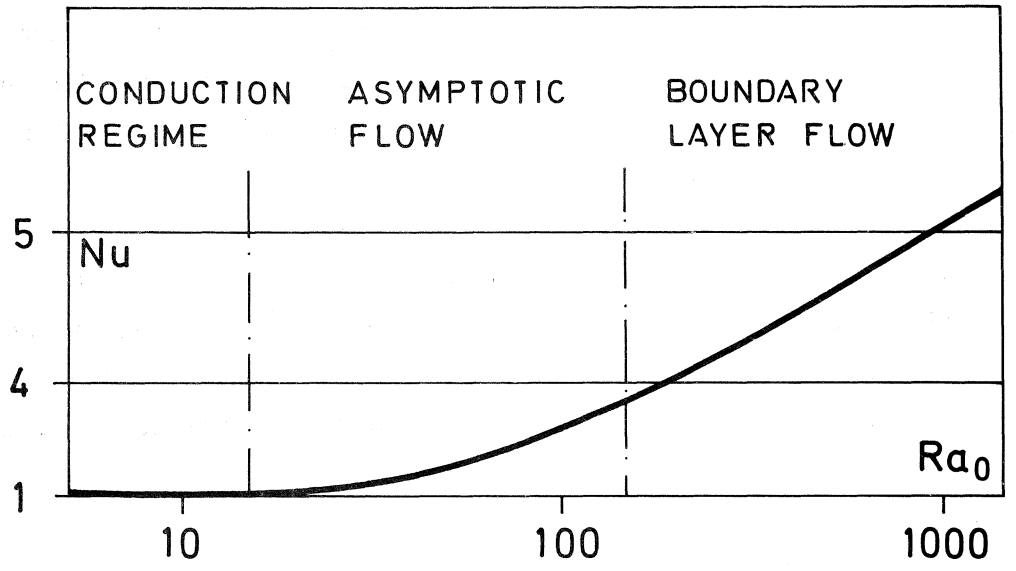

FIG. 5.5. Natural convective heat transfer in permeable vertical space (h/d ≈ 10).

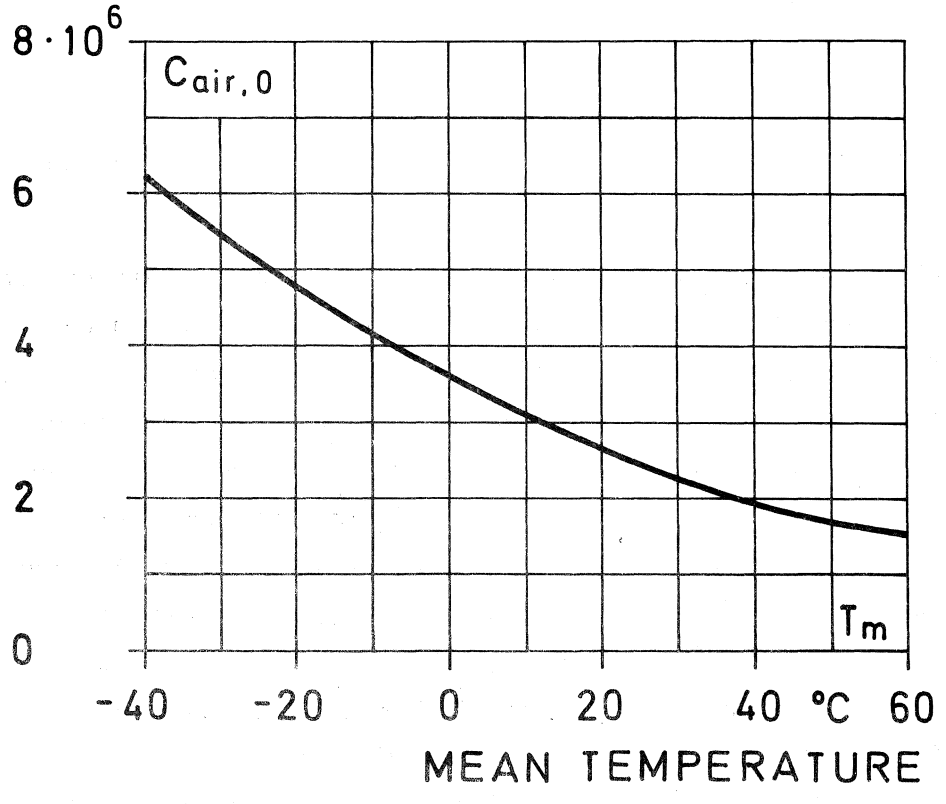

FIG. 5.6. Coefficient for calculation of Ra_o-value for a permeable space, $Ra_o = C_{air,o} \cdot \Delta T \cdot B_o \cdot d / \lambda_o$.

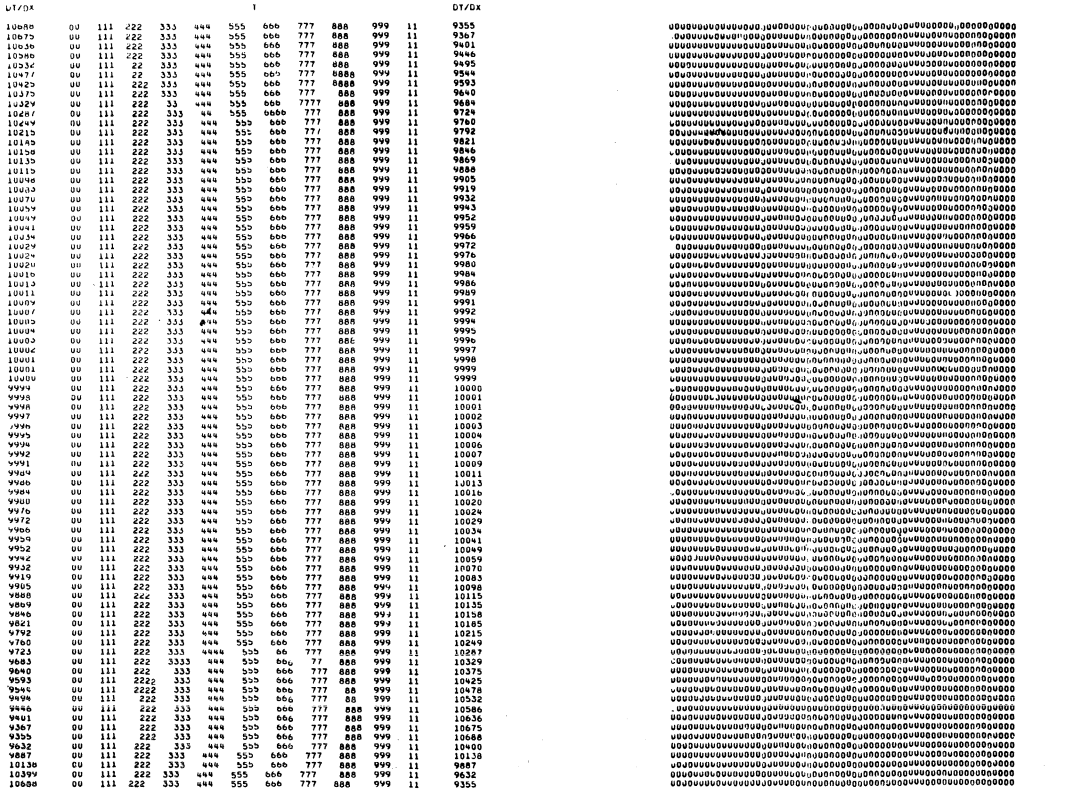

Ra = 1.0 Nu = 1.0

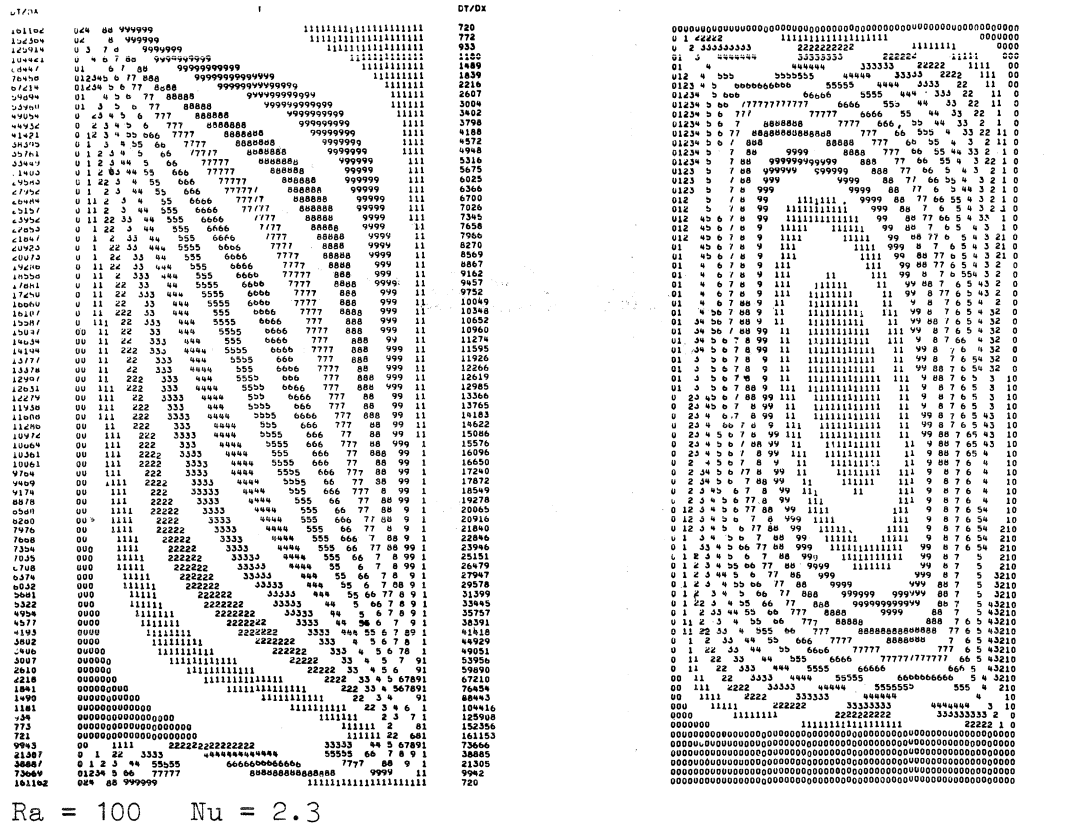

Ra = 100 Nu = 2.3

FIG. 5.7-5.8. Temperature field and streamfunction for permeable space with different Ra_o-value, h/d = 5.

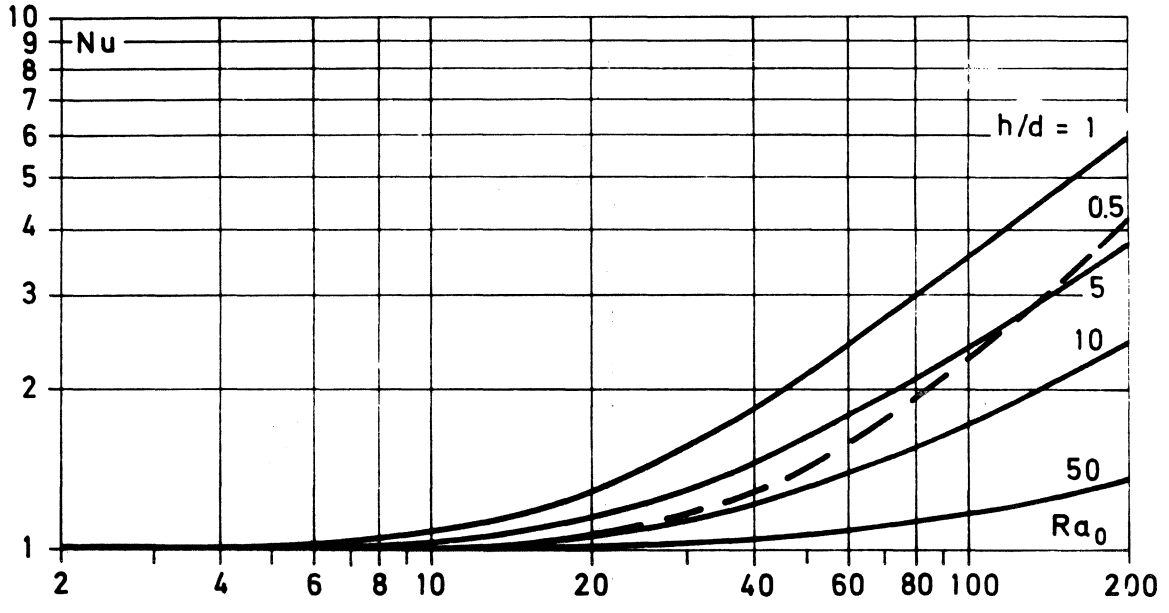

FIG. 5.9. Natural convective heat transfer in permeable space with isothermal vertical and insulated horizontal boundaries.

h/d = 5 with insulated horizontal boundaries. As the streamfunction develops, the temperature field is deformed and the heat flow through the bottom of the warm side and the top of the cold side is increased; the opposite is true at the top of the warm side and the bottom of the cold side. Calculations indicated velocities below 0.01 m/s. This is within the validity of the Darcy law and warrants the omission of the viscous force.

The influence of the aspect ratio h/d and the modified Rayleigh number on the convective heat transfer in the space is calculated in FIG. 5.9 for insulated horizontal boundaries. As could be expected, it is found that the heat transfer decreases as the aspect ratio increases. This phenomenon is explained by the convective flow from one vertical side to the other at the top and at the bottom of the space. In a space with large height this end region flow will influence a comparatively small part of the total space. If the aspect ratio on the other hand decreases below one the convective flow will be restricted and the convective heat transfer will diminish again. In this latter case, of course, the horizontal boundary conditions are of paramount importance. These changes in the flow and temperature fields are illustrated in FIG. 5.10-5.12, in the same manner as before. The variation in Nusselt number with h/d for a given Rayleigh number is illustrated in FIG. 5.13. Additional calculations have indicated a slight shift of the maximal value of the curve towards lower aspect ratio for increasing Ra_o-value.

In the previous theoretical calculations the horizontal boundaries have been considered as perfectly insulating. This has been done because this is the situation where the convective flow most influences the heat transfer. As the conductivity of the horizontal boundaries increases, the temperature field at the boundaries will restrict the deformation of the temperature field in the insulated space and reduce the convective flow. This is illustrated in FIG. 5.14 where the Nu-value is shown for given Ra_o-values as a function of the ratio between the thermal conductivity in the insulation and the horizontal crossbars. The different temperature fields in the limiting cases, the perfectly conducting and insulating horizontal boundaries, respectively,

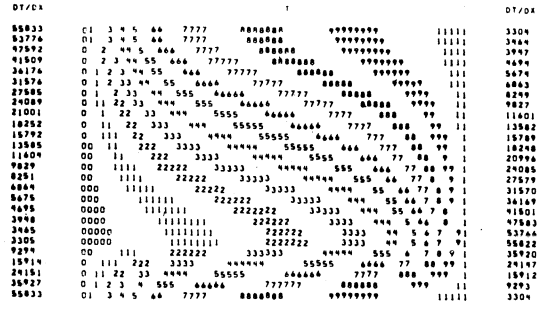

Ra = 50 h/d = 1 Nu = 2.0

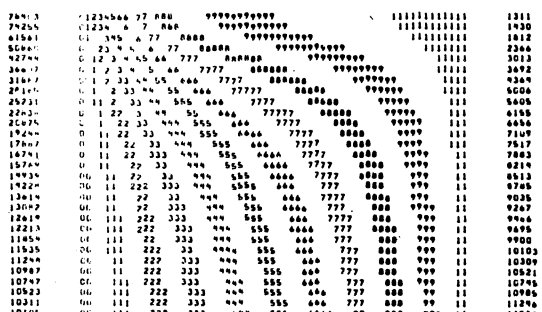

Ra = 50 h/d = 5 Nu = 1.6

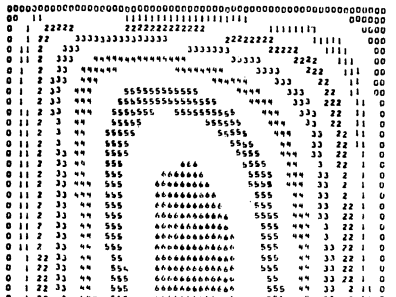

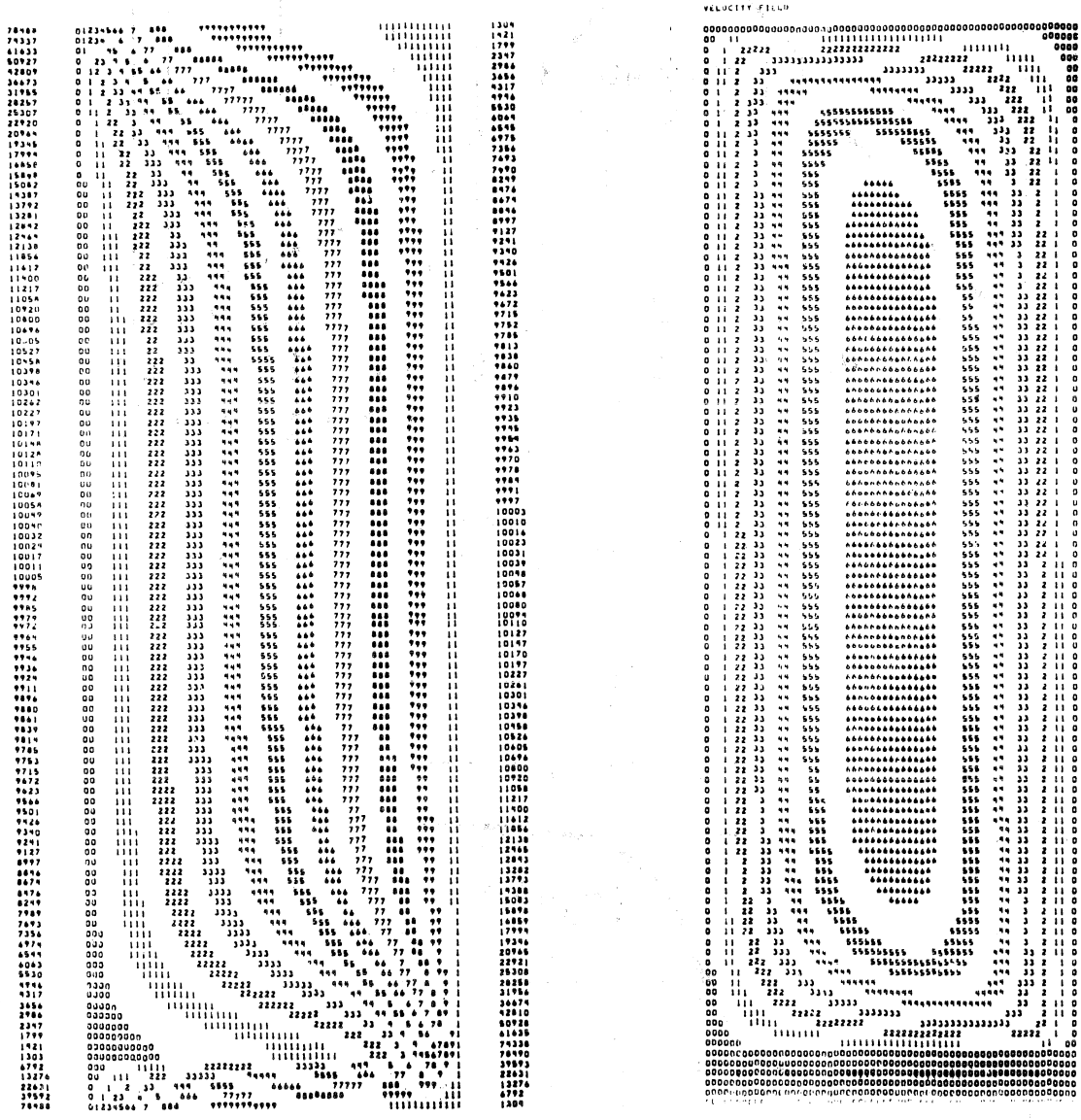

Ra = 50 h/d = 10 Nu = 1.3

FIG. 5.10-5.12. Temperature field and streamfunction for permeable space of different aspect ratio.

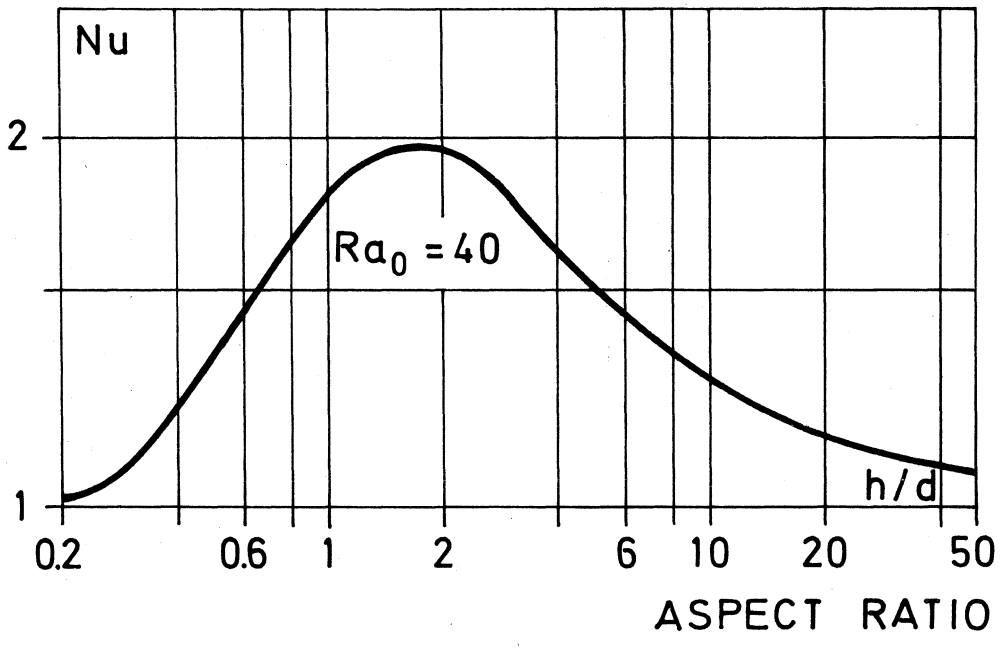

FIG. 5.13. The influence of aspect ratio upon the convective heat transfer in a vertical permeable space.

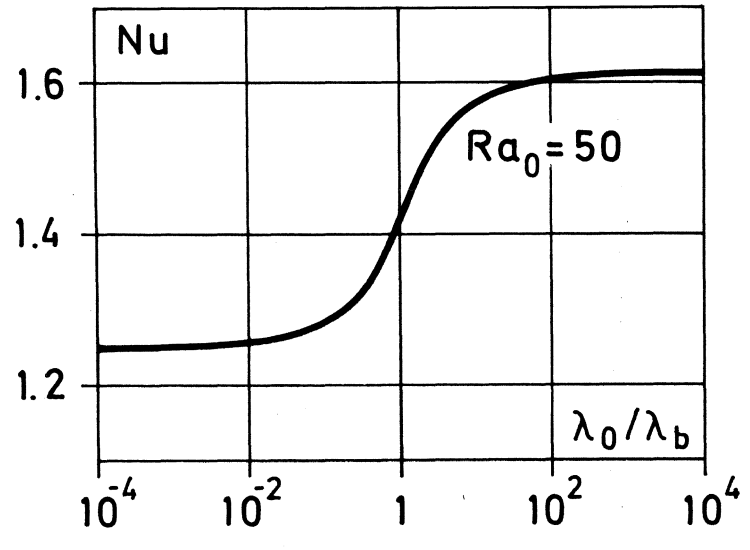

FIG. 5.14. The influence of thermal conductivity ratio upon the convective heat transfer in a vertical structure (0.5 × 0.10 insulated space and 0.05 × 0.10 crossbar).

are shown in FIG. 5.15 and 5.16. The former figure clearly shows the restriction of the temperature field deformation at the horizontal boundaries. The heat transfer in these cases is illustrated in FIG. 5.17 as a function of Ra_o for h/d = 1 and 10.

The vertical boundaries in the theoretical calculations have thus far been considered as having constant temperature. As was pointed out before, however, it is quite simple to assume any other temperature distribution on the boundaries. In FIG. 5.18 and 5.20 the vertical temperatures have been assumed to vary linearly over the height of the space with forty percent of the temperature difference. The horizontal boundaries have been assumed insulated. In FIG. 5.18 the temperature increases with the height. This situation leads to a further deformation in the convective temperature field and heat transfer increases as compared to constant temperature boundaries in FIG. 5.19. In FIG. 5.20 the situation is reversed.

From the above, it can generally be stated that the influence from the temperature boundary conditions, on the convective flow and heat transfer in the space, depends upon whether they restrict the convective flow deformation of the temperature field or not. This is actually self-evident.

It is obvious that, with the addition of the specific permeability, the same factors influence the permeable space as the air (fluid) space (cf. section 3.3). These factors and their interaction have presented considerable difficulties in many investigations. The natural convection phenomena have, under certain conditions, been observed in permeable materials by many research workers though few have realized the importance of all the influencing factors. Allcut (1951) observed convection in materials under increased pressure and this was also the subject of an investigation by Martin and Haselden (1963). They also noted the possibility of an aspect ratio giving maximal convection. Similar measurements were later performed by Baker and Haselden (1970) and Betbeder and Jolas (1972). Achtziger (1960) and Zehendner (1964) made measurements upon light mineral-wool insulations in guarded hot plates. Since their experiments were performed at low mean temperatures and high temperature differences they observed the influence of

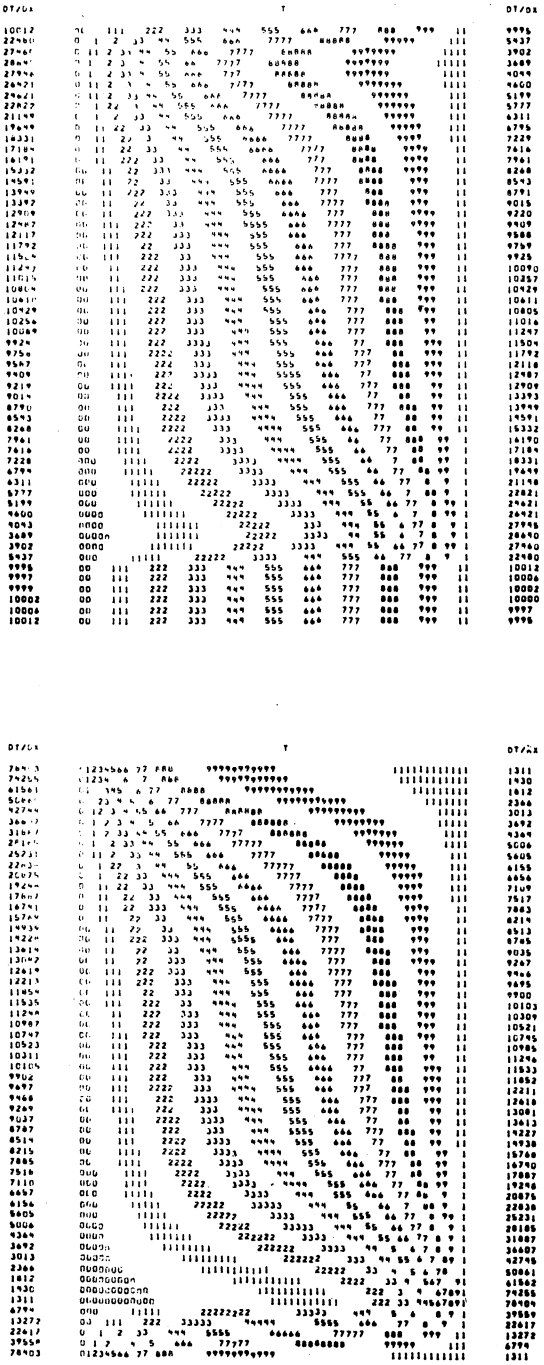

FIG. 5.15-5.16. Temperatur fields for conducting and insulating horizontal boundaries in the permeable space, Ra = 50, h/d = 5, Nu = 1.2 and 1.6 respectively.

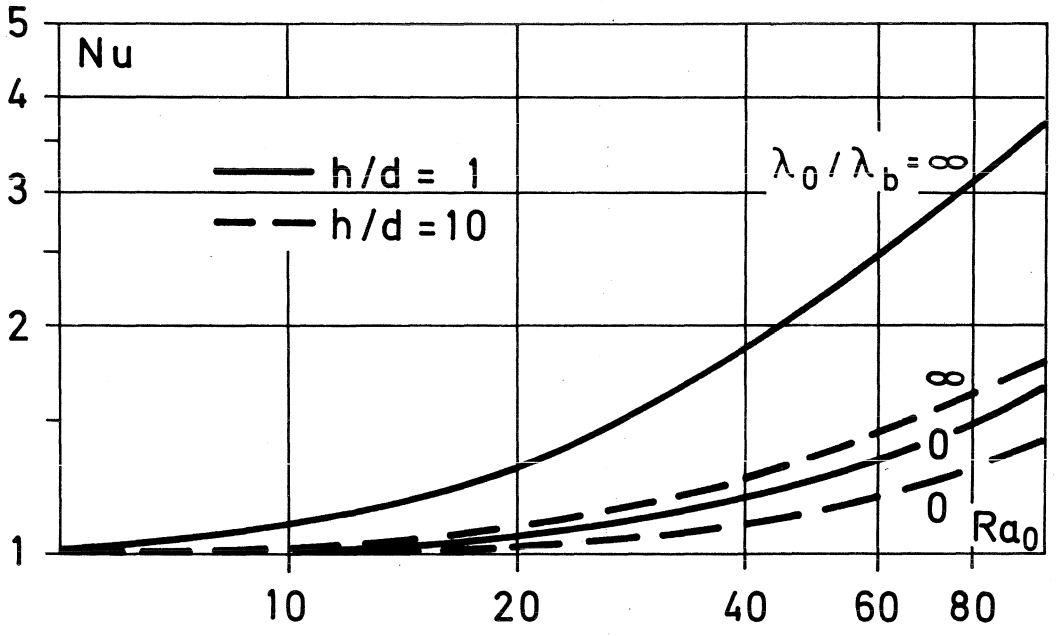

FIG. 5.17. The influence of horizontal boundary conditions on the convective heat transfer in the vertical space.

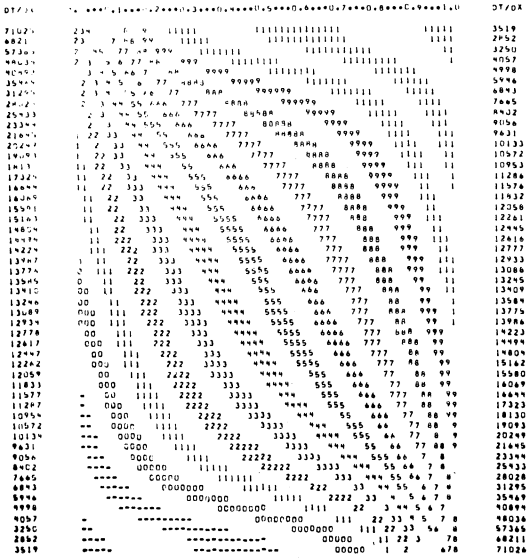

Linear increase with height of vertical boundary temperatures, Nu = 1.8.

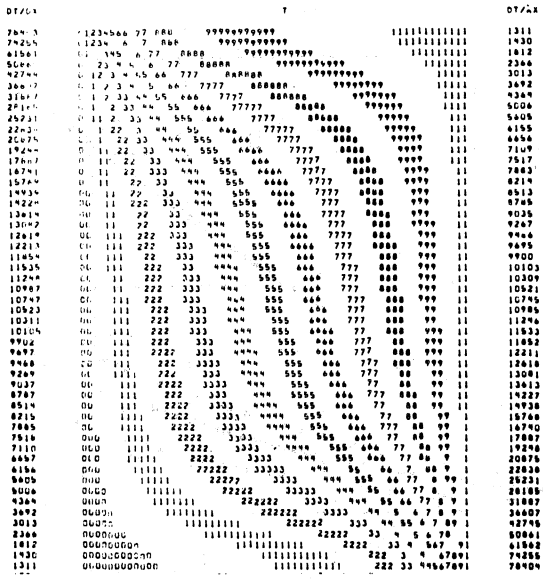

Isothermal vertical boundaries, Nu = 1.6.

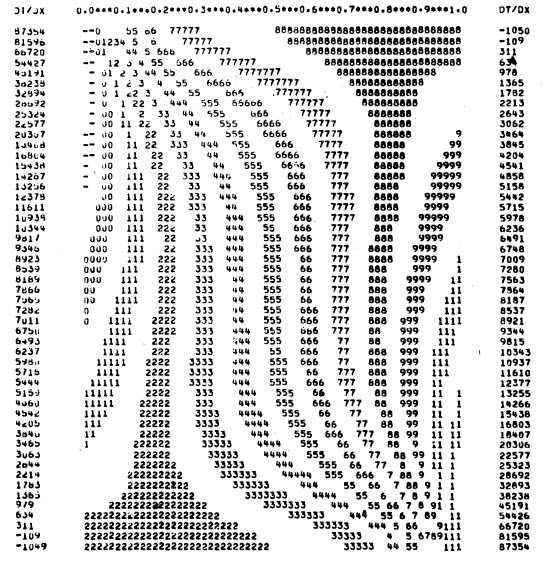

Linear decrease with height of vertical boundary temperatures, Nu = 1.5

FIG. 5.18-5.20. The influence from different vertical boundary conditions upon the convective heat transfer in the permeable space, Ra = 50, h/d = 5.

convection in accordance with the previous considerations in this section. To these additional references can also be added the special studies, with references to geothermal activities, made by Wooding (1958, 1960, 1962, 1963).

5.5 Horizontal space.

In the previous sections the natural convection in the vertical insulated space was treated in some detail. It is quite possible to calculate the convective heat transfer in the horizontal permeable space in the same way. In this case, however, extensive analytical and numerical calculations are available in the literature. The conditions of convection are also well established experimentally.

As in the case of the horizontal fluid space, it has been found that there exists a critical modified Rayleigh number value above which natural convection will be present in the space. For a space defined as in FIG. 5.21 the critical Ra_o-value is

$$Ra_o = \frac{g \cdot \beta \cdot \Delta T \cdot h \cdot B_o}{\nu \cdot a_o} = 4\,\pi^2 \qquad (5.22)$$

The breakdown of stability of a permeable horizontal space was discussed by Horton and Rogers (1945). Essentially the same linearized analytical approach was used as had earlier been used for fluid layers (cf. Section 3.4), but they did not use the modified thermal diffusivity a_o. This was also the case in the treatment by Lapwood (1948). Experimental verifications of the critical value for convection were therefore not very successful as performed by Morrison, Rogers and Horton (1949). Rogers and Morrison (1950), Rogers and Schilberg (1951) and Rogers (1953) extended the theoretical analysis but still used the thermal diffusivity a for the fluid. Wooding (1957) stated the governing equations using the modified thermal diffusivity a_o, and applied this in an analytical and numerical treatment of the temperature field in a geothermal area. The results were reported to be in fair agreement with measured temperatures (cf. references in Section 5.4 also). The experimental measurements by Schneider (1963) on

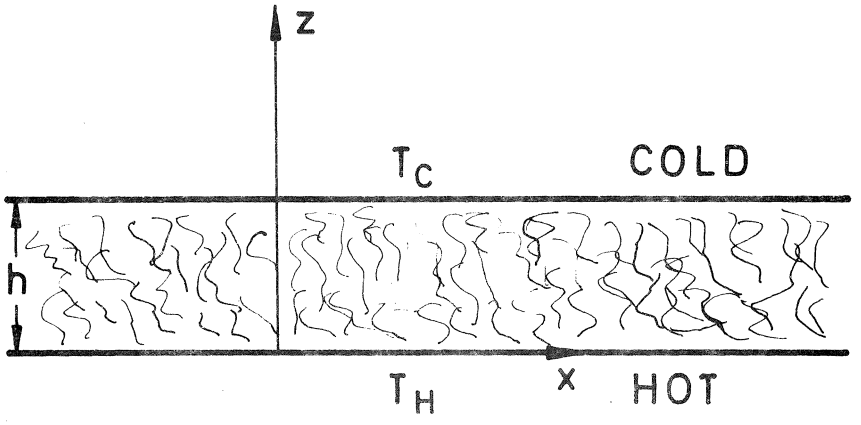

FIG. 5.21. Horizontal permeable space notation.

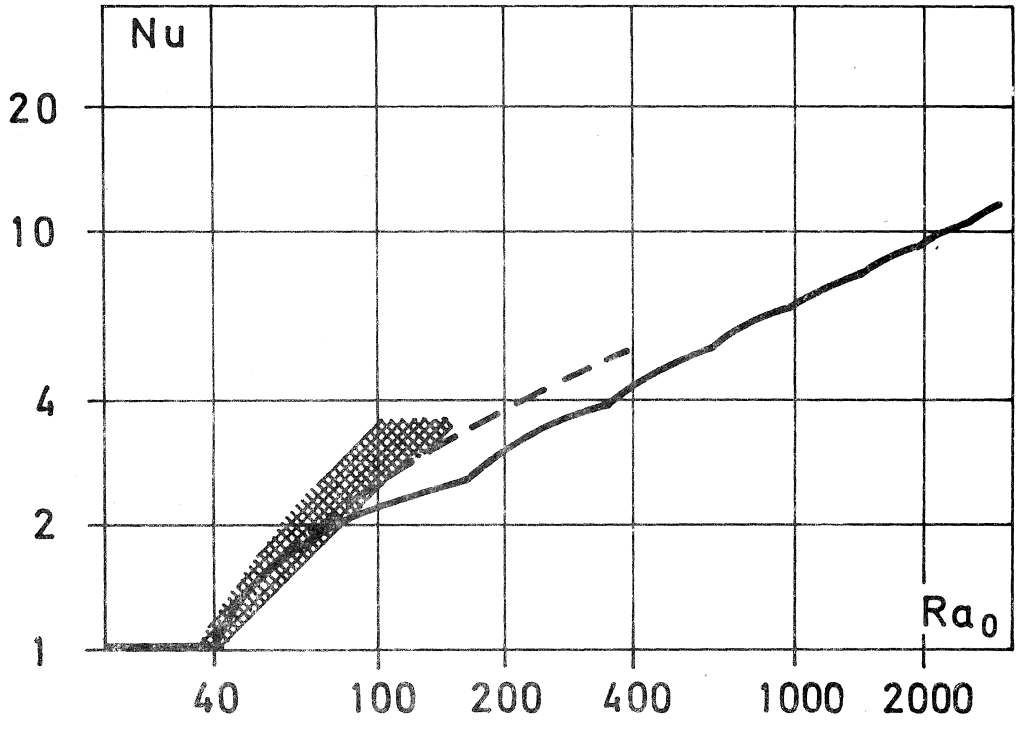

FIG. 5.22. Convective heat transfer in horizontal permeable space. Comparison between analytical results (- Aziz & Combarnous, 1970), numerical calculation (-- Combarnous, 1970) and experimental results (marked area, Schneider, 1963, Boires, 1970, and Combarnous, 1970).

granular materials clearly showed the existence of a critical $Ra_o \simeq 40$. His experiments also indicated that the a_o-value should be used. Katto and Masuoka (1967) measured the criterion for the onset of convective flow and verified the value $4\pi^2$. They also confirmed the importance of the modified thermal conductivity a_o, and so did Elder (1967) in his experiments and numerical calculations. Combarnous and Le Fur (1969) experimentally studied different modes of convection and also found the critical Ra_o-value $\simeq$ 40.

A criterion for the stability under arbitrary disturbances of the convective flow in a porous medium was considered by Westbrook (1969). His considerations also led to equations (5.22). In recent years several investigations have been published in this field. Aziz and Combarnous (1970) discussed the development of different convective modes in analogy with the fluid space considerations by Malkus and Veronis. The theoretical results deviated somewhat, however, from the experimental results at high Ra_o-value. This was also the case when comparisons were made with the numerical solution presented by Combarnous (1970), and Combarnous and Bia (1971). This situation is illustrated in FIG. 5.22. Boires (1970) made an analytical and experimental exposition of the natural convection phenomena in the horizontal permeable space. Combarnous and Aziz (1970) noted that, for insulating horizontal boundaries the critical Ra_o-value was reduced to less than half of that of the isothermal boundaries case. The transient three-dimensional natural convection in the horizontal space was discussed by Holst and Aziz (1972) and the influence of inclination from the horizontal upon the convective heat transfer was investigated by Boires and Monferran (1972). Analytical studies of the horizontal permeable space have been presented by Beck (1972) and Palm et al. (1972). The differences between the most recent presentations are generally the discussion of the higher convective modes and the influence of boundary conditions and three-dimensional flow. The critical value for natural convection is, however, well established.

The criterion for natural convection in an air filled permeable material is

$$Ra_o = C_{air,o} \frac{h \cdot \Delta T \cdot B_o}{\lambda_o} \geq 4\,\pi^2 \qquad (5.23)$$

The coefficient $C_{air,o}$ is given in FIG. 5.6 for different mean temperatures.

From the above it is obvious that, as in the case of the air space, the convective flow in the horizontal permeable space is phenomenologically slightly different from that in the vertical space. The important influencing factors in the horizontal case are included in the Ra_o-value.

6 EXPERIMENTAL INVESTIGATIONS.

6.1 Introduction.

The factors influencing the natural convection in an insulated structure have been established theoretically in the previous sections. In order to study these factors in applied building physics, two different types of experiments were undertaken. The behaviour of the horizontal space was investigated in a guarded hot plate apparatus and the behaviour of the vertical space was tested in an insulated wall structure. This choice of different experimental procedures in the two cases was based on the previous theoretical findings. Numerous measurements were made on the wall structure, in order to ascertain under what conditions natural convection can be found in a wall insulation.

6.2 Convective heat transfer through horizontal insulated space, investigated in a guarded hot plate apparatus.

In the horizontal insulated space, the aspect ratio h/d is generally small and the vertical boundary conditions are of little interest. The important factor is the modified Rayleigh number. Tests were therefore made in a one-sided, rotatable guarded hot plate apparatus. This unit has been described in a previous report (cf. Bankvall, 1972a), and consists basically of a hot and a cold plate. The test specimen is placed between the plates and its thermal conductivity is calculated from the measurement of heat flow and temperatures.

The thermal conductivity of the permeable horizontal space, was measured in the guarded hot plate as a function of temperature difference and heat flow orientation. Measurements were first performed on a light mineral wool with air, then the material was filled with water and a situation reached where the critical modified Rayleigh number was, according to the theoretical considerations, exceeded.

FIG. 6.1 illustrates the results from the measurements on the insulation with air. No indication of convective heat transfer

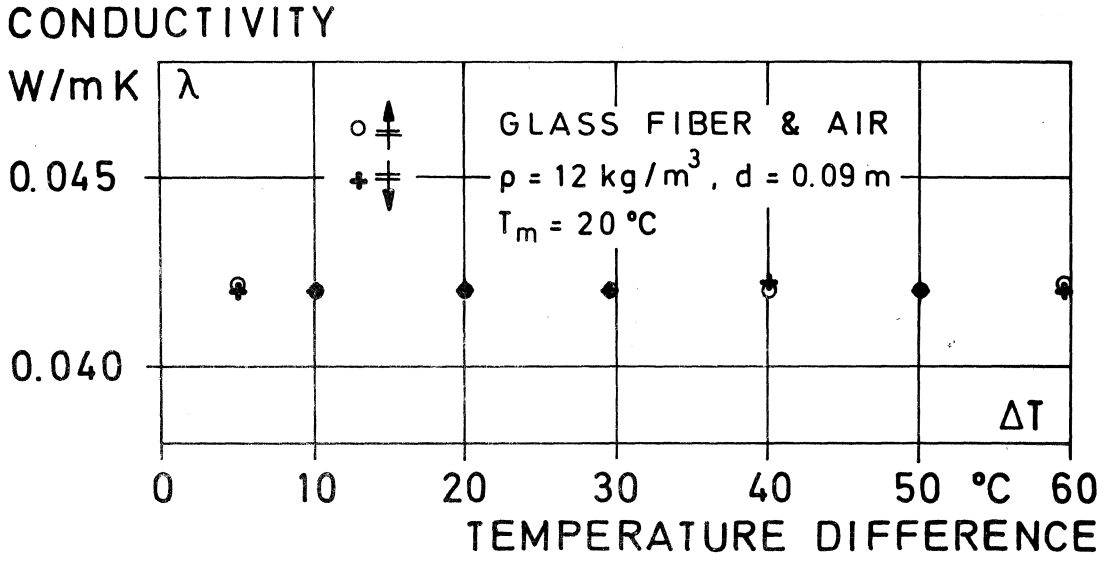

FIG. 6.1. The influence of temperature difference and heat flow direction on thermal conductivity of glass fiber insulated horizontal space. Guarded hot plate investigation.

was found. This is also predicted by the theoretical Ra_o-value, which, in this case, is 3 for $\Delta T = 60\ ^oC$. The case with the material saturated in water gave the results shown in FIG. 6.2 and 6.3. The variation in Nu-value from temperature difference and heat flow direction is illustrated in the first figure, in the second the Ra_o-values have been calculated. This figure shows that the Nu-value increases when the modified Rayleigh number exceeds a value of about 40. In these calculations, the specific permeability value parallel to the fiber planes has been used, $B_o(\parallel)$. If the other lower value, $B_o(\perp)$, is used, the critical modified Rayleigh number will be reached at about 30. Fournier and Klarsfeld (1970, 1971) found in similar measurements that the choice of $B_o(\parallel)$ agreed best with the theories. This was further confirmed in the recalculations they made of the measurements by Zehendner (1964) on mineral wool at low mean temperatures and with large temperature differences. Paljak (1969) presented measurements on mineral wool with different heat flow orientation. The Ra_o-value, calculated from the information found in the report, was $\simeq 1.5$. No indication of convective heat transfer was reported.

The above confirms the theoretical considerations concerning the convective heat flow in a horizontal permeable space. The existence of a critical Ra_o-value for this type of natural convection has been verified.

6.3 Convective heat transfer through vertical insulated space, the crossbar wall.

The convective heat flow in the vertical space is influenced by the modified Rayleigh number, the aspect ratio and the boundary conditions. In order to investigate this influence measurements were performed on a crossbar wall between a cold room and a warm room. The wall structure was 5.4 m high and 3.5 m wide. The crossbars of wood were covered with sheets of hard fiberboard. In this insulated structure, a space of 1.5×0.6 m was studied in detail. Different mineral wool insulations were used, glass fiber or diabase fiber. The density of the fibrous material varied from

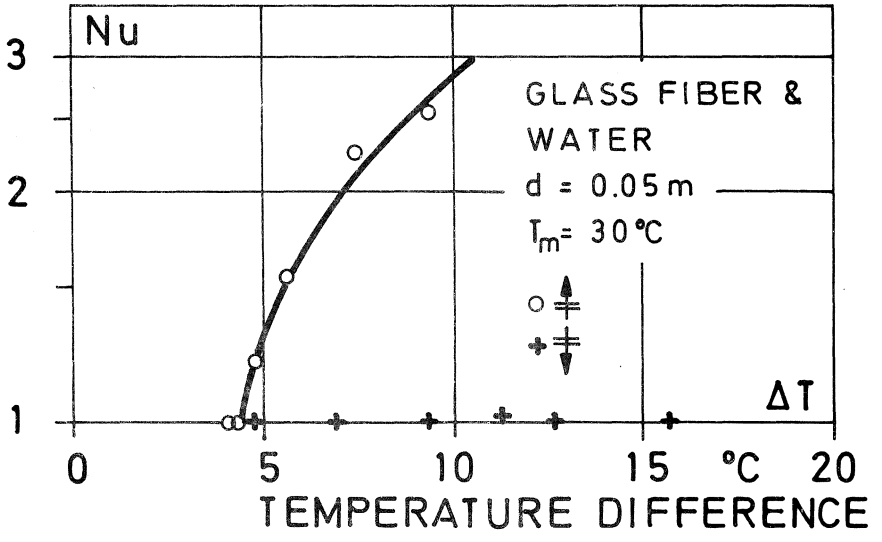

FIG. 6.2. The influence of temperature difference and direction of heat flow upon the convective heat transfer in a horizontal water filled, glass fiber insulated space. Guarded hot plate investigation.

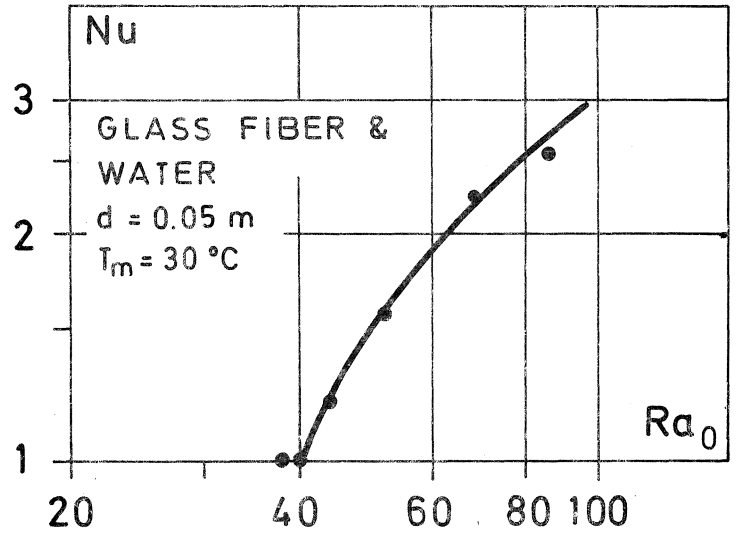

FIG. 6.3. The convective heat transfer values in FIG. 6.2 vs Ra_o-value

10 to 60 kg/m^3 and its thickness from 0.05 to 0.145 m. In some of the tests the insulated space was divided horizontally by insertion of thin fiberboards. The temperature at the warm side was +15 to +20 ^{o}C, while the cold side had a temperature between -25 and +5 ^{o}C in different measurements.

Measurements of temperatures and heat flows were taken during the investigations. The temperatures were measured on both sides of the covering fiberboards in all experiments. In some of the measurements on low density materials, the temperature field inside the insulation was also investigated. The heat flow was measured over the height of the space on the warm side as well as the cold side. FIG. 6.4 shows the placement of heat flow meters and thermocouples on the boards. "Inside" indicates the side turned towards the insulation. The two covering boards were identical. Details concerning measurement techniques and instrumentation are given in the Appendix.

In the theoretical considerations the interesting variables for the measurements have been pointed out. The influences from varying mean temperature, temperature difference and dimensions were therefore investigated for different insulations. The properties of the permeable materials, i.e. specific permeability and thermal conductivity, had been investigated in advance. The permeability measurements have already been described. The measurements of thermal conductivity, λ_o, were performed in the guarded hot plate for different densities and temperatures. The results of the measurements are shown in FIG. 6.5. These results have been recalculated in FIG. 6.6 to show the influence from mean temperature more clearly.

Detailed results of the measurements on the wall structure are given in diagrams in the Appendix. The heat flows measured over the height of the space and the temperatures measured at the surface of the insulation, i.e. the inside of the boards, are shown in these diagrams. Since the change of temperature horizontally over the boards was insignificant, the temperatures measured at the place corresponding to the center of the heat flow meters have been indicated. The effective thermal conductivity of the

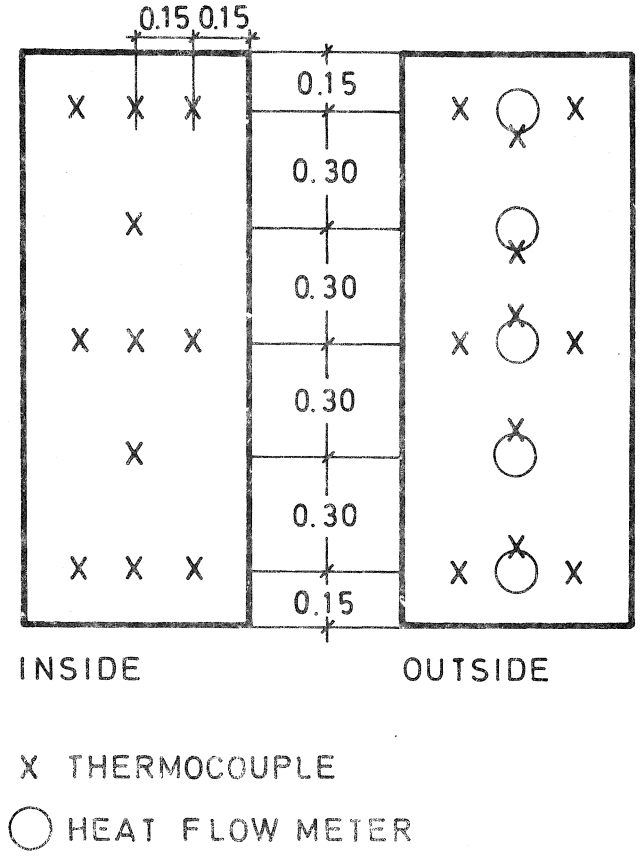

FIG. 6.4. Placement of heat flow meters and thermocouples on the (identical) covering boards. "Inside" indicates the side turned towards the insulation.

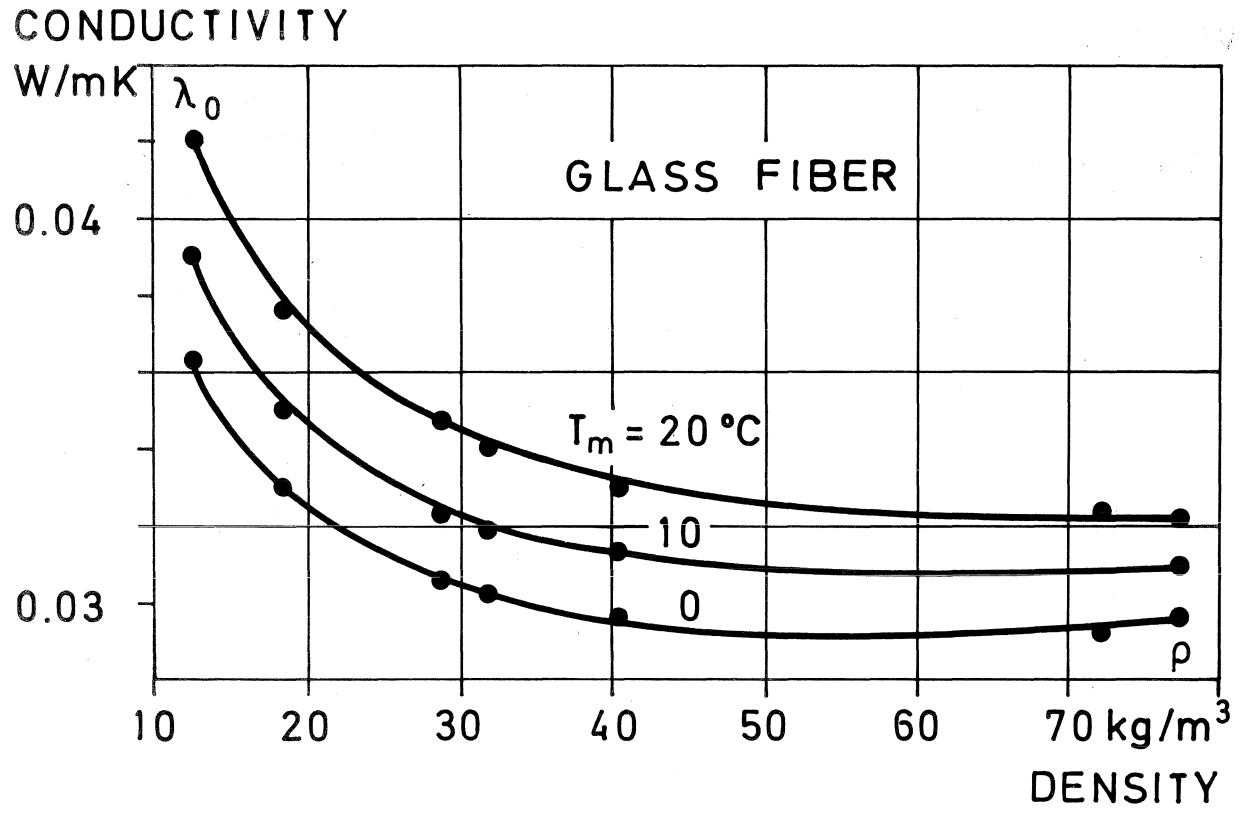

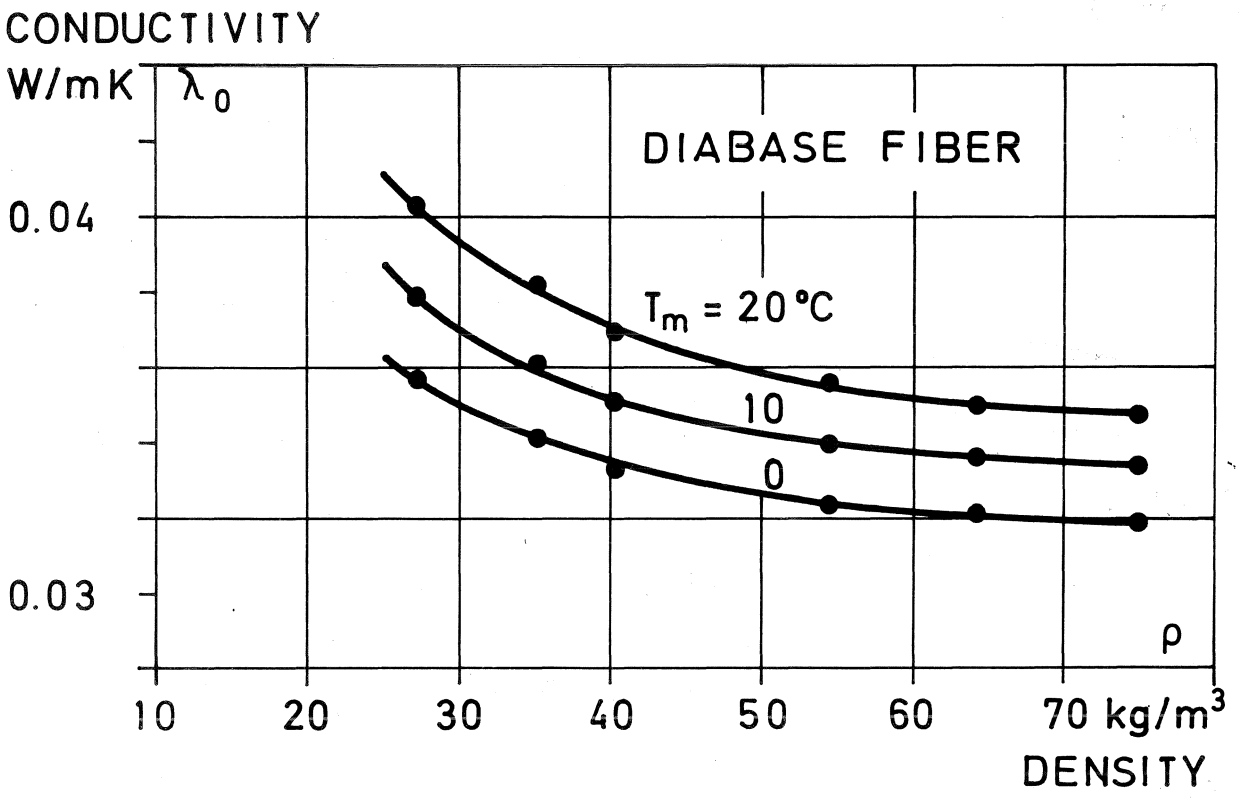

FIG. 6.5. Thermal conductivity, λ_o, measured in the guarded hot plate apparatus, for different densities and temperatures.

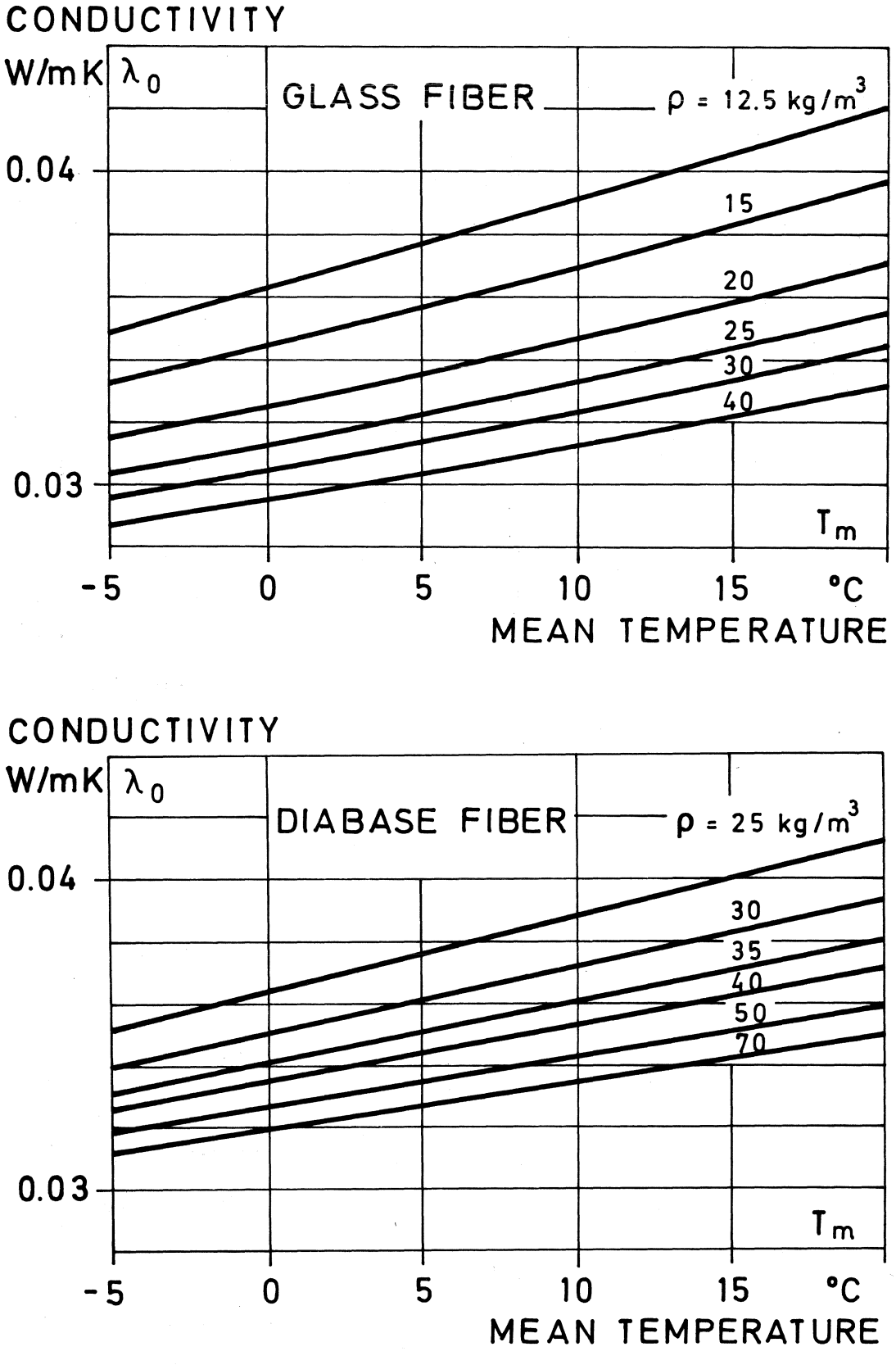

FIG. 6.6. Influence of mean temperature upon thermal conductivity, λ_o (from FIG. 6.5).

wall insulation was calculated from the mean of the heat flows and the mean of the temperature differences. The measured density of the insulation and its thickness together with the calculated thermal conductivity and the mean temperature are given in each diagram. In cases where the space was divided horizontally, this has been indicated by contineous lines. FIG. 6.7 shows examples of this. In the measurements on diabase fiber insulation, the space was divided with specimens of slightly different densities in the different sections. This was due to the fact that the commercially available dimensions for the material was 0.9×0.6 m.

From the wall measurements, it was possible to investigate the influencing factors characteristic for natural convection. An examination of the heat flows over the height of the space revealed no variations that were typical for natural convection. The same heat flow was generally measured on the warm as on the cold side at each height. To protect the heat flow meters from the direct and somewhat irregular cooling air flow on the cold side, an impermeable cover was errected outside the measuring area. This created a large air space with steady, regular air flow, gave stable readings from the heat flow meters, but led in some cases to a marked temperature variation over the height of the space. This did not, however, adversely influence the results. Calculations of the thermal conductivity at each height showed a variation in conductivity-value consistent with the simultaneous change in mean temperature.

The measurements of the temperatures inside some of the low density materials, did not reveal any distortions of the temperature field characteristic for natural convective air flow. These measurements, done with thermocouples inserted into the insulation, were, however, not accurate. In spite of careful installation and that the test specimen was cut to pieces after the test, it was difficult to establish the location of the measuring points accurately enough.

The influence of mean temperature upon the heat transfer in the insulated space is shown in FIG. 6.8. The ratio between the thermal conductivity measured in the wall insulation, λ, and measured in the guarded hot plate, λ_o, (from figures 6.5 and 6.6) is illustrated

DIABASE FIBER

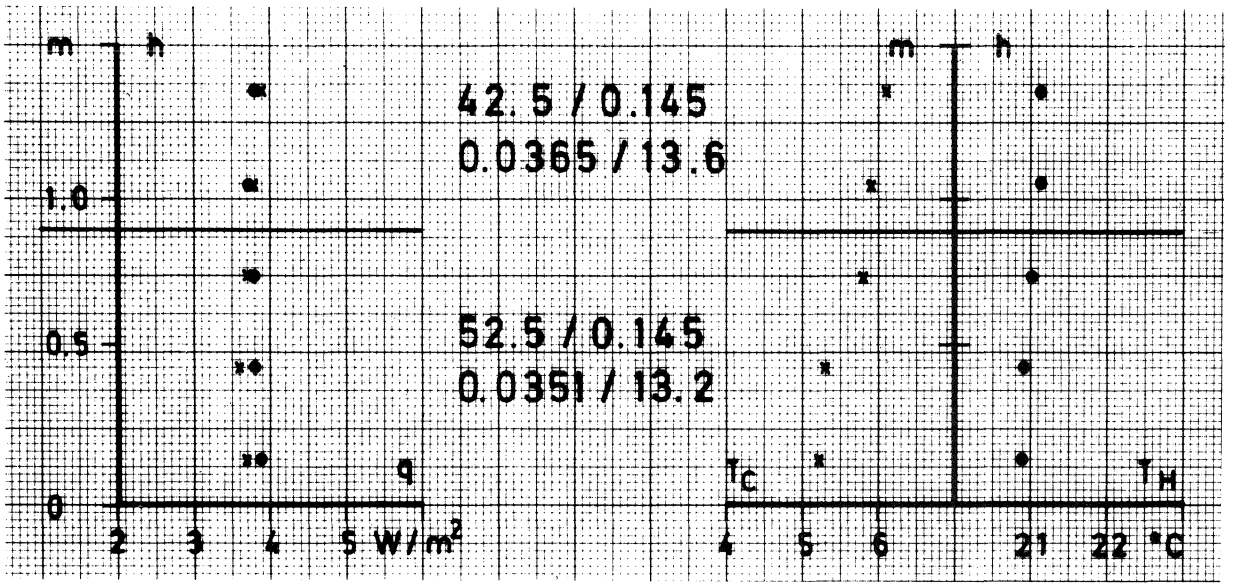

GLASS FIBER

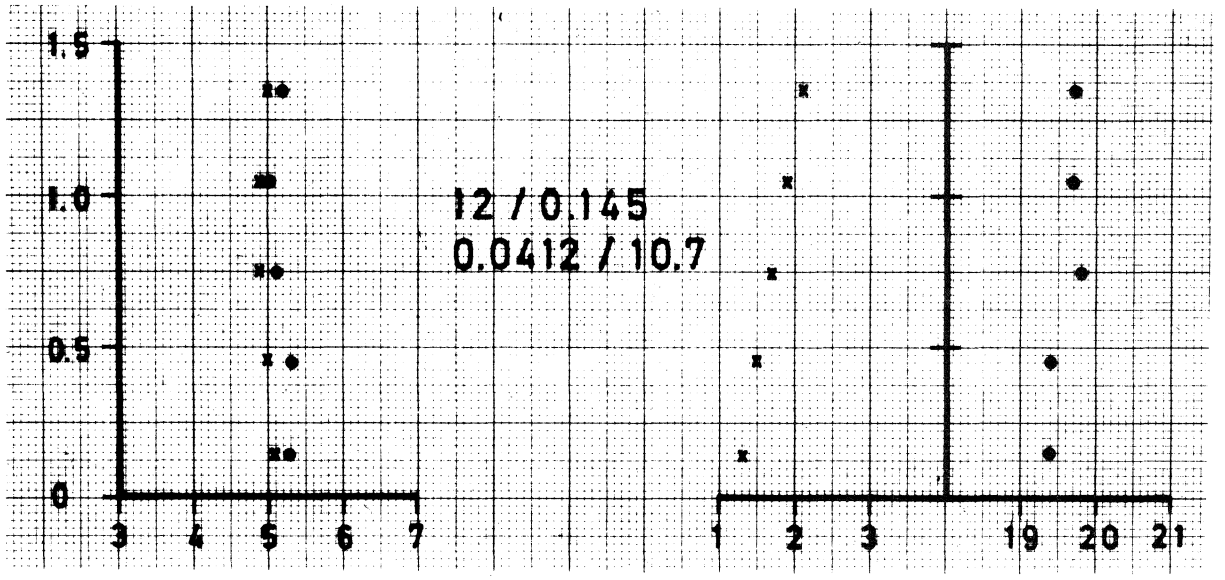

FIG. 6.7. Examples of measured results showing heat flows and surface temperatures over the height of the insulation. (x) indicates cold side and (•) warm side. Density/thickness and thermal conductivity/mean temperature are given in SI-units. In the upper diagram the space was divided and specimens of different densities were used.

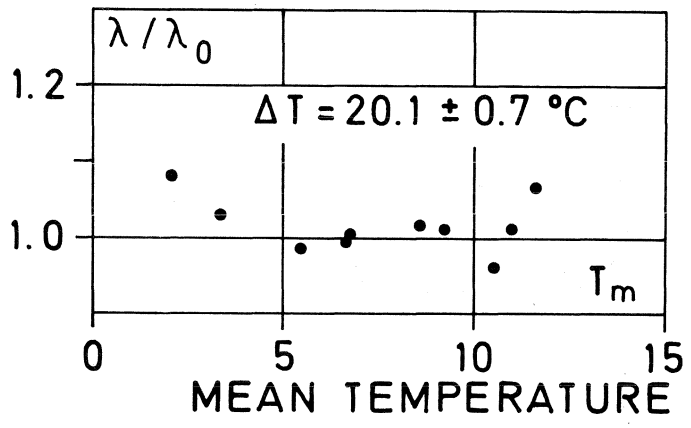

FIG. 6.8. Influence of mean temperature upon Nu-value ($= \lambda/\lambda_o$) measured in wall insulation.

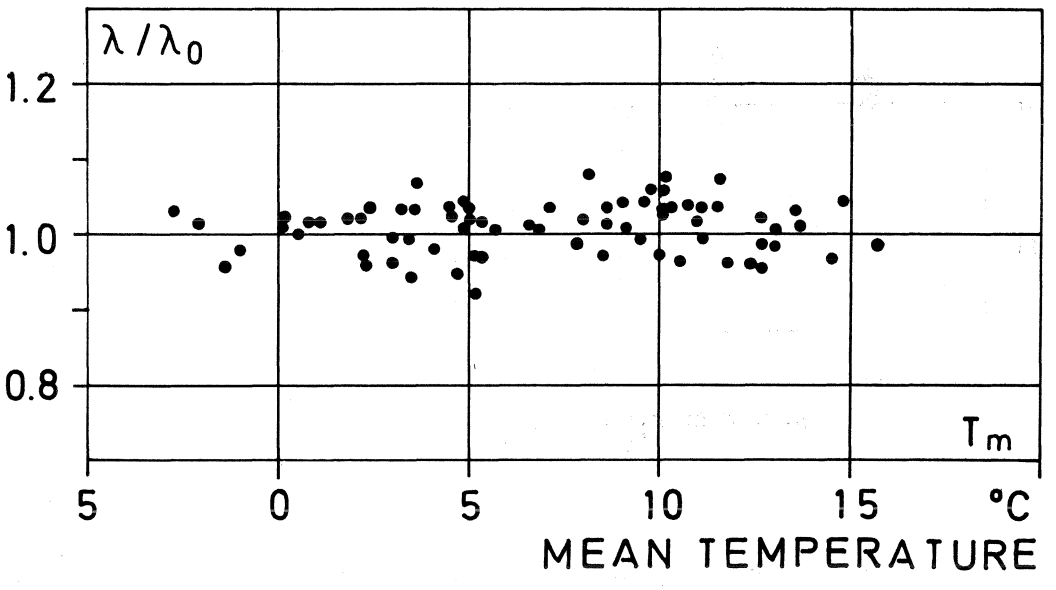

FIG. 6.9. Nu-value vs. mean temperature for all tests on vertical space, arbitrary temperature difference.

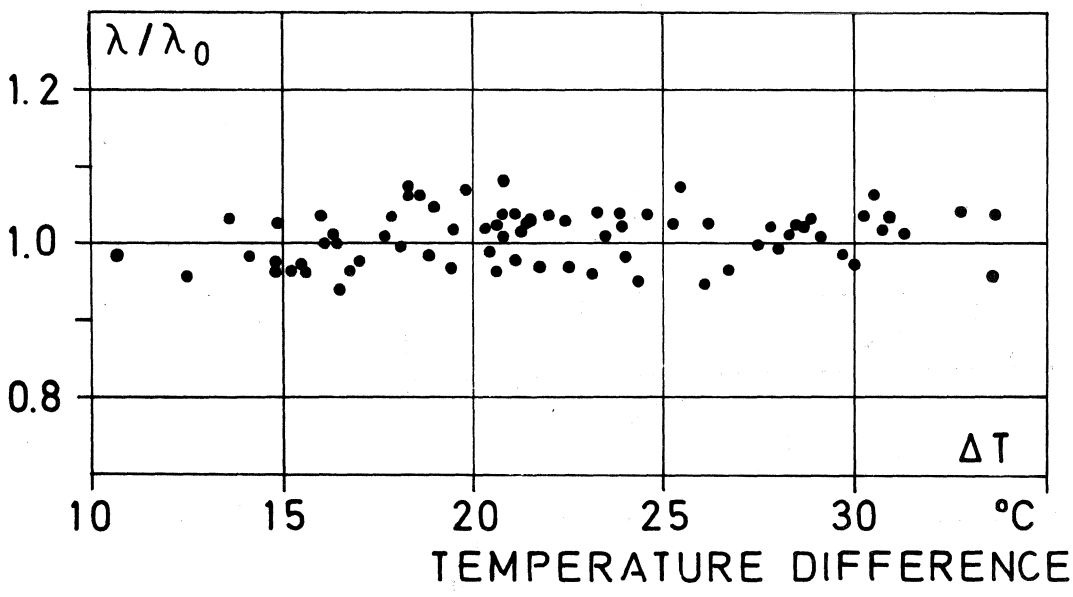

FIG. 6.10. Nu-value vs. temperature difference for all tests on vertical space, arbitrary mean temperature.

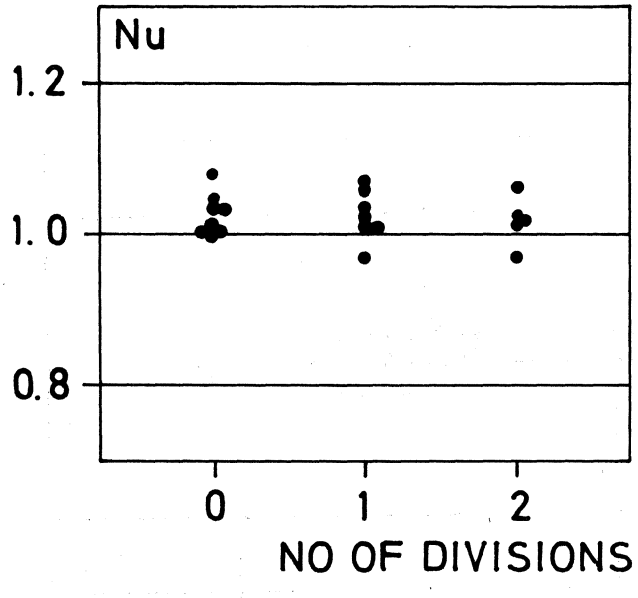

FIG. 6.11. The influence upon the Nu-value from dividing the insulated space horizontally.

for different mean temperatures. The variation of the temperature difference for these measurements was within ± 0.7 °C of the mean value. No significant influence upon the ratio, i.e. the Nu-value, from the mean temperature can be found. The slight variation in temperature difference, which was as a matter of fact completely arbitrary, does not alter this conclusion. A conservative estimation of the error in the measured λ-value indicates a maximal error of 9 %. In FIG. 6.9 all measurements upon wall insulation are shown as a function of mean temperature, regardless of the temperature difference. No significant regression line can be found, and the conductivity ratio, Nu, is represented by the entire mean value, which is $Nu = 1.0074$.

If the influence of temperature difference upon the Nu-value is illustrated instead, then the points are rearranged in another arbitrary pattern. This is shown in FIG. 6.10 regardless of mean temperature. The restricted possibility to change the temperature of the hot side of the insulated space, did, however, make it impossible to change the mean temperature and the temperature difference completely independently. In order to test whether any such simultaneous variation of the two variables could be found to influence the measurement results, a multiple regression analysis was made. A stepwise linear analysis (cf. Draper, N.R. & Smith, H., 1966) was performed on computer. No significant variables were found, which confirms the conclusion that neither the mean temperature nor the temperature difference influenced the Nu-value.

The influence of height, i.e. aspect ratio, upon the heat transfer in the insulated space was investigated by inserting horizontal partitions of fiberboard. A comparison between the undivided space and the divided space gives the results shown in FIG. 6.11. No significant change in the Nu-value can be detected, though these measurements were performed on the low density materials.

In a similar manner as before the influence of insulation thickness may be tested. This is illustrated in FIG. 6.12 for all the materials tested. It is found that this variable does not influence the Nu-value.

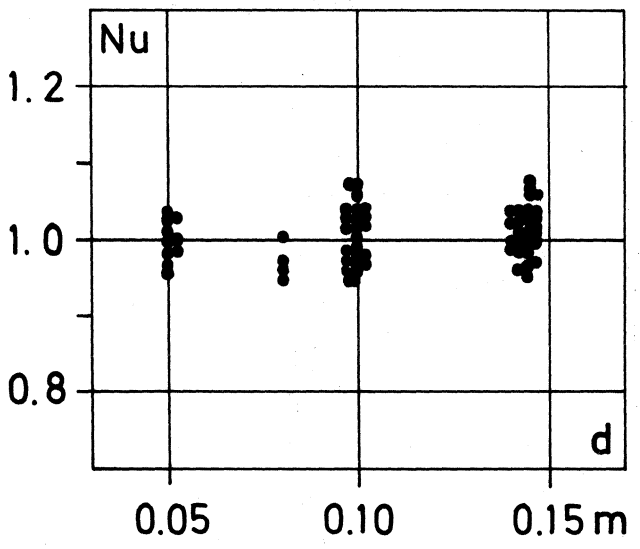

FIG. 6.12. The influence of thickness upon the convective heat transfer for all tests in the vertical space. The tested thicknesses were 0.05, 0.08, 0,10 and 0.145 m.

So far it has been found that neither the heat flow, the temperature field inside the insulation, the influences of mean temperature, temperature difference, aspect ratio nor the influence of insulation thickness do, in the measurements, indicate any noticeable heat transfer due to convective air flow in the permeable vertical space.

The specific permeability of the insulation and its thermal conductivity, λ_o, are closely related to the bulk density. A final comparison was therefore made between the thermal conductivity values measured in the guarded hot plate and in the wall structure for different insulations. The results of this are shown in FIG. 6.13, where all values from the wall measurements have been adjusted to a mean temperature of 10 °C. As is seen, the insulated space behaves as can be expected from the laboratory measurements in the guarded hot plate apparatus. A theoretical calculation of the modified Rayleigh-value in the most critical experimental case is of interest. This case is $d = 0.145$ m, $T_m = -3$ °C, $\Delta T = 35$ °C and $\rho = 12$ kg/m^3, i.e. $\lambda_o = 0.0355$ W/mK and $B_o(\,||\,) = 110 \cdot 10^{-10}$ m^2, which gives a Ra_o-value of 5. A comparison with FIG. 5.9 (on page 52) shows that this is theoretically not enough to give any appreciable convective influence on the heat transfer in the experiments, regardless of the aspect ratio. The boundary conditions in the wall structure will not alter this conclusion. The horizontal boundaries were not perfectly insulating, which will compensate for the vertical boundaries not being perfectly isothermal (cf. Section 5.4).

The Ra_o-values in the performed experiments were not sufficiently high to cause any appreciable convective heat transfer according to the theories. The experimental results show no indication of convective air flow in any of the factors influenced by such flow. The mean thermal conductivity ratio between wall and guarded hot plate measurements, λ/λ_o is as a matter of fact 1.0074, i.e. the measurements on the insulated vertical space are on an average less than 1 % higher than the guarded hot plate results.

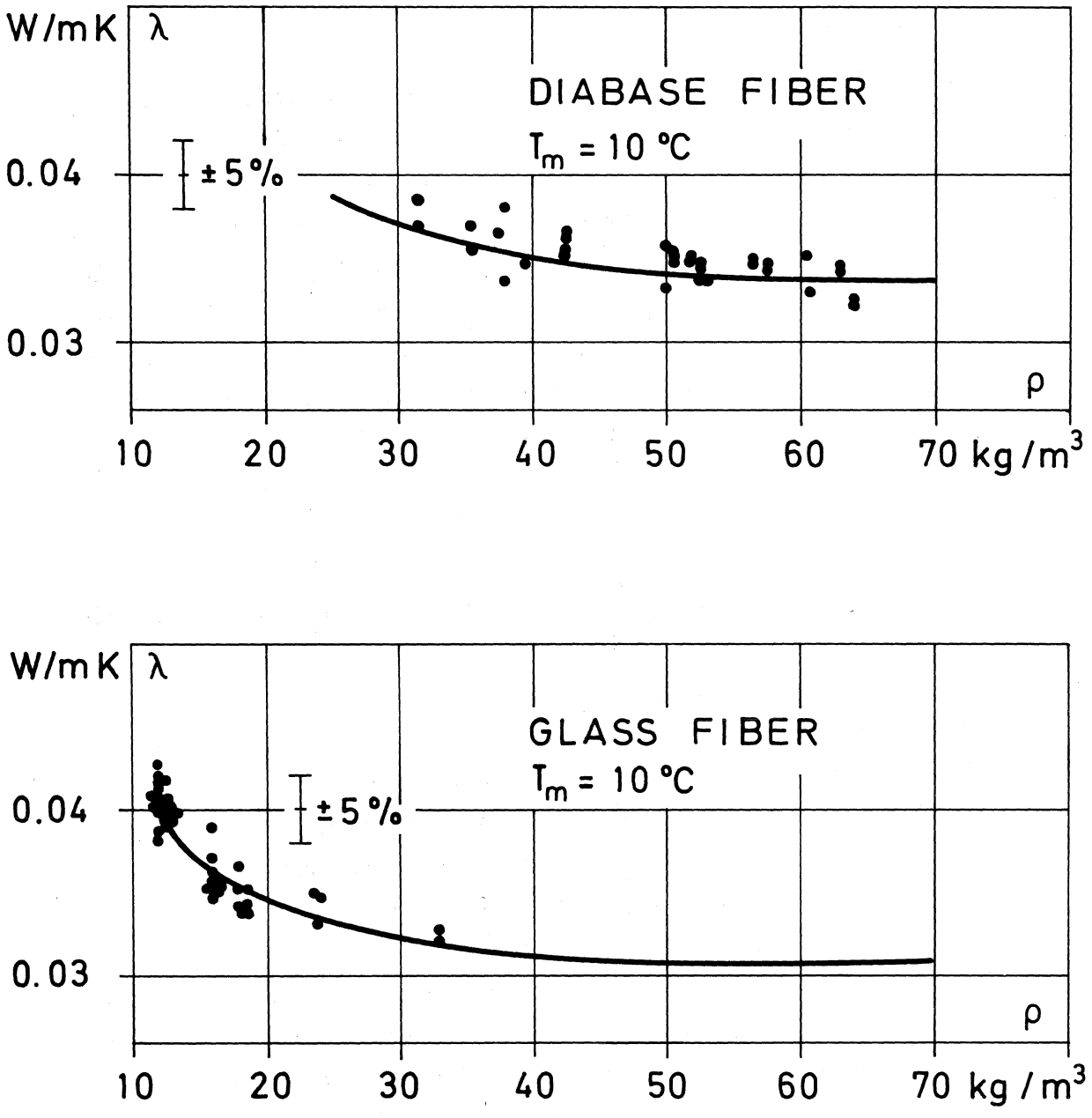

FIG. 6.13. Measurements of thermal conductivity on insulated walls (•) as compared to guarded hot plate results (—).

6.4 The insulation in combination with air spaces.

In normal building applications, there may be slits and openings between slabs of insulation if the insulating work is not carefully done. Also in this situation the limiting case is the air space, because this represents a case with no insulation at all. The opposite limit, of course, is when the insulation completely fills the space. This was the case in the previous sections.

It is difficult to evaluate the influence of slits and openings in an insulation, first because even when the number and dimension or these small air spaces are known, the situation presents a very extensive theoretical and calculatory problem, and secondly because the problem is seldom well defined, i.e. the number, size and location of the openings due to more or less careful insulation work differs, and are generally unknown. In this situation two questions are of interest for the insulating performances of the structure. The first is whether it is more difficult to achieve good workmanship with one material than with another. The second is whether the thermal performances of the material are influenced by the presence of small air spaces, e.g. if a material with high permeability is appreciably influenced by the convective air flow in the air space and thus gets an increase in thermal conductivity due to convection in part of the material.

Field investigations have shown that inferior workmanship can lead to openings going from the warm side to the cold side of an insulating space or to an air space between the insulation and one of the covering boards, or any arbitrary combination of these two alternatives, the latter generally being the case.

To what extent small air spaces or openings will influence the thermal conductivity of a permeable material is an interesting question from a physical stand point. Since it is difficult to solve this problem theoretically, a tentative experimental investigation was performed. In the wall structure a space with a thickness of 0.095 m and a surface area of 0.9×0.6 m was

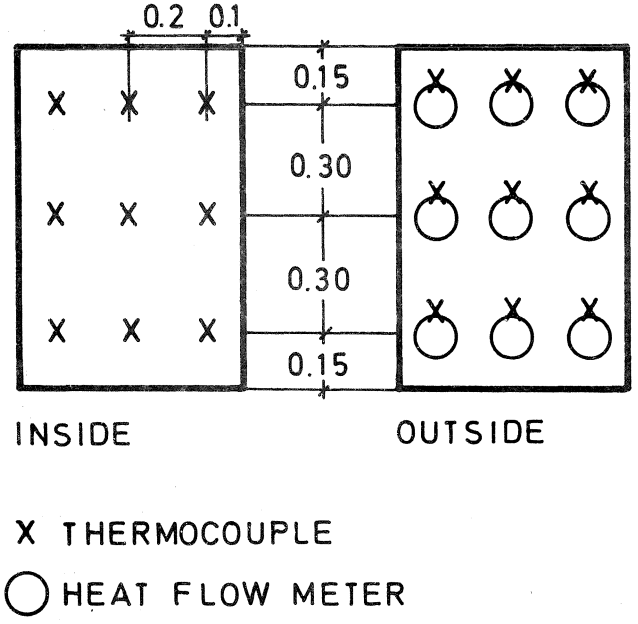

FIG. 6.14. Placement of thermocouples and heat flow meters on the two identical covering boards. "Inside" indicates the side turned towards the insulation.

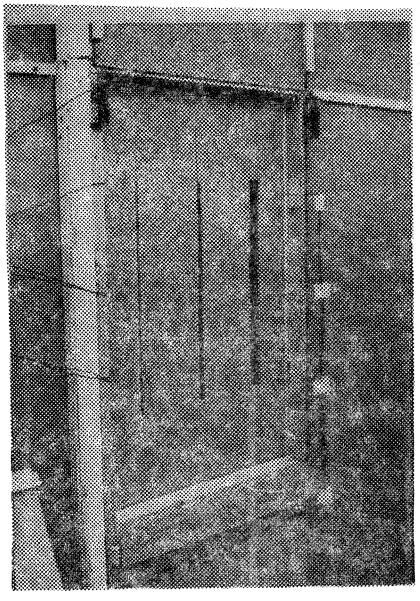

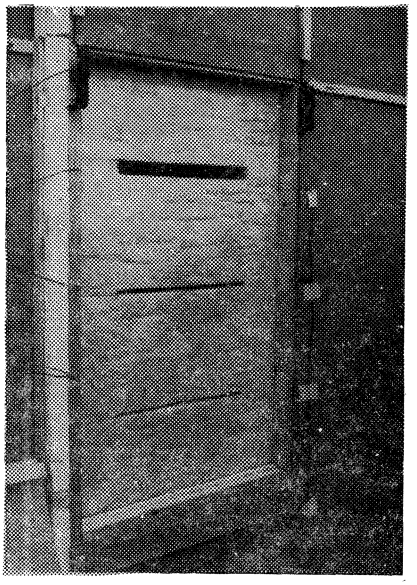

FIG. 6.15-6.16. Vertical and horizontal slits in the insulation. Viewed from cold side before the erection of the covering board.

studied in detail. This area was divided into nine parts. In each part the heat flow through the insulation and the temperatures at the surfaces of the insulation were measured. FIG. 6.14 shows the placement of heat flow meters and thermocouples on the covering boards. The two boards, on the warm and the cold side, respectively, were identical. "Inside" indicates the side turned towards the insulation. The temperatures measured on the inside of the boards, i.e. at the surface of the insulation, were used together with the mean of the heat flow values measured in each part of the insulated space to calculate the thermal resistance of that part. The instrumentation and measurement techniques, together with the detailed results, are given in the Appendix. The results are stated as thermal resistance and mean temperature in each part of the space. The temperature difference was between 19 and 24 ^{o}C in all measurements. The materials investigated were glass fiber, $\rho \simeq 17$ kg/m^3, diabase fiber, $\rho \simeq 46$ kg/m^3 and cellular plastic (expanded polystyrene), $\rho \simeq 15$ kg/m^3. The two mineral wool insulations had nearly the same thermal conductivity values, but the permeability of the glass fiber was more than twice that of the diabase. The permeablility of the cellular plastic of course was very small. This choice of materials was made in order to, under otherwise equal conditions, test the influence from small air spaces and different specific permeability upon the thermal conductivity of the insulation.

Three different series of tests were made, each beginning with a measurement of the completely insulated space. In the first series vertical slits were cut through the material. The slits were 5, 10 and 30 mm in width and the tops and bottoms of the slits were situated between a horizontal pair of a warm and a cold side heat flow meter. In this way, the heat flow in the end regions of the slit was measured together with a measurement in between. FIG. 6.15 shows a photograph of this situation taken from the cold side before the covering board has been erected. All three materials were tested in this way.

In the second series of tests, the slits were made horizontally but otherwise the same, as is shown in FIG. 6.16. The mineral

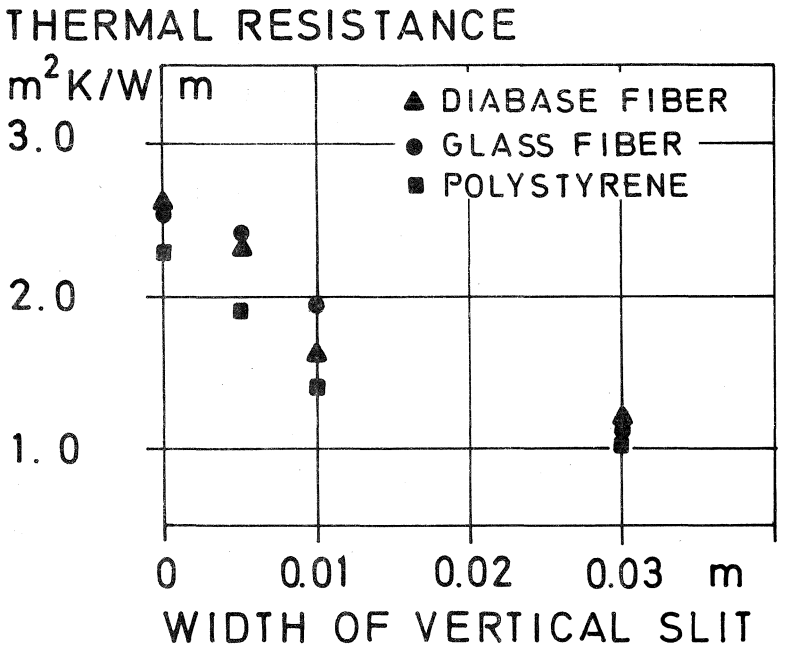

FIG. 6.17. The influence of width of vertical slit upon the measured thermal resistance.

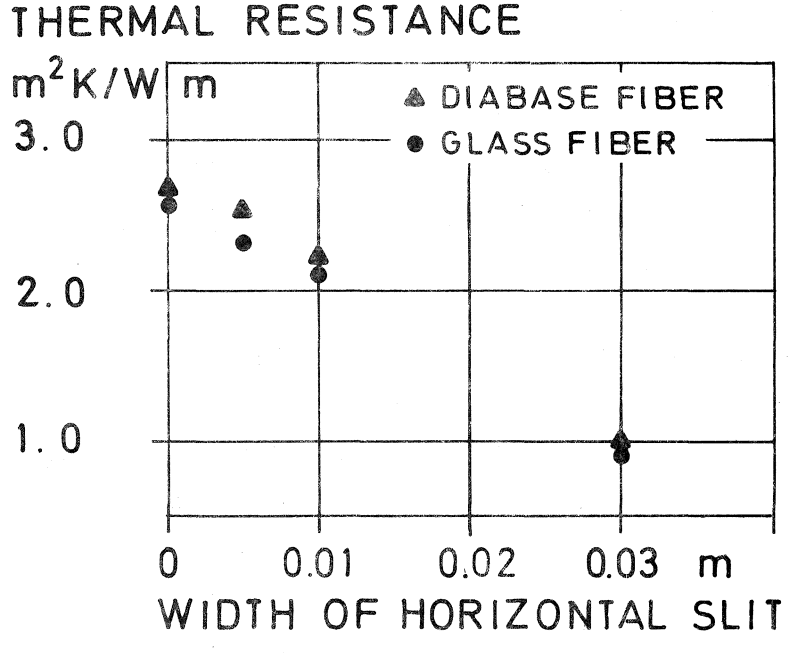

FIG. 6.18. The influence of width of horizontal slit upon the measured thermal resistance.

wool insulations were tested in this way.

The final series of tests was made with the space insulated with slabs of decreasing thickness, full thickness 0.095 m, 0.085 m, 0.07 m and finally only 0.045 m insulation on the warm side and a 0.05 m air space on the cold side. This was accomplished by sawing up the initial slab of insulation. All three types of insulation were tested.

The results from the measurements on the vertical slits are shown in FIG. 6.17, where the decrease in thermal resistance is given as a function of the width of the slit. It should be noted that these values are referred to the area covered by the heat flow meters (0.10 m diameter). In the case of the 30 mm slit, it is not unlikely that the three-dimensional heat flow around the slit will also distort the isotherms outside the measured area. Since a theoretical evaluation is difficult, the measurements are only used to note that in spite of the large differences in specific permeability in the materials tested, the decrease in thermal resistance due to vertical slits is roughly the same. The measurements on the horizontal slits gave results as shown in FIG. 6.18. It is also evident in this case that the permeability of the material is of no importance under the conditions of measurement.

The thermal resistance of the space when the insulation in it was combined with an air space on the cold side is illustrated in FIG. 6.19. In this case, the combination of air space and insulation can easily be calculated theoretically. This calculation agrees very well with the measured values and no influence from the specific permeability of the material can be found.

In practical applications, of course, different types of slits and openings are combined. Investigations at building sites have shown good insulation installations combined with examples of widely varying inferior work. Laboratory measurements, at the Lund Institute of Technology, have shown that inferior insulation work may considerably reduce the thermal resistance

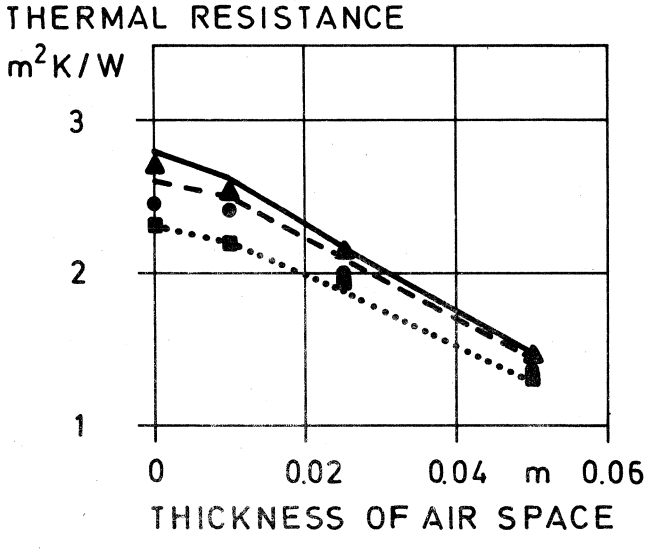

FIG. 6.19. The influence of an air space on the cold side in the insulated space (total thickness 0.095 m). The lines connect theoretically calculated values and the points indicate measured results; - ▲ diabase fiber, -- ● glass fiber and ····■ cellular plastic.

of a space, to what extent being entirely dependent on the arbitrary workmanship in the actual case. The simplest solution to these problems is, of course, a careful installation of the insulation.

6.5 Measurements on insulated structures in the literature.

Measurements on insulated structures are numerous in the literature. In some cases, the influence of natural convection has been reported, but in others, not. This can partly be attributed to an insufficient theoretical background, which has obscured the important influencing factors. In many cases, however, the basic mechanisms of heat transfer in a permeable material have been misinterpreted. Heat transfer due to radiation has been attributed to convection etc.. This situation has been discussed before (Bankvall, 1972b). In the following, only investigations on insulated structures will be considered.

The influence from natural convection on insulated structures has generally been indicated when air spaces have been included in the structure, or when the temperature conditions have been exceptional, e.g. in cold storage insulations.

Wilkes and Vianey (1943) reported on effects of convection in ceiling insulations. Though their results included the cross-bars in their test section, the values found for unprotected loose fill mineral wool indicated an influence from convection., Depending upon the permeability of the insulation, which was not given in the report, the Ra_o-value in the tests may exceed the critical value, especially since a free upper surface can indicate a lower value of this kind than in the enclosed horizontal space. Many investigations on insulated walls including air spaces have treated the installation of a permeable foil- or paper-enclosed material in the space. These investigations have shown the importance of sealing the insulation blankets to the surrounding structural parts so as to prevent air circulation round the insulation (cf. Handegord & Hutcheon 1952, 1953, Robinson et al. 1957, Lund & Lander, 1961). In these cases the permeability of the insulation was of little interest.

Lorentzen and Brendeng (1960) reported on the influence of free convection in insulated, vertical freezer room walls. The height of the wall was 2.4 m and its thickness 0.21 m. The insulation was mineral wool, loose fill, in mats or as bats, in some tests expanded polystyrene or cork was used. In all cases natural convection was reported. The temperature difference was 25-40 ^{o}C and the mean temperature about 0 ^{o}C. The authors pointed out that some of the convective heat transfer was due to leakages through small crevices between individual slabs and that due to this cork and polystyrene slab insulation offered no advantage over fiber materials of sufficiently high density. In the measurements the influence from natural convection in the case of loose fill insulation was especially noticeable. No explicit information on the permeability of the fiber material was given. The fiber diameter for the loose fill fiber material, with densities down to 17 kg/m^3, was, however, referred to, and indicated that the permeablility might have been several times as high as in the materials used in the present investigation. The aspect ratio for the convective flow in the more or less evenly distributed loose fill insulation could have been anywhere below approximately ten. The theories indicate the possibility of a considerable amount of natural convective heat transfer.

Cammerer (1962) discussed the thermal conductivity of wall insulations of mineral wool. This report included a short inventory of findings in the literature and the author noted the inconsistency and contradictions as to the nature of free convection in early measurement results. The report presented investigations on a mineral wool insulation with varying height, 0.3-1.3 m, and thickness, 0.05-0.20 m. Measurements were also made in a guarded hot plate with different heat flow directions. The mean temperature varied from -2 to +250 ^{o}C with a temperature difference of 20 ^{o}C/cm. No references as to the permeability of the material were made. The density, however, was high, 100 kg/m^3 and the author concluded that no influence from natural convection could be found in any of the measurements.

Höglund (1963) reported on laboratory-investigations of insulated

walls. The height of the insulation was 2.4 m and its thickness 0.1 m. The fiber insulation used had a density of 15 and 45 kg/m^3. The corresponding permeability was $74 \cdot 10^{-10}$ and $23 \cdot 10^{-10}$ m^2, $B_o(\parallel)$. The mean temperature was about 0 °C and the temperature difference was varied between 30 and 41 °C. In measurements on the two materials completely filling the space the author reported an increase in thermal conductivity with increasing temperature difference due to natural convection. This influence was, however, small and based on the heat flow measurements made only on the warm side in a total of nine measurements. A theoretical calculation of the Ra_o-values for $\Delta T = 40$ °C and $T_m = 0$ °C in the two materials gives $Ra \simeq 2$ and 0.5 respectively. This indicates that the convective heat transfer should have been negligible. Two measurements with 0.08 m mineral wool and 0.02 m air space in the 0.10 m space were presented. Both measurements showed heat flow variations over the height characteristic for convective flow. The reported measured mean thermal conductivities are, however, in agreement with a simple calculation of the thermal resistance in the insulation plus that in the air space. Only one measurement on 45 kg/m^3 material, when installed, at both surfaces, with air spaces that interconnected at the top and at the bottom of the space, showed a significant reduction in the total conductivity value.

In a subsequent report, Höglund and Hansson (1964) reported on measurements on mineral wool insulation of a height of 1.5 m and a thickness of 0.10 m. The permeability, $B_o(\perp)$, varied from $5 \cdot 10^{-10}$ to $50 \cdot 10^{-10}$ m^2. The temperature difference varied between 17 and 39 °C at a mean temperature of 0 to 40 °C in different tests. The analyzed results presented showed a successively greater influence from convection as the permeability increased. An even more marked influence was reported for insulation with air space. Examination of these results, which were based on measured heat flow distributions on the warm side, does not verify the conclusion about convective heat flow in the case without air space. The case with air space was really based on measurements without covering board on the cold side.

Lotz (1964) reported on results from nine years of field observations of the thermal performance of fibrous glass insulations in the walls of refrigerated warehouses. These results were combined with laboratory measurements in a guarded hot box on materials with a density of 25 and 130 kg/m^3, $\Delta T \simeq 60$ °C, $T_m \simeq 10$ °C and d = 0.12 m. The author concluded that, though the presence of convection currents was indicated in some tests, the net effect of convection on the total heat transfer was negligible for constructions containing an air-impermeable facing on at least one surface of the insulation. Wolf et al. (1966) and Wolf (1966) presented an investigation of the convective air flow effects with mineral wool insulation in wood-frame walls. Tests were made with insulation installed with air spaces at one or both sides and with or without an air-impermeable polyethylene covering. The density of the material was 12 - 38 kg/m^3, $\Delta T \simeq 45$ °C and $T_m \simeq 0$ °C. 0.05 m insulation was installed with either 0.04 m air space at one side or 0.025 m air spaces at both sides, all with or without covering. The authors concluded that convective air flow effects were negligible when the insulation was isolated from the air space by an impermeable membrane, or when at least one of the air spaces was eliminated.

Investigations of the influence of natural convection in walls with insulation from rigid, air-tight, slab-type insulation were presented by Lorentzen and Nesje (1966). They showed that slits between the insulation slabs might give a marked convective heat transfer, dependent upon the number and size of slits and the temperature conditions in a cold storage wall. Ogston (1970) studied the influence of natural convection heat transfer in a wall of granular material. The conditions were $B_o = 150 \cdot 10^{-10}$ m^2, d = 0.152 m, $\Delta T = 60$ °C, $T_m = 0$ °C and $\lambda_o = 0.0425$ W/mK, which gives $Ra_o \simeq 15$. The height of the space was originally 1.07 m and subdivided 0.173 m, i.e. h/d = 7 and 1.2. The author noted deformations of the temperature field chracteristic for convective flow. The rise in the thermal conductivity value found experimentally was, however, small, in the first case $\lambda/\lambda_o \simeq 1.06$ and in the second 1.10. The author also stated that these values were obtained at insulating horizontal boundary

conditions. The theories used in this report give 1.06 and 1.16, respectively.

It is obvious from the above that the experiments found in the literature agree well with those presented in this report. It is also evident that the theoretical considerations presented, consistently explain the qualitative and quantative results.

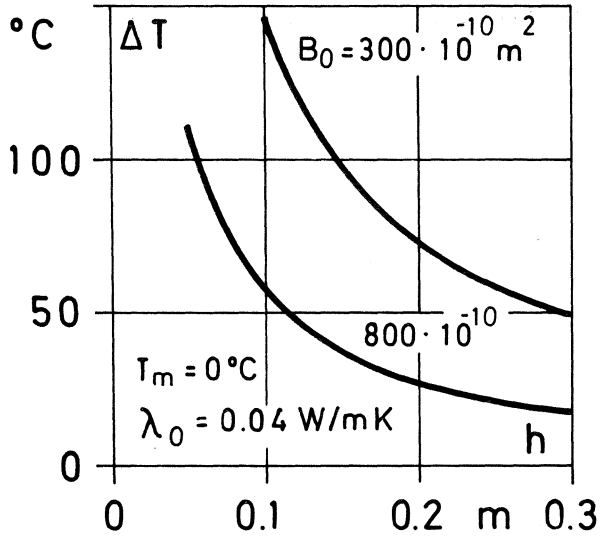

FIG. 7.1. The minimal specific permeability of the insulation in a horizontal space for natural convective heat flow.

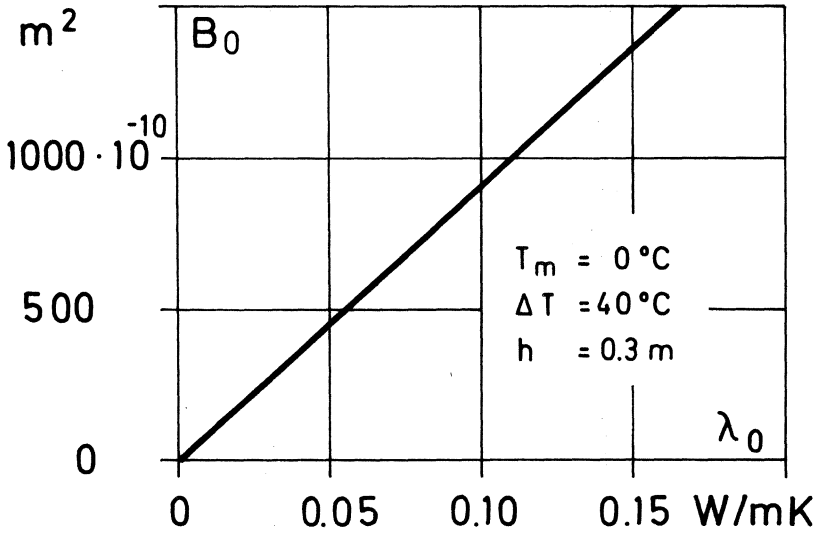

FIG. 7.2. Minimal specific permeability for natural convective heat flow in horizontal insulations of different thermal conductivity.

7 CONCLUSIONS

In the preceeding sections the factors influencing the natural convection in a space insulated with a permeable material have been investigated theoretically and experimentally. The two extreme limits, the air space and the solid structure, have been pointed out and a discussion made of the convective heat transfer phenomena in the air space. These considerations together with investigations of the flow in a permeable material have lead to the permeable space. The natural convection in such a space has been treated theoretically in considerable detail, and measurements have been presented on insulated structures. It has also been shown that these findings theoretically, as well as experimentally, are in good agreement with previous experimental results presented in the literature, and that the theories consistently explain the behavior of the natural convection in these cases.

This permits the following conclusions to be drawn:

The natural convection in a fully insulated space is governed by the modified Rayleigh number, Ra_o the aspect ratio, h/d and the boundary conditions.

In the case of the <u>horizontal</u> space, a critical Ra_o-value exists, i.e.

$$Ra_o = \frac{g \cdot \Delta T \cdot h \cdot B_o}{\nu \cdot a_o \cdot T_m} = C_{air,o} \cdot \frac{\Delta T \cdot h \cdot B_o}{\lambda_o} = 4\pi^2 \qquad (7.1)$$

$C_{air,o}$ depends upon the air and its mean temperature and is given in FIG 5.6 (on page 50). The consequences of this equation are shown in FIG 7.1 for a material with $\lambda_o = 0.04$ W/mK at a mean temperature of 0 °C. It should also be pointed out that if the upper surface is free, there are indications in the literature that the critical value may be somewhat reduced.

If only normal building physical applications are considered,

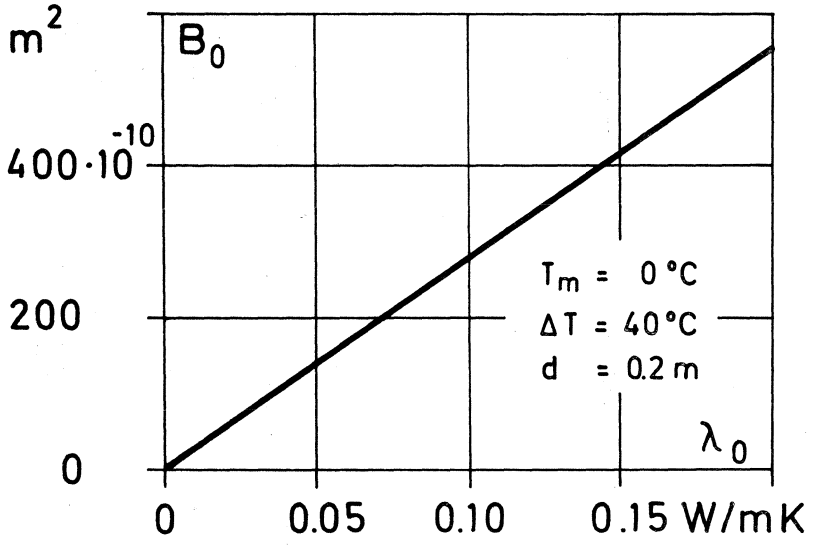

FIG. 7.3. Minimal specific permeability for 5 % natural convective heat flow in vertical insulations of different thermal conductivity (h/d = 1).

the temperature of the warm side can be assumed to be 20 °C and on the cold side it is seldom below -20 °C. In FIG. 7.2 the minimal specific permeability-values necessary to exceed the critical Ra_o-value at $\Delta T = 40$ °C and $T_m = 0$ °C are given as a solid line for different λ_o-values and $h = 0.30$ m. This figure gives an indication of what the conditions have to be to induce natural convective heat transfer in the horizontal space. The aspect ratio and boundary conditions are normally of little interest in this case.

In the vertical permeable space, the situation is slightly more complicated, since both aspect ratio and boundary conditions often influence the amount of natural convective heat transfer in the space. The Ra_o-value is given by

$$Ra_o = C_{air,o} \frac{\Delta T \cdot d \cdot B_o}{\lambda_o} \qquad (7.2)$$

FIG. 5.9 (on page 52) gives the amount of convective heat transfer in the space as a function of h/d and for isothermal vertical boundaries and insulating horizontal boundaries. In order to investigate the implications of this under normal applications, the same assumptions are made as in FIG. 7.2, $\Delta T = 40$ °C, $T_m = 0$ °C and $d = 0.20$ m. Unlike the horizontal case no critical Ra_o-value exists in the vertical case. The condition for 5 % natural convective heat transfer is therefore illustrated in FIG. 7.3 for different specific permeabilities, B_o and thermal conductivities, λ_o. The Ra_o-value when calculating FIG. 7.3 was taken from FIG. 5.9 (on page 52) and is valid for those boundary conditions. The aspect ratio was chosen as one, since this represents a situation with maximal convective heat transfer. In order to evaluate the influence of arbitrary boundary conditions or other aspect ratios, Section 5.4 should be consulted.

When air spaces or slits are included in the insulated space the following conclusions, valid in circumstances similar to those in the experimental investigation, can be drawn from

the experiments and the literature.

For normal building physical applications a structure, where the insulation has an air space of normal thickness on only one side, will behave thermally as the insulation plus an air space. If the material is placed with air spaces at both sides its permeability may influence the convective heat transfer. Slits from the warm to the cold side in the material will give convective heat transfer independent of the permeability of the material. This is also true if slits and spaces are interconnected and facilitates a convective flow round the insulating slabs.

In general, it can be concluded that in normal temperature conditions, the natural convective heat transfer in an insulated space takes very high permeability values to be of any importance, and that if uncontrolled air spaces and slits are introduced into the insulating structure, any amount of convective heat transfer can be expected. In this case, knowledge about the behaviour of the air space is useful to estimate the ultimate result.

8 APPENDIX

8.1 Measurements of specific permeability.

The specific permeability coefficient is defined by

$$B_o = \frac{Q}{A} \cdot \frac{\eta}{\text{grad } p}$$

This coefficient is generally evaluated by the simultaneous measurements of pressure-drop and volume flow for a test material. The problem is to establish a true one-dimensional flow through a representative part of the material. This is done conventionally by placing the test specimen in a circular tube and measuring the flow through the tube and the pressure-drop over the specimen. This method is similar to the one used by Darcy in his experiments and is the one that the standardized DIN (1958) and ASTM (1968) methods are based upon. The critical part of this method is whether the material adhere to the wall and how to avoid slits or flow in slits between the tube-wall and the test piece.

In one part of the investigation, measurements were performed in a unit designed according to the conventional method. The unit is shown in FIG. 8.1. The connection between the test specimen and the wall was achieved in different ways, dependent upon the compressibility of the material tested. For materials with low compressibility, the test specimen was cut to give a tight fit against the tube walls. This could not be done on high compressibility specimens without their compression. In this case, the diameter of the test piece was made slightly smaller than that of the tube and the material was wrapped in an adhesive paper. After inserting this configuration in the tube, the ends of the paper-wrapping were sealed by wax to the tube walls. This is shown in FIG. 8.1. Measurements were made in tubes with diameters from 0.05 to 0.15 m. The pressure-drop was varied, giving an apparent velocity of 0.01-0.1 m/s, and in some experiments, 0.08-0.39 m/s. In a few measurements, the pressure-drop was measured inside the material as well. No difference in calculated permeability value was found, however. To ensure that the fit of the

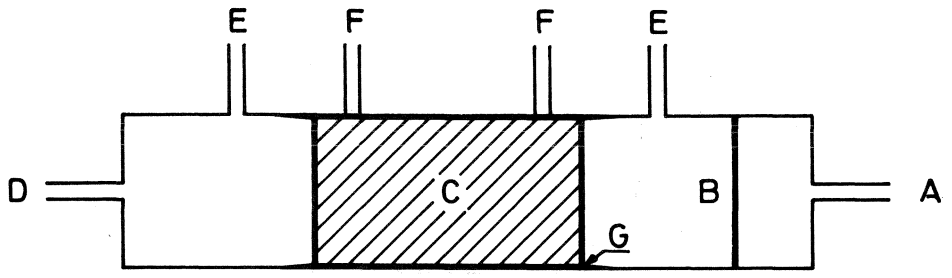

FIG. 8.1 Conventional permeability test tube.

A Air inlet from flow regulation and rotameter.

B Screen for flow normalizing.

C Test specimen.

D Air outlet or open end.

E Pressure taps connected to manometer.

F Alternative pressure taps to faciliate measurement in the test specimen.

G Adhesive wrapping sealed to the test tube (used in case of high compressibility specimens).

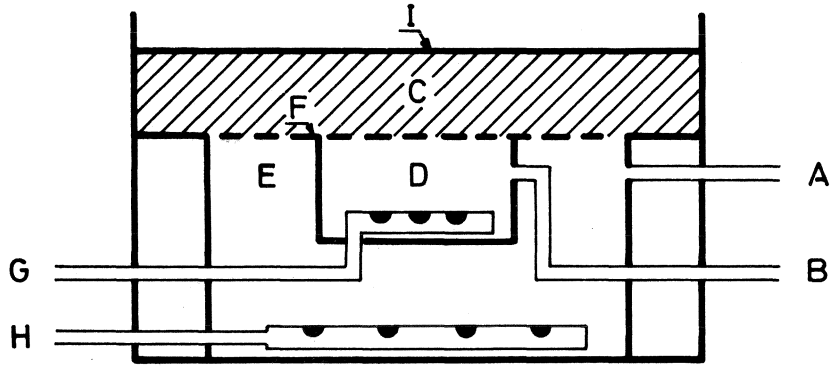

FIG. 8.2. Permeability measurement by guard ring technique.

A Pressure tap from guard ring, connected to differential manometer.

B Pressure tap from test area, connected to differential manometer and to manometer for pressure difference measurement over test specimen.

C Test specimen.

D Test section.

E Guard section.

F Screen.

G Air inlet, test section, from flow regulator and rotameter.

H Air inlet, guard section, from precision flow regulator.

I Open end.

low compressible materials was sufficient, some of these were measured with adhesive wrapping as well, and showed no difference between the respective results. It was generally found that this conventional method had fairly high reproducability, but that the fitting of the material was sometimes a tedious work.

Measurements of permeability were also performed in a unit manufactured according to principles developed at the Statens Provningsanstalt (National Swedish Institute for Materials Testing) in Stockholm. The unit is shown in FIG. 8.2. This method applies a guard ring technique to ensure one-dimensional flow in the test area. At the same time the problem of flow between the test piece and the wall is more or less avoided. The flow through the guard ring is regulated so as to give zero differential pressure between the inflow regions of the guard and the test sections. The dimensions of the guard and test area together with the thickness of specimen and its permeability will decide to what extent one-dimensional flow is actually achieved. This method naturally simplifies the installation of the material as compared to the previous one. On the other hand it was found it was slightly more difficult to achieve high reproducability.

The results from the measurements are shown in FIG. 8.3-8.6, where permeability is given versus density. Measurements paralell to the fiber planes were made exclusively in the guard ring unit after pieces of the test material had been glued together to yield a sufficiently large area of maesurement. It is not believed that this method influenced the results in any appreciable way. Measurements at right angle to the fiber planes were performed in both units, and showed no differences in the results from the two units. In the diagrams, regression lines give the approximate relationship between density and specific permeability.

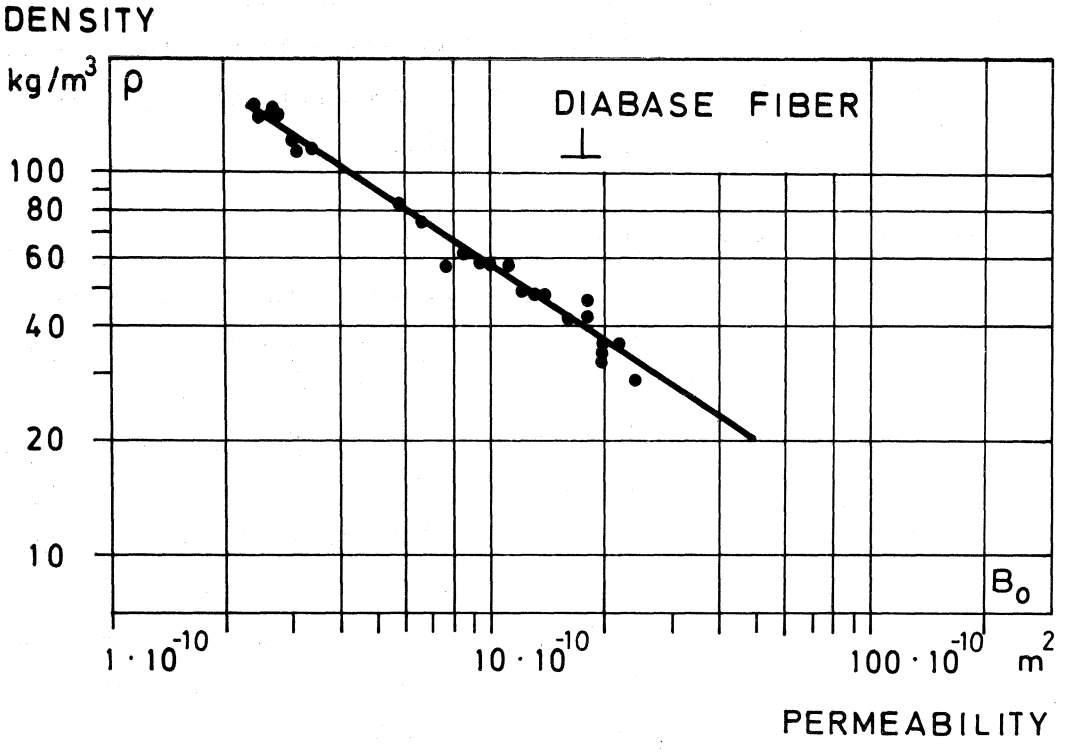

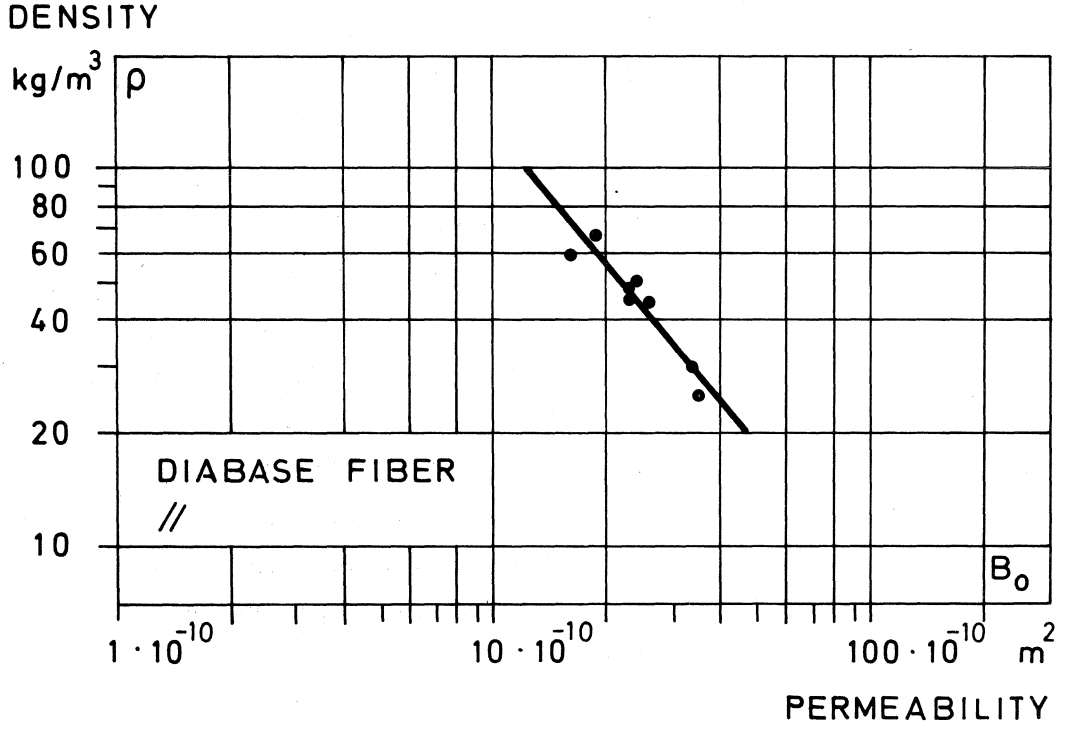

FIG. 8.3-8.4. Experimental specific permeability values.

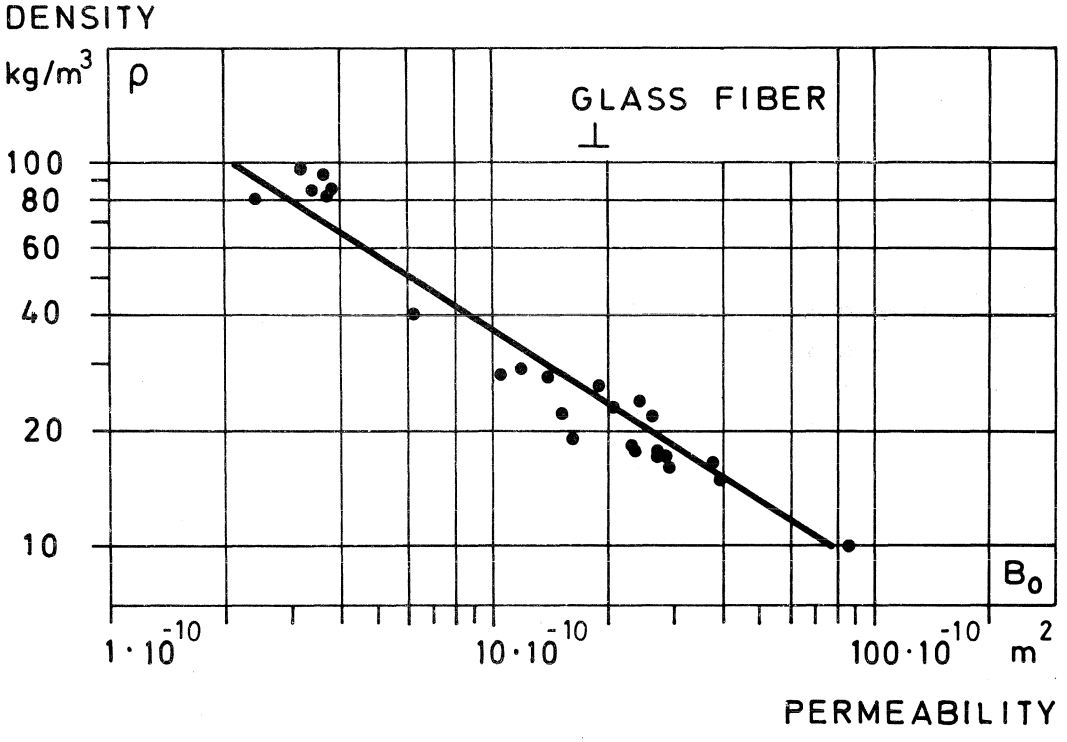

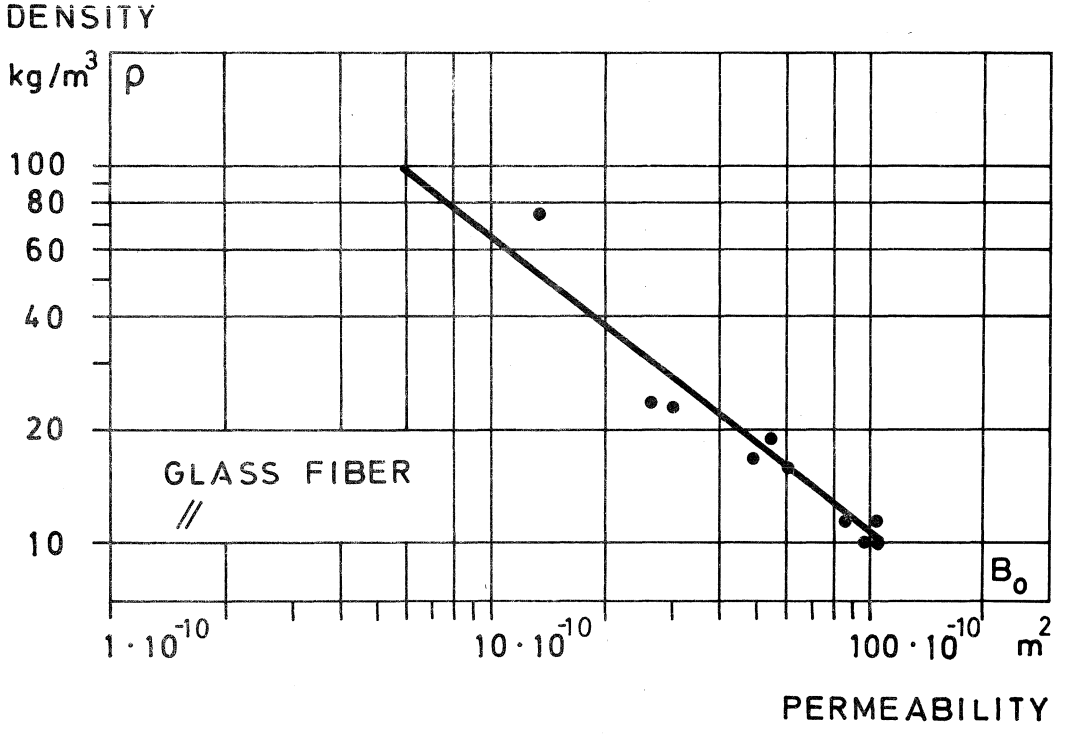

FIG. 8.5-8.6. Experimental specific permeability values.

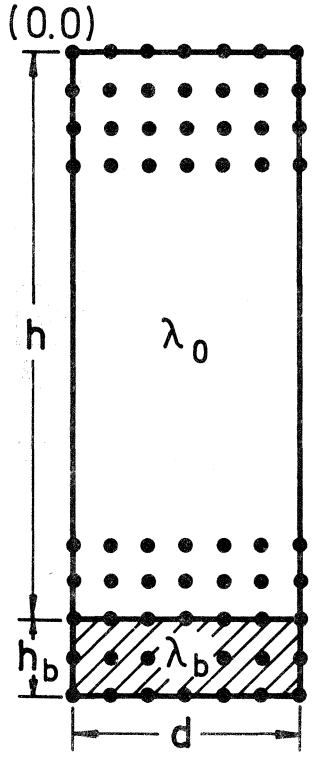

FIG. 8.7. Numerical problem.

8.2 Vertical space, numerical solution.

The governing equations for the vertical insulated space were formulated and simplified in Section 5.2 to give, in dimensionless form,

$$-Ra_o \frac{\partial \theta}{\partial X} = \nabla^2 \psi$$

and

$$\frac{\partial \psi}{\partial Z} \frac{\partial \theta}{\partial X} - \frac{\partial \psi}{\partial X} \frac{\partial \theta}{\partial Z} = \nabla^2 \theta$$

The problem considered was primarily that of an insulated space and a crossbar (cf. FIG. 5.2 on page 46) with different boundary conditions. The vertical boundaries were generally kept at constant temperature. The conduction heat transfer in the solid crossbar was calculated from

$$\frac{\partial^2 \theta}{\partial X^2} + \frac{\partial^2 \theta}{\partial Z^2} = 0$$

The problem was solved numerically by the introduction of mesh points, as in FIG. 8.7.

In the differential equations the partial derivatives were approximated by finite-differences. Inside the space and the crossbar three point central-difference approximations were used and at the vertical boundaries three point forward - or backward - difference approximations. At the boundary between the space and the crossbar a simple heat flow balance with three point temperature approximations was used. The temperatures of the bottom horizontal boundary of the crossbar were set equal to the temperatures of the top horizontal boundary of the space.

The numerical explicit procedure is illustrated in FIG. 8.8. Constants and boundary conditions for temperature field and streamfunction are stated, at first. The initial temperature field and streamfunction-values are specified, usually equal to the non-convective state, i.e. linear temperature variation and zero

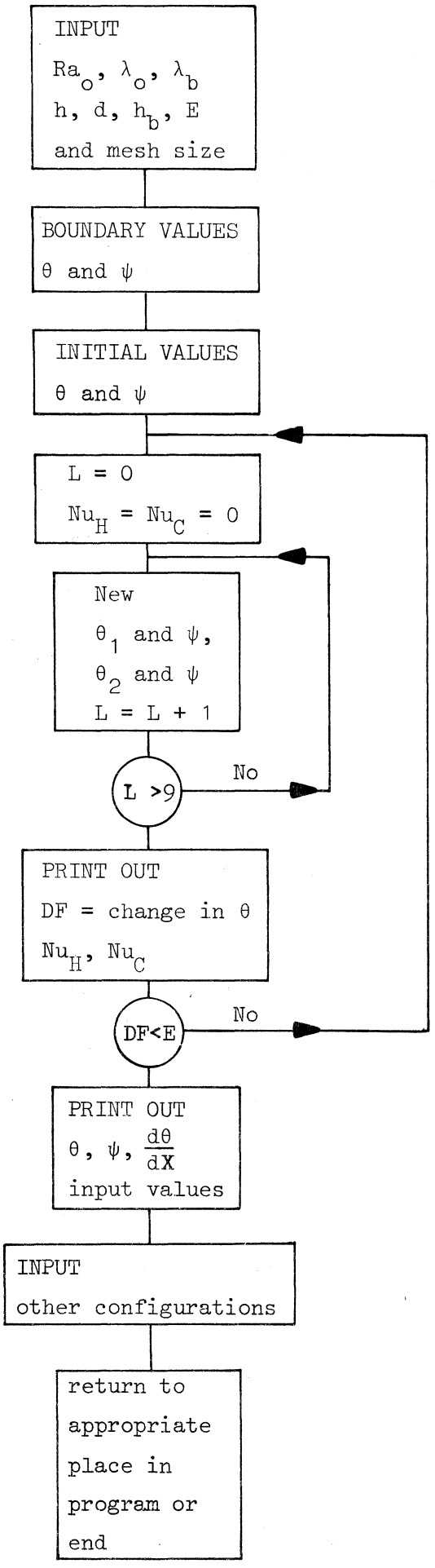

FIG. 8.8. Numerical procedure

streamfunction-values. New θ and ψ values are calculated in each mesh point. Two temperature fields, at the n-th and (n+1)-th iterations, are retained in the computer. After twenty iterations, the difference between these two fields is established. The Nu-values are calculated at the hot and the cold sides and are printed out together with the difference. If this difference is sufficiently small a print out is also made of the temperature field and the streamfunction-values. These values are then used as initial values if further calculations are to be made on the same structure.

The stability of the numerical solution depends upon the Ra_o-value and on the mesh size. In the case of the air space more sophisticated numerical procedures have been developed to extend the stability to high Ra-values (cf. the Bibliography). It should be pointed out that the extention of the solution to high Ra- and Ra_o-values, respectively, may involve a certain risk, since the original basic equations were developed under certain assumptions of e.g. flow-velocity and the viscous force. In the present case, the method used is thought to be stable at sufficiently large modified Rayleigh numbers. Depending upon the specific problem the solution is stable up to a Ra_o-value of about 200.

In testing the change in the temperature field a certain number of mesh point values adjacent to the hot side is used. If the total absolute difference calculated from these points is sufficiently small, the iterations are terminated. FIG. 8.9 shows the calculated difference and the Nu-value as a function of the number of iterations. Test runs like this were made to decide what difference would give an acceptable approach to the final value, and how many mesh points should be used in the calculation of the change in the temperature field.

The number of mesh points influences the accuracy of the solution and the computational time. FIG. 8.10 shows the change in final value as a function of the number of mesh points for a space with h/d = 1. A closer approach to the numerically correct value is achieved as the number of mesh points increases, at the same time

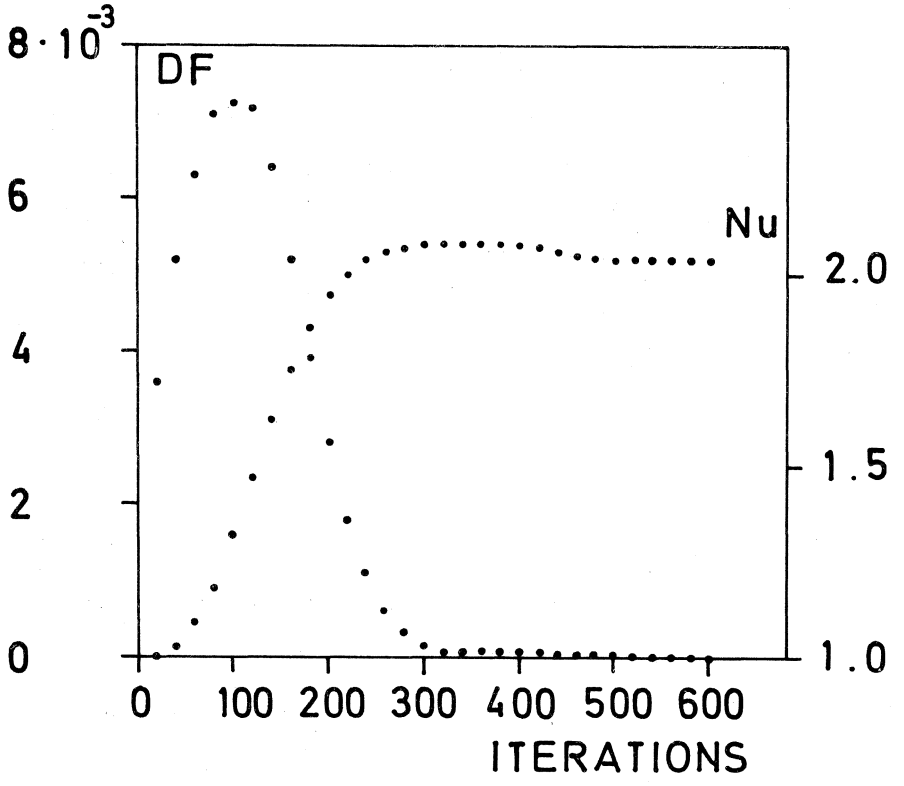

FIG. 8.9. Change in calculated temperature field difference, DF, and Nu-value as a function of the number of iterations.

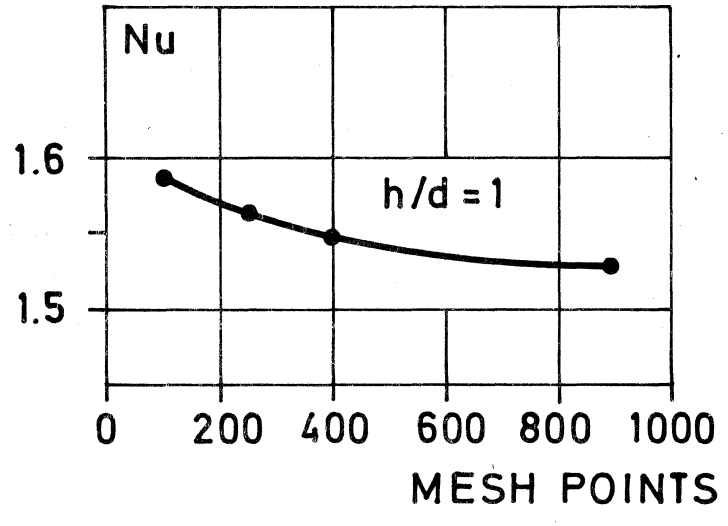

FIG. 8.10. Change in Nu-value as a function of the number of mesh points.

the computational time will, of course, increase. The program was run on a UNIVAC 1108 computer and for a 21×21 mesh the time for 20 iterations was about 4 seconds. The number of 20-iterations required to complete the calculation depends upon the initial values and the Ra_o-value. A separate run for Ra_o = 50 took in this case 27 such iterations.

In Section 5.3 comparisons have been made between results calculated numerically and measured experimentally. A close agreement is found, which verifies the validity of the numerical procedure developed.

8.3 Instrumentation, measurement techniques and results.

Measurements of heat flows and temperatures were made on the insulated wall structure. The temperature measurements were made by thermocouples with an accuracy of 0.2 ^{o}C. The heat flow meters, which were glued to the boards, had a stated accuracy of 5 %. Calibrations made on three of the meters indicated that the accuracy was well within this value. FIG. 8.11 shows the installation of the heat flow meters in the measurements on the insulation in combination with air spaces.

The registration of the measurements were made by a hundred-channel data-logging unit and the measured values were punched on tape (cf. FIG. 8.12). After the temperatures and heat flows had stabilized, measurements were made for a duration of about three hours. In a computer the heat flows and temperatures were linearized and calculations made of mean values, deviations etc.

The detailed results from these measurements are given in the following.

The results for the experiments on insulation without air spaces are shown in diagrams. The heat flows and temperatures measured at the surfaces of the insulation over its height are indicated in these diagrams. The measured mean density and thickness of the insulation, together with the calculated thermal conductivity and mean temperature, are given for each specimen tested.

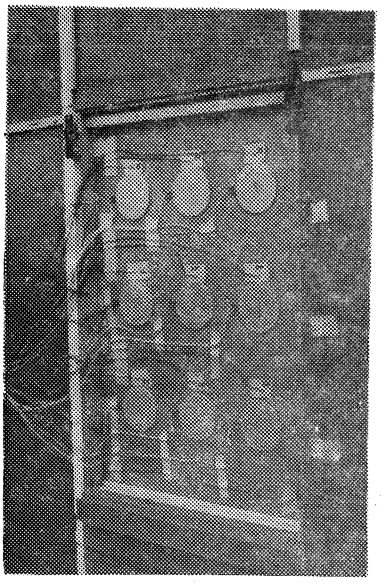

FIG. 8.11. Placement of heat flow meters and thermocouples on the board on the cold side.

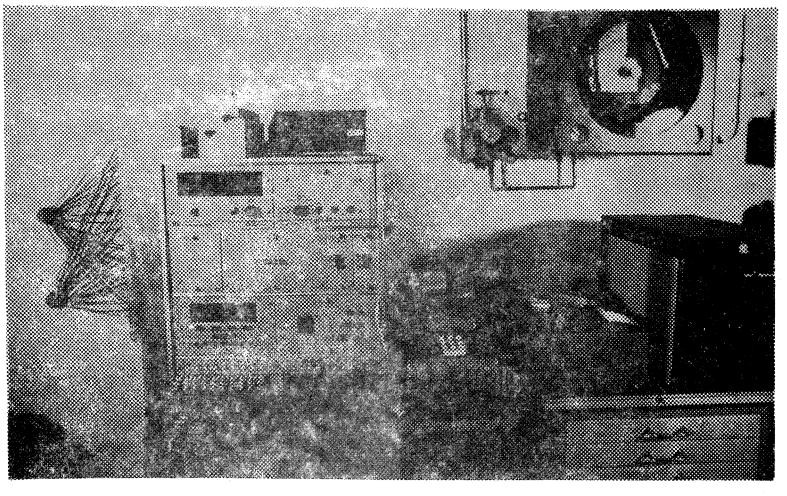

FIG. 8.12. Datalogging unit used for the measurements of heat flows and temperatures. Printer and punch on the right.

A horizontally, divided space is indicated by continuous lines in the diagram. All values are in SI-units unless otherwise stated.

The measurement results for walls with air spaces and openings are explicitly noted as thermal resistance and mean temperature for each part of the space under investigation, as viewed from the cold side.

GLASS FIBER

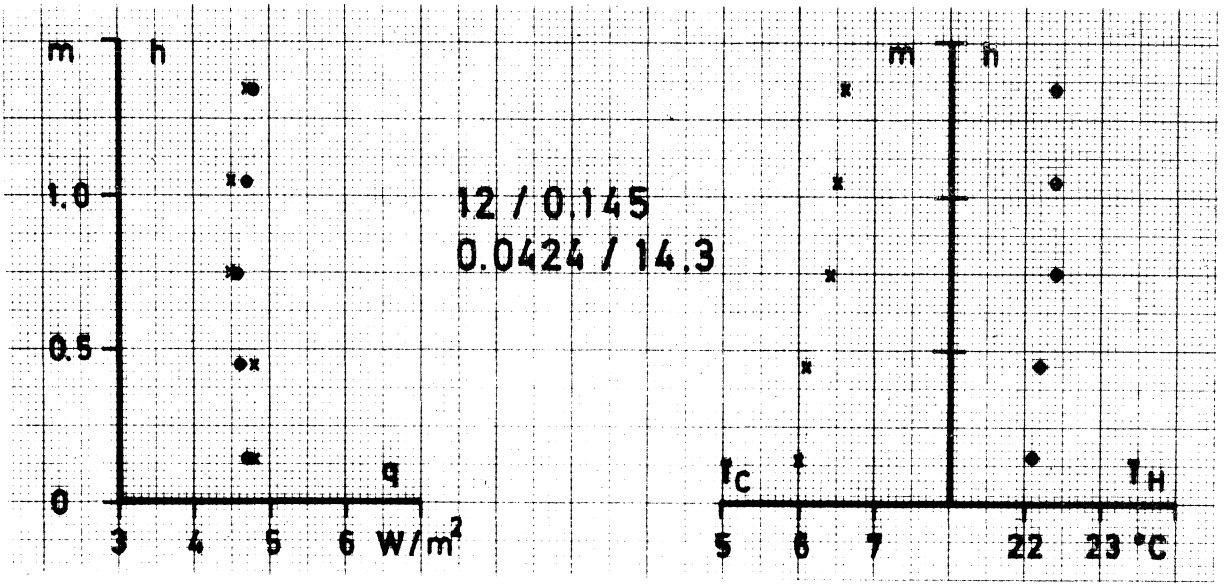
m
h
1.0
0.5
0
q
3
4
5
6 W/m²
12 / 0.145
0.0424 / 14.3
m
h
t_C
t_H
5
6
7
22
23 °C

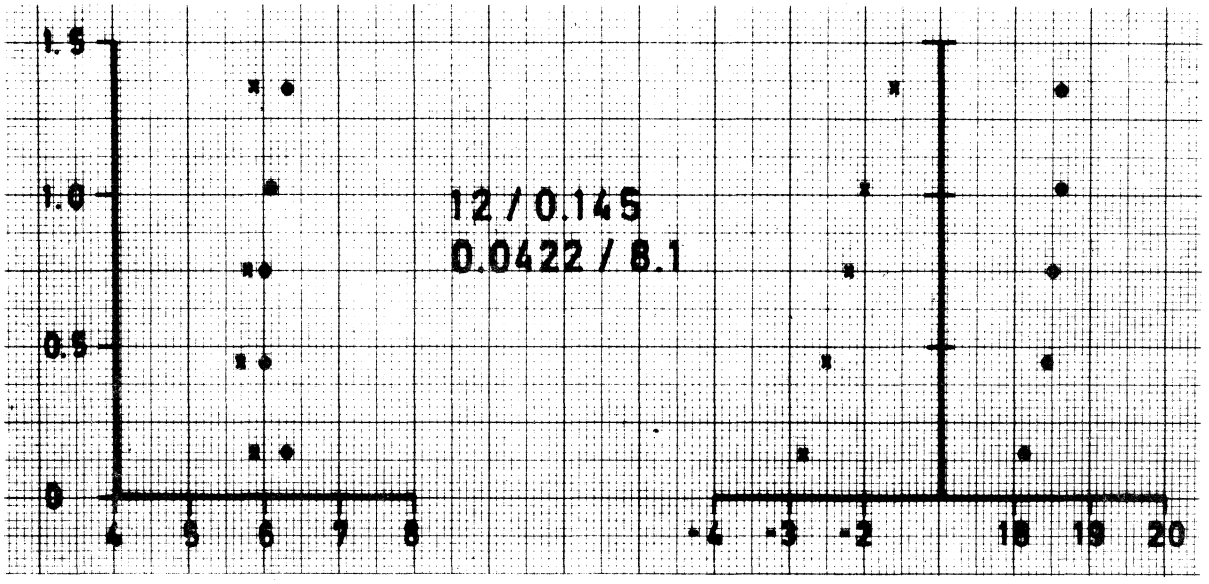
1.5
1.0
0.5
0
4
5
6
7
8
12 / 0.145
0.0422 / 8.1
-4
-3
-2
18
19
20

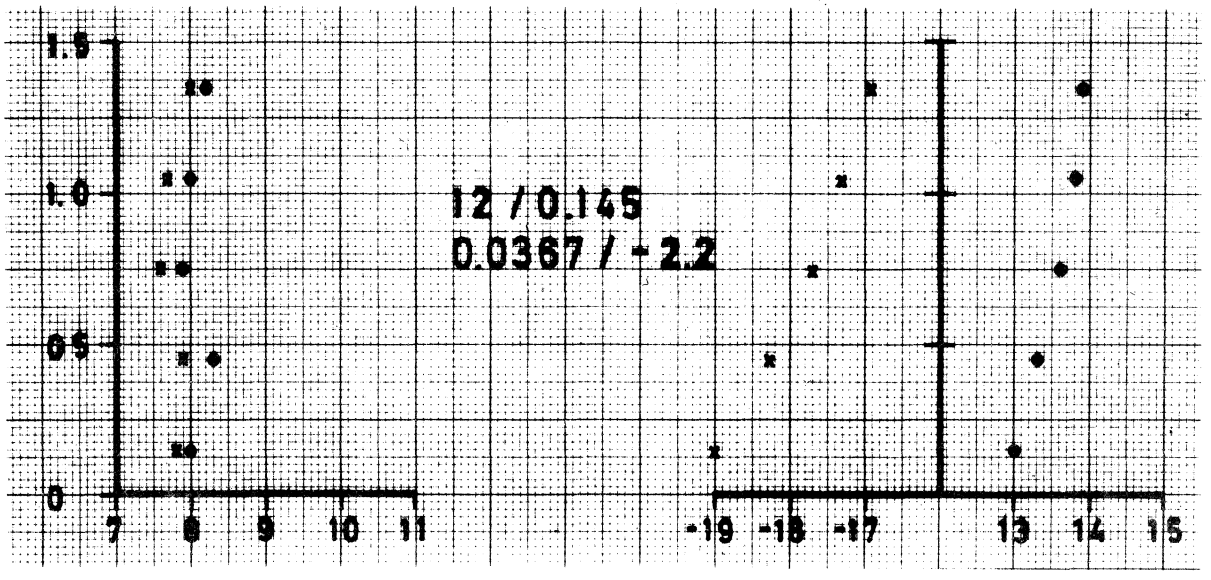
1.5
1.0
0.5
0
7
8
9
10
11
12 / 0.145
0.0367 / -2.2
-19
-18
-17
13
14
15

GLASS FIBER

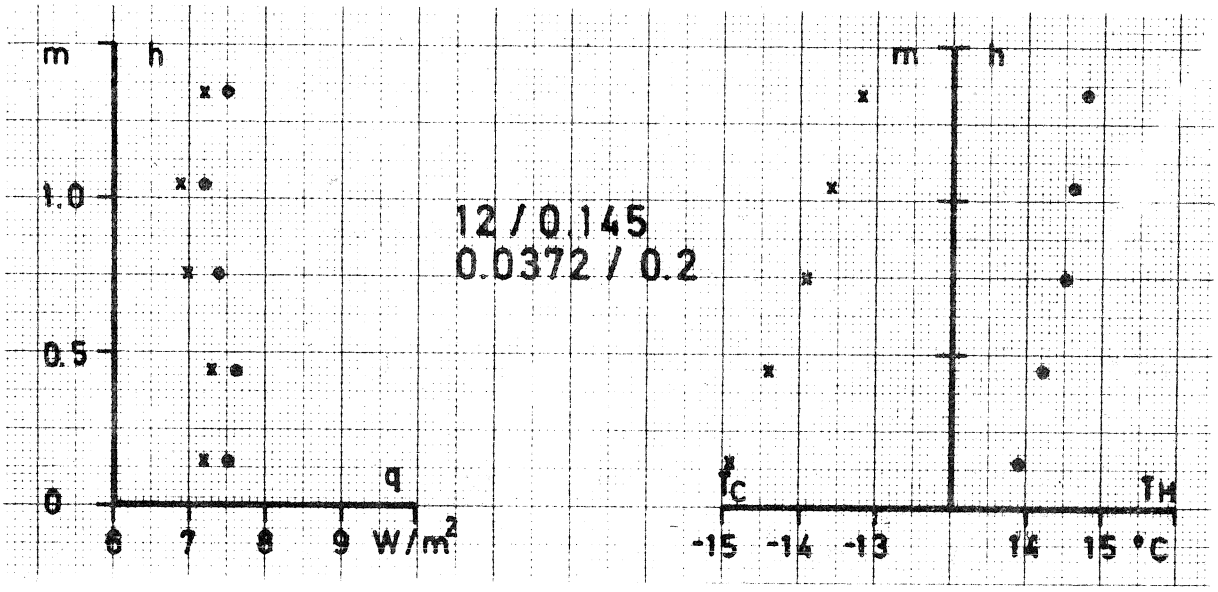
m
h
1.0
0.5
0
q
6
7
8
9 W/m²
12 / 0.145
0.0372 / 0.2
m
h
TC
TH
-15
-14
-13
14
15 °C

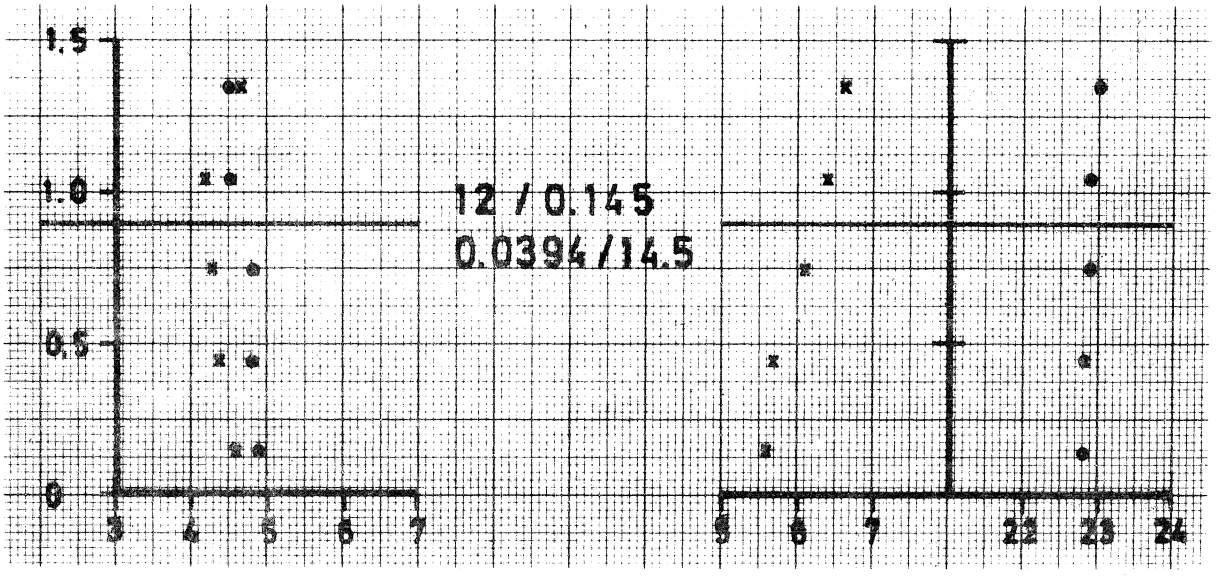
1.5
1.0
0.5
0
3
4
5
6
7
12 / 0.145
0.0394 / 14.5
5
6
7
22
23
24

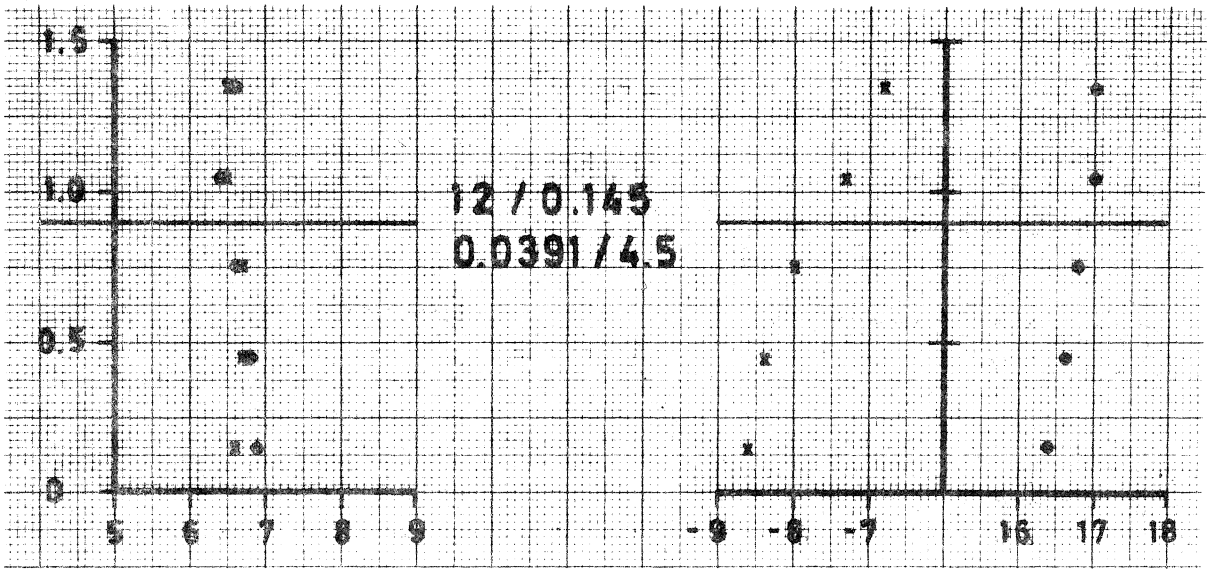
1.5
1.0
0.5
0
5
6
7
8
9
12 / 0.145
0.0391 / 4.5
-9
-8
-7
16
17
18

GLASS FIBER

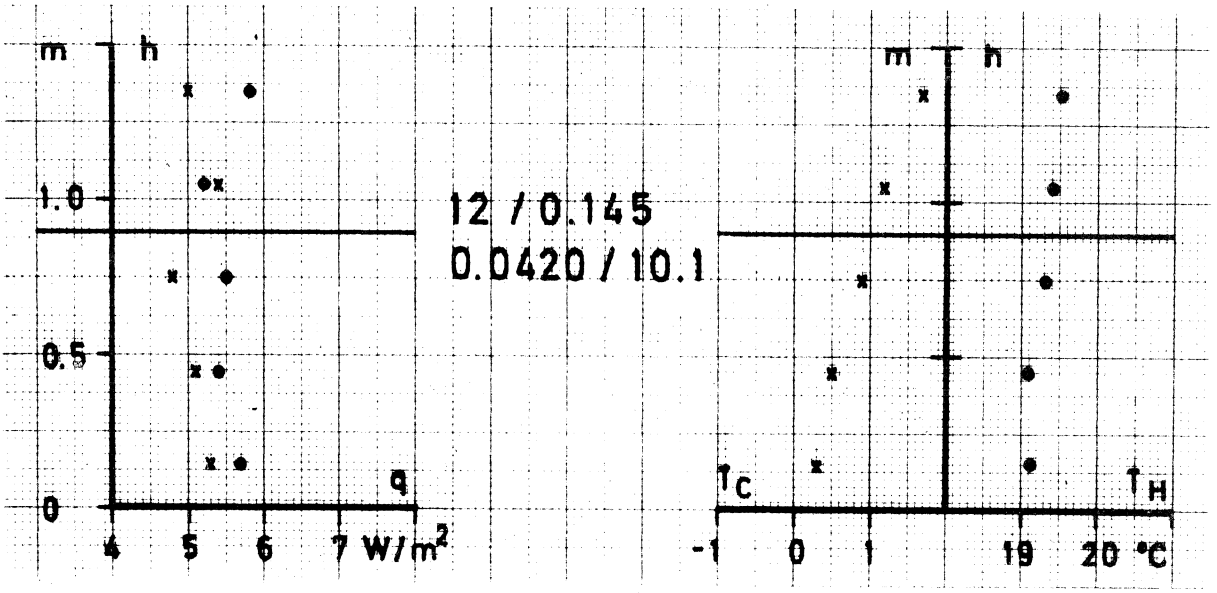
m
h
1.0
0.5
0
q
4
5
6
7 W/m²
12 / 0.145
0.0420 / 10.1
m
h
T_C
T_H
-1
0
1
19
20 °C

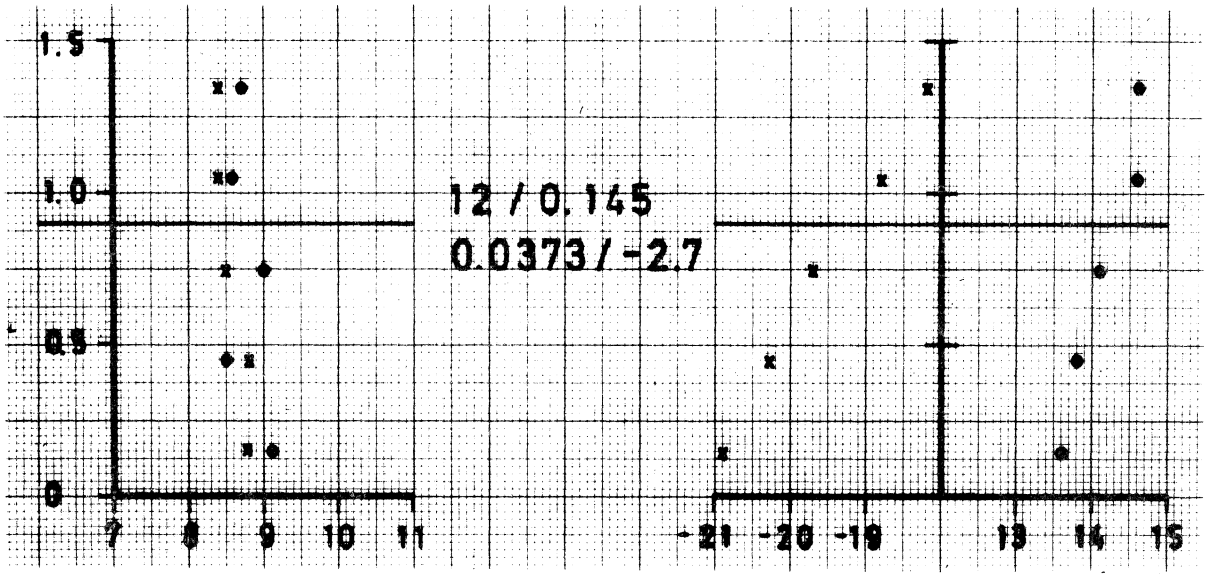
1.5
1.0
0.5
0
7
8
9
10
11
12 / 0.145
0.0373 / -2.7
-21
-20
-19
13
14
15

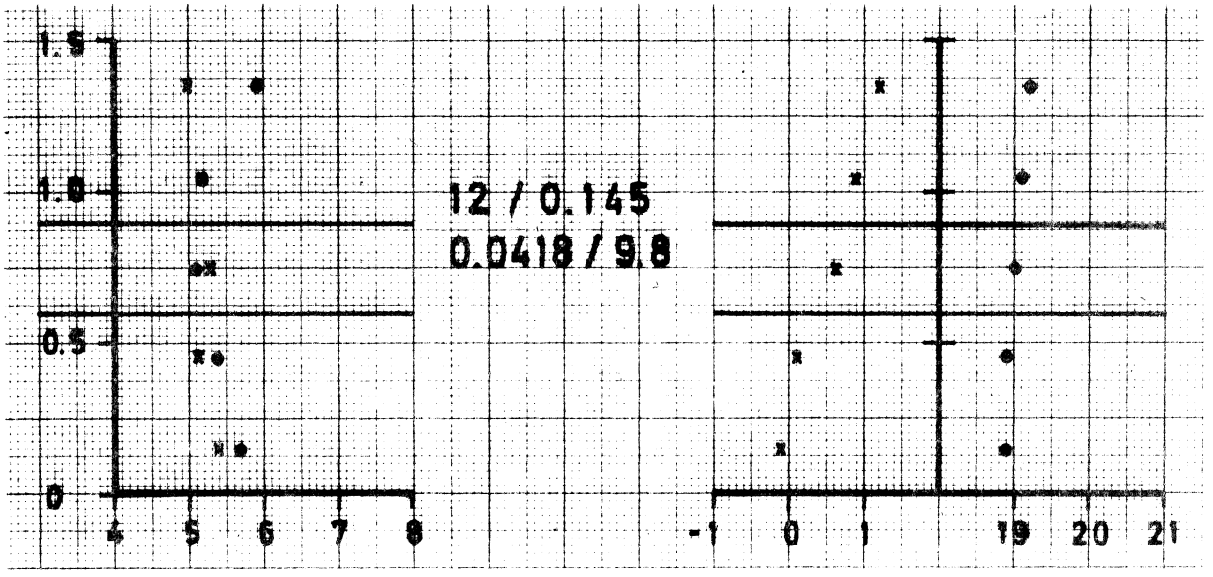
1.5
1.0
0.5
0
4
5
6
7
8
12 / 0.145
0.0418 / 9.8
-1
0
1
19
20
21

GLASS FIBER

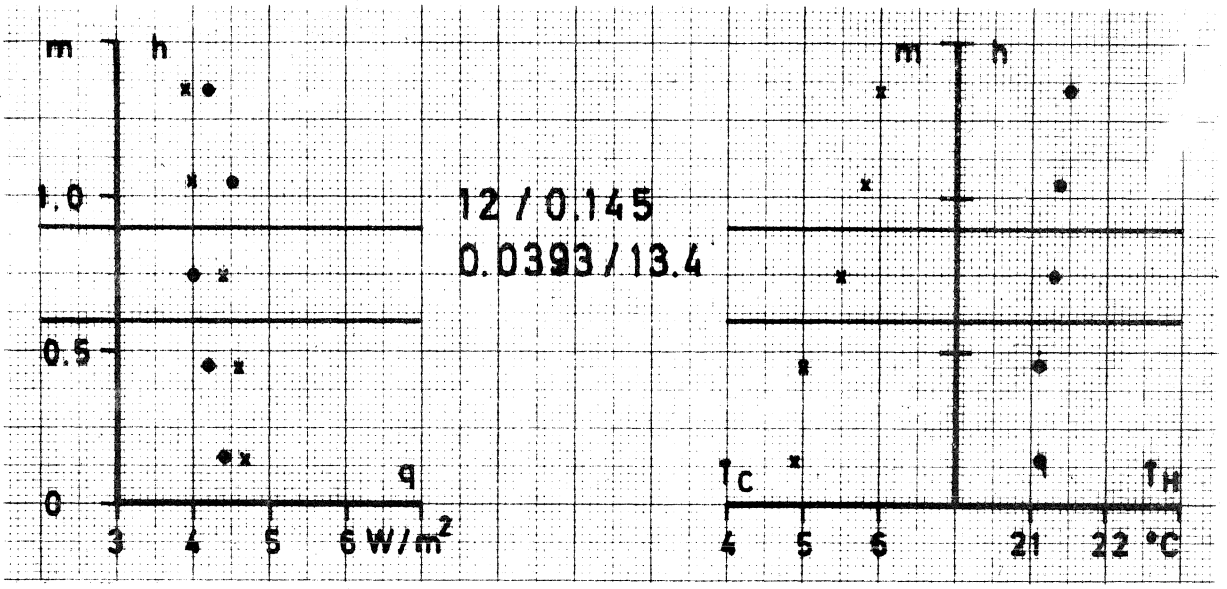
m
h
1.0
0.5
0
q
3
4
5
6 W/m²
12 / 0.145
0.0393 / 13.4
m
h
t_C
t_H
4
5
6
21
22 °C

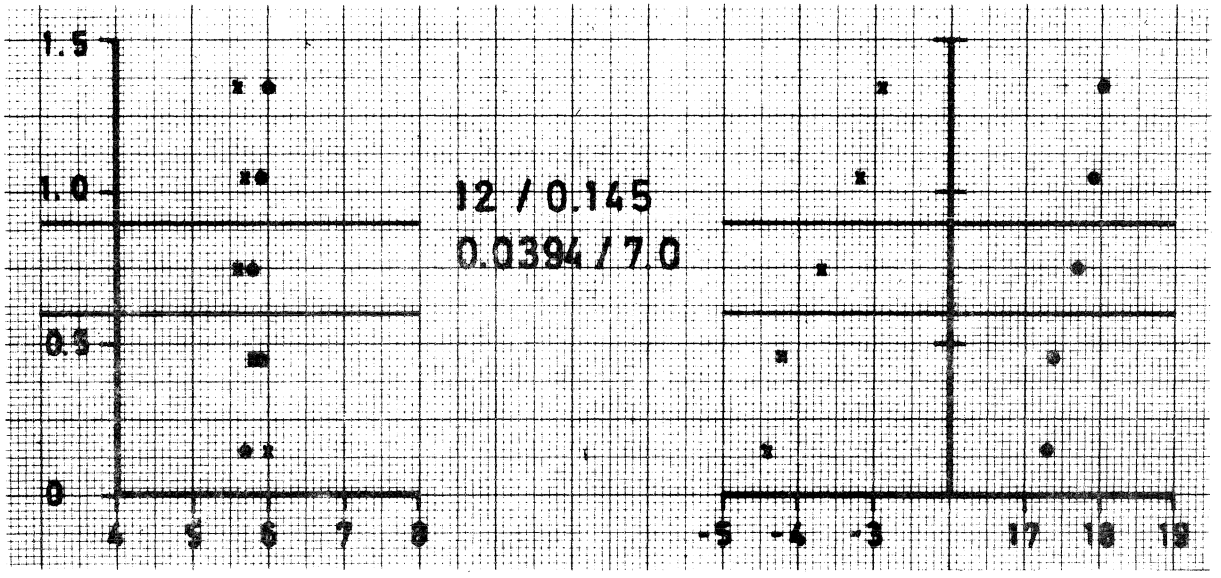
1.5
1.0
0.5
0
4
5
6
7
8
12 / 0.145
0.0394 / 7.0
-5
-4
-3
17
18
19

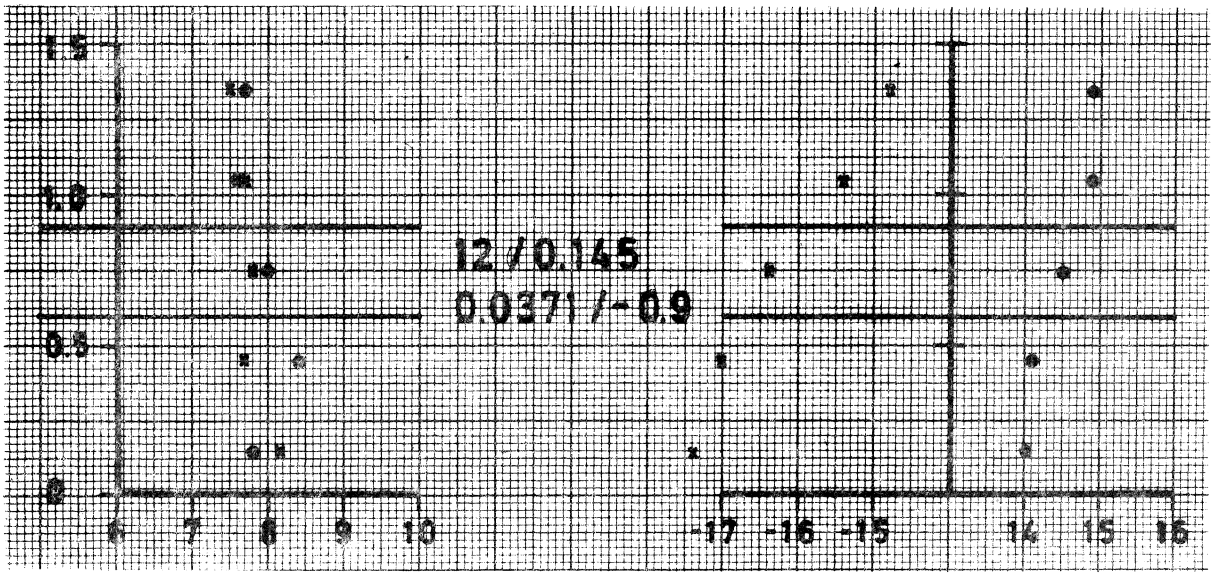
1.5
1.0
0.5
0
6
7
8
9
10
12 / 0.145
0.0371 / -0.9
-17
-16
-15
14
15
16

GLASS FIBER

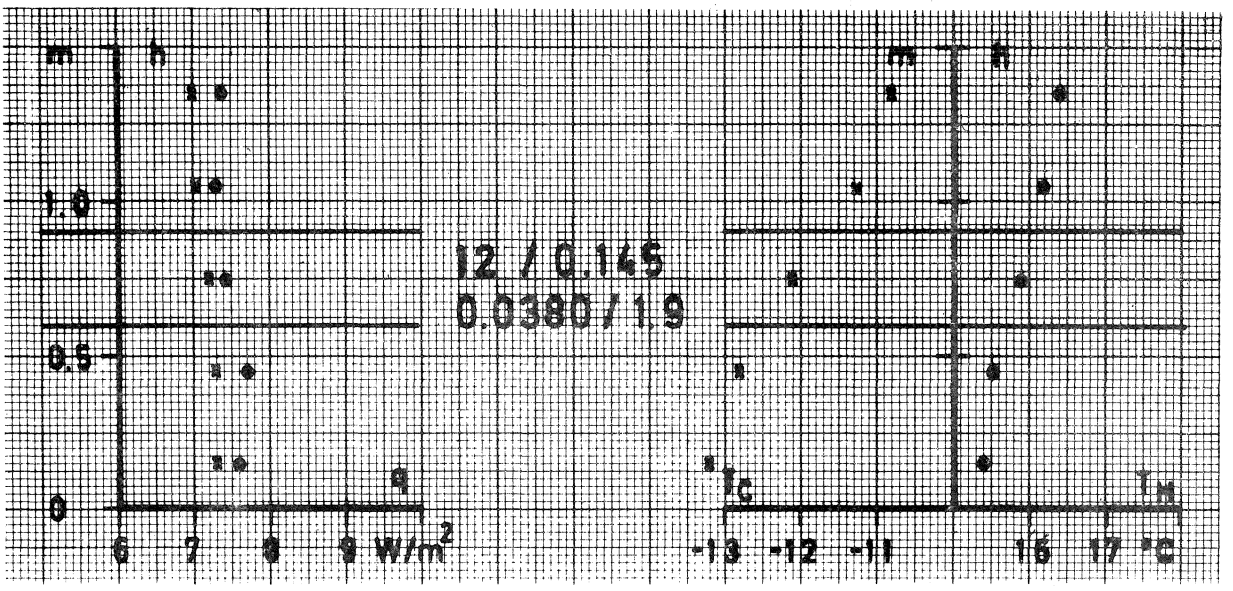
m
h
1.0
0.5
0
q
6 7 8 9 W/m²
12 / 0.145
0.0380 / 1.9
m
h
Tc
Tm
-13 -12 -11 16 17 °C

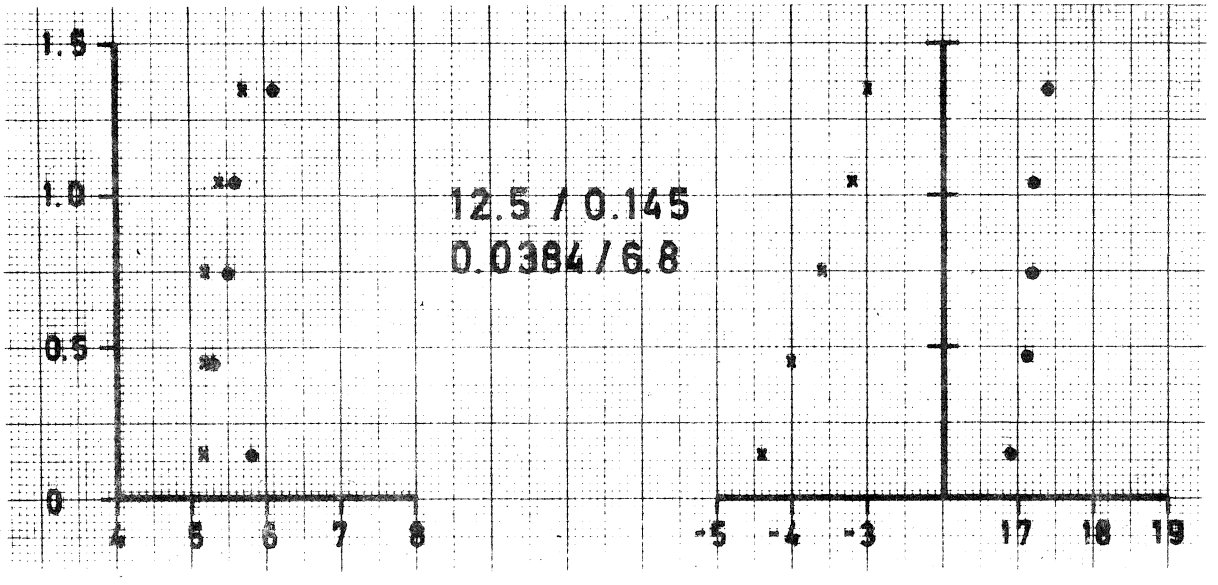
1.5
1.0
0.5
0
4 5 6 7 8
12.5 / 0.145
0.0384 / 6.8
-5 -4 -3 17 18 19

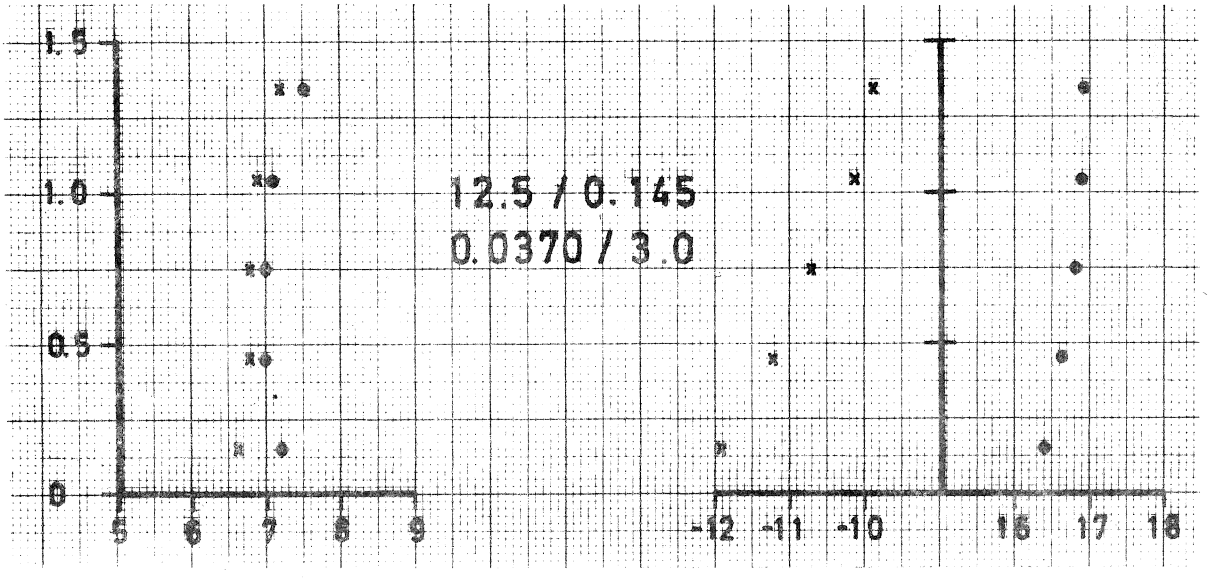
1.5
1.0
0.5
0
5 6 7 8 9
12.5 / 0.145
0.0370 / 3.0
-12 -11 -10 16 17 18

GLASS FIBER

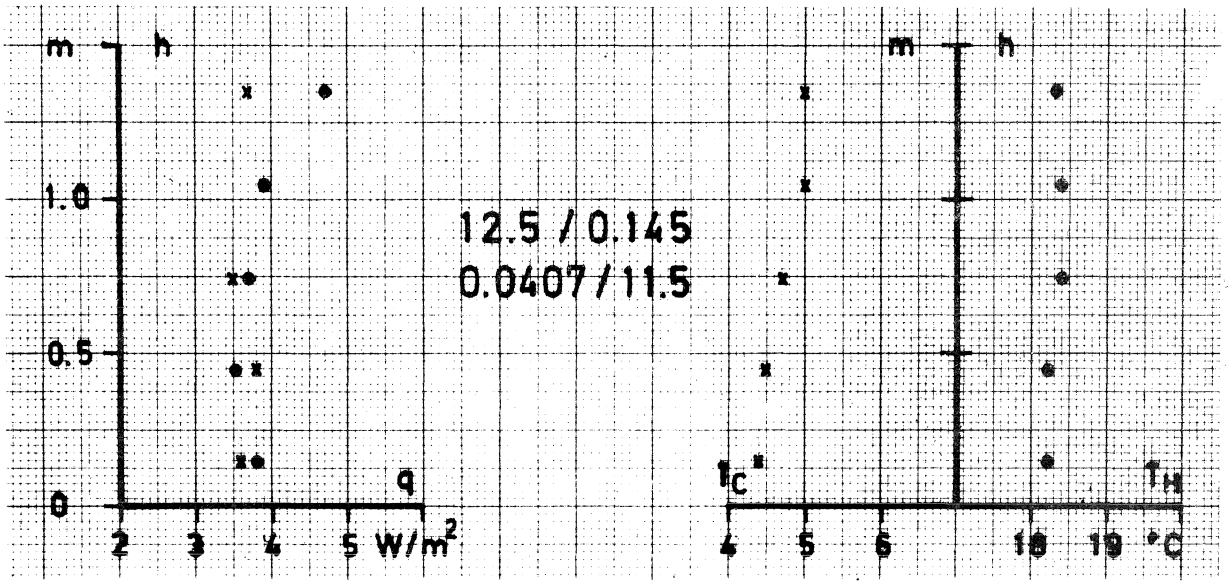
m
h
1.0
0.5
0
q
2
3
4
5 W/m²
12.5 / 0.145
0.0407 / 11.5
m
h
t_C
T_H
4
5
6
18
19
°C

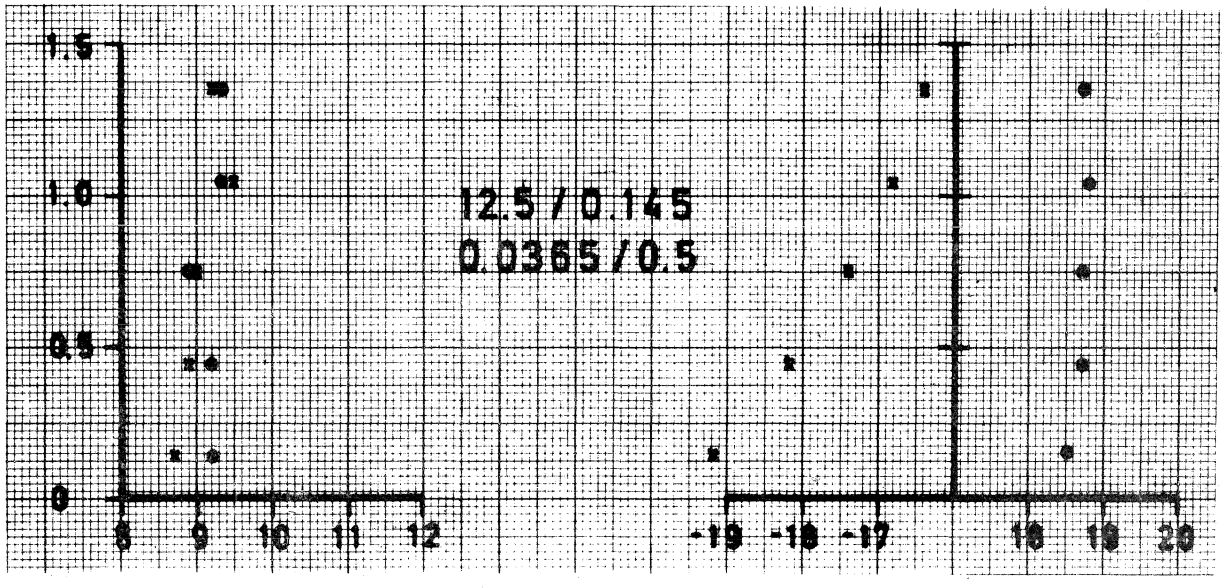
1.5
1.0
0.5
0
8
9
10
11
12
12.5 / 0.145
0.0365 / 0.5
-19
-18
-17
18
19
20

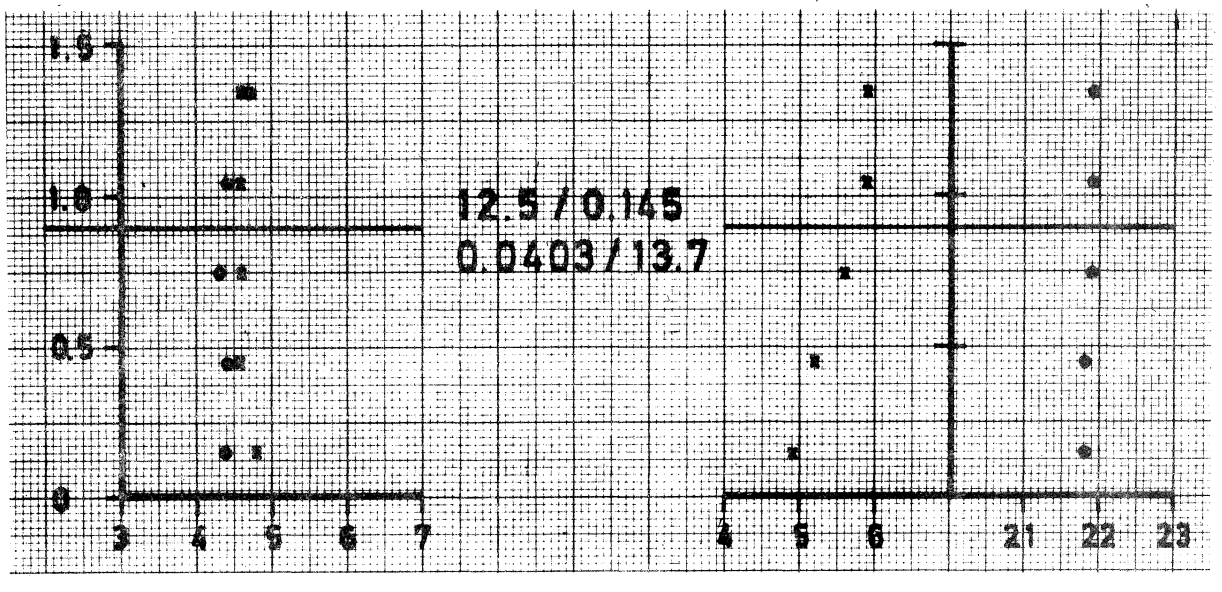
1.5
1.0
0.5
0
3
4
5
6
7
12.5 / 0.145
0.0403 / 13.7
4
5
6
21
22
23

GLASS FIBER

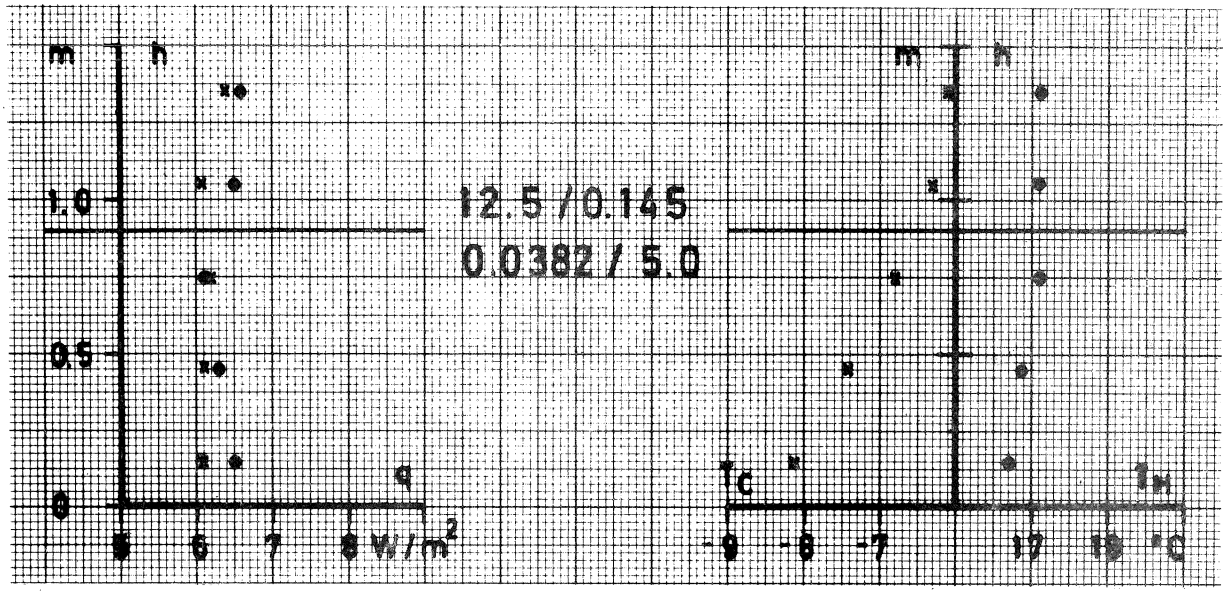
m
h
1.0
0.5
0
q
6
7
8 W/m²
12.5 / 0.145
0.0382 / 5.0
m
h
T_c
T_M
-9
-8
-7
17
18
°C

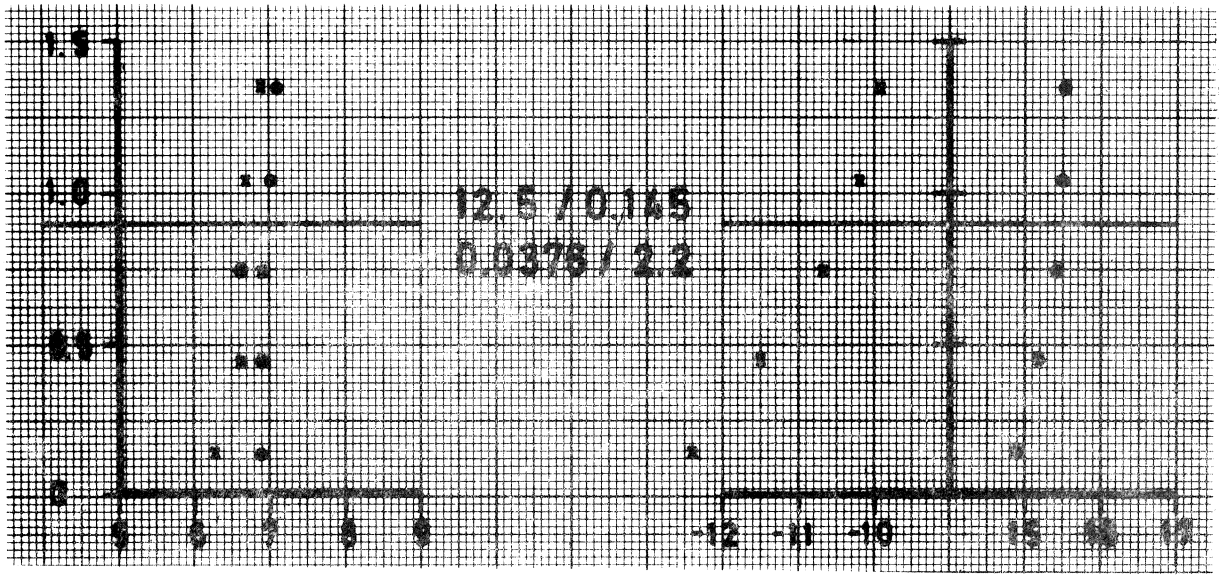
1.5
1.0
0.5
0
-12
-11
-10
12.5 / 0.145
0.0378 / 2.2

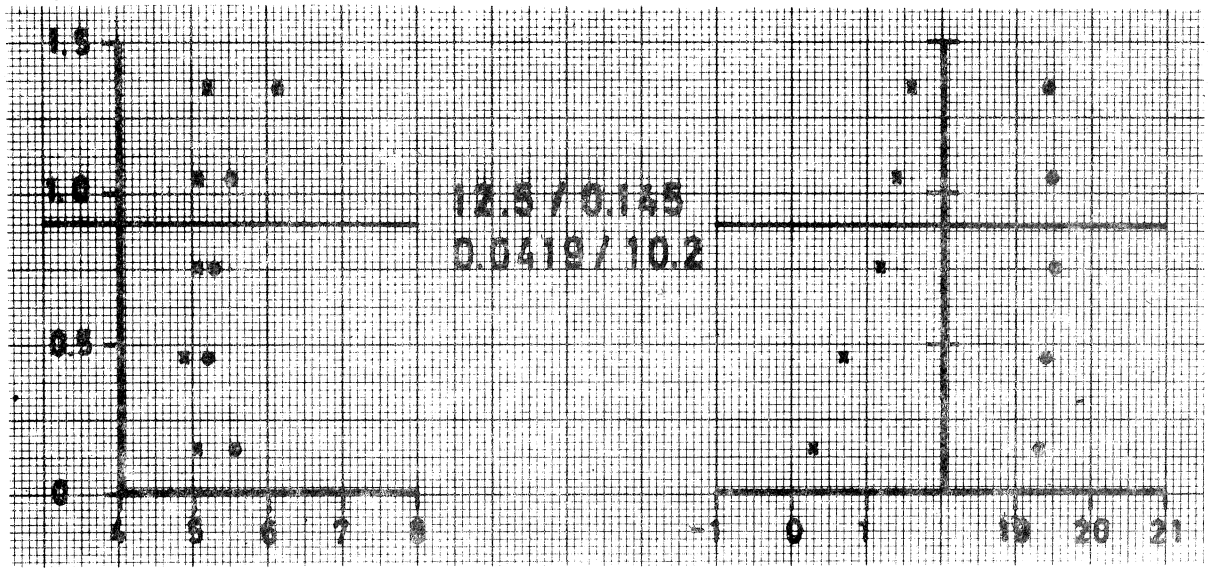
1.5
1.0
0.5
0
4
5
6
7
8
-1
0
1
19
20
21
12.5 / 0.145
0.0419 / 10.2

GLASS FIBER

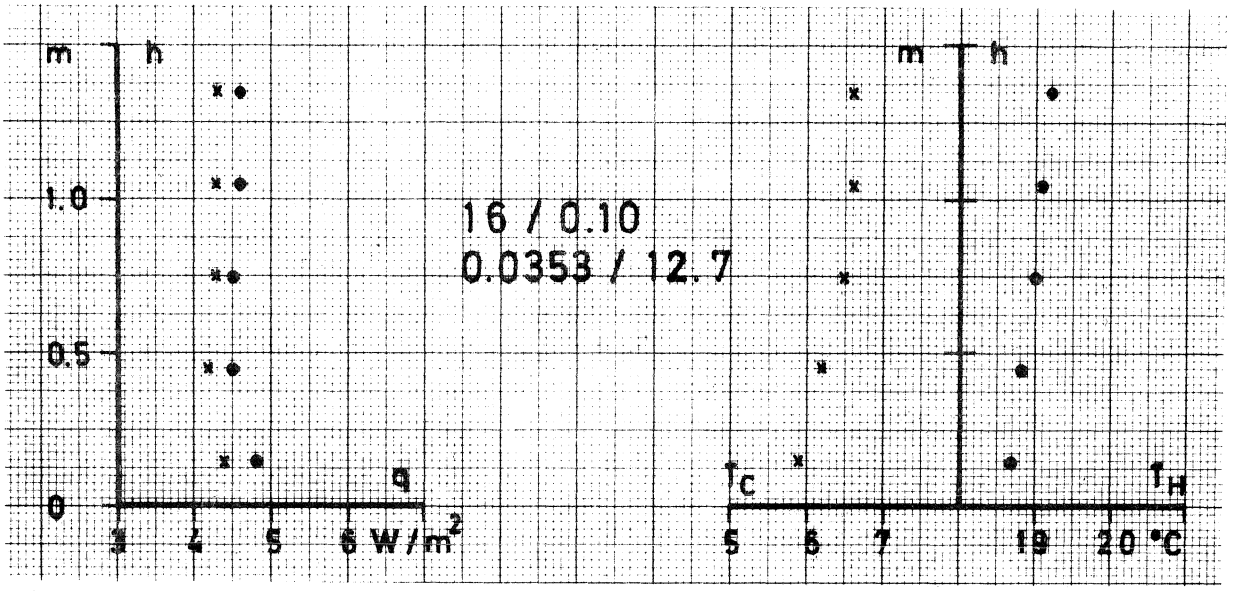
m
h
1.0
0.5
0
q
3
4
5
6 W/m²
16 / 0.10
0.0353 / 12.7
m
h
T_C
T_H
5
6
7
19
20 °C

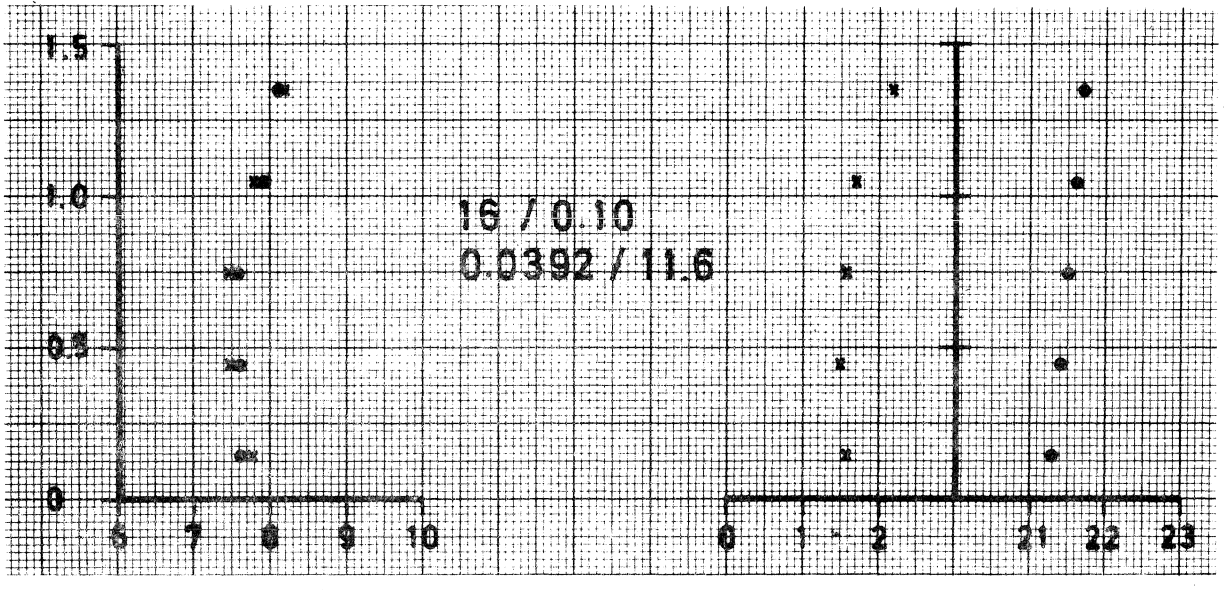
1.5
1.0
0.5
0
5
7
8
9
10
16 / 0.10
0.0392 / 11.6
0
1
2
21
22
23

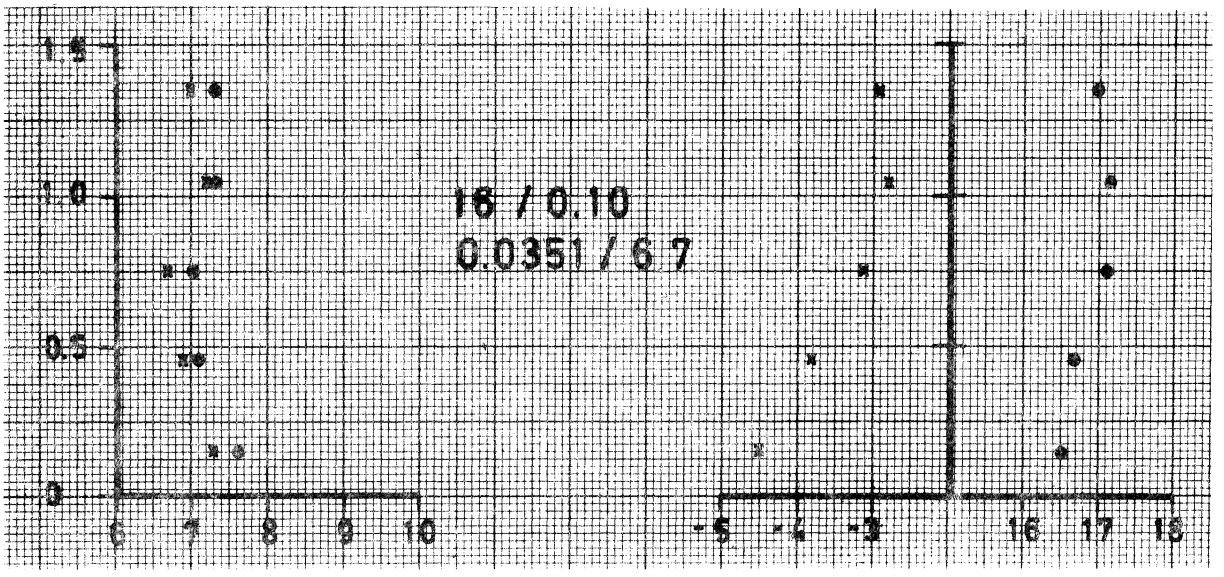
1.5
1.0
0.5
0
6
7
8
9
10
16 / 0.10
0.0351 / 6.7
-5
-4
-3
16
17
18

GLASS FIBER

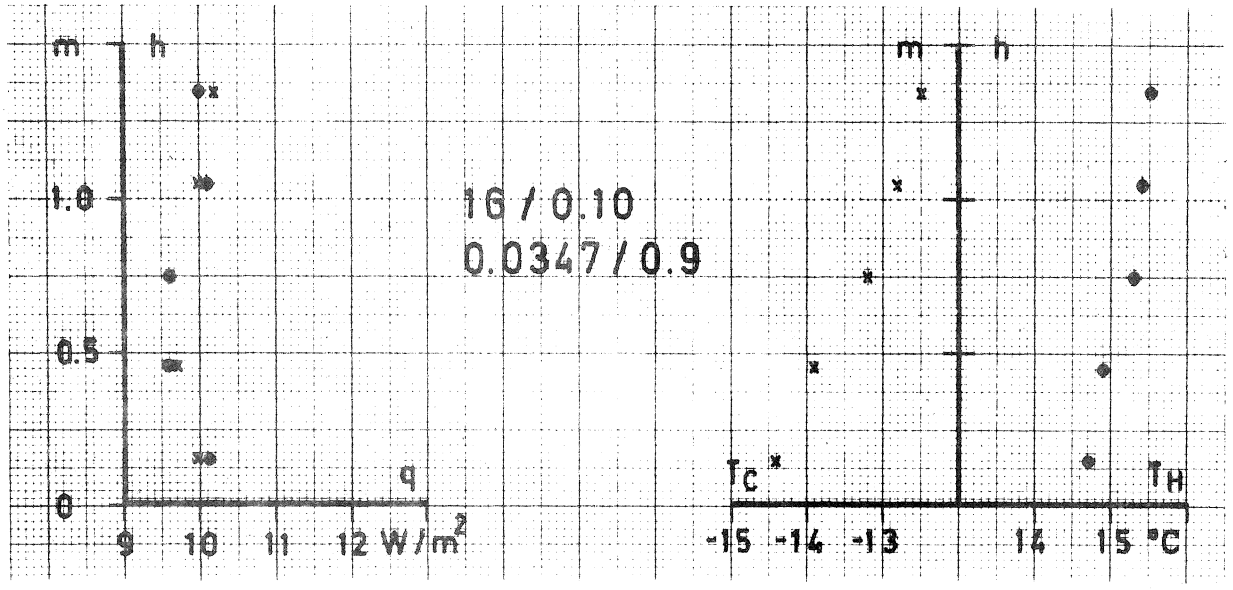
m
h
1.0
0.5
0
q
9
10
11
12 W/m²
16 / 0.10
0.0347 / 0.9
m
h
T_C
T_H
-15
-14
-13
14
15 °C

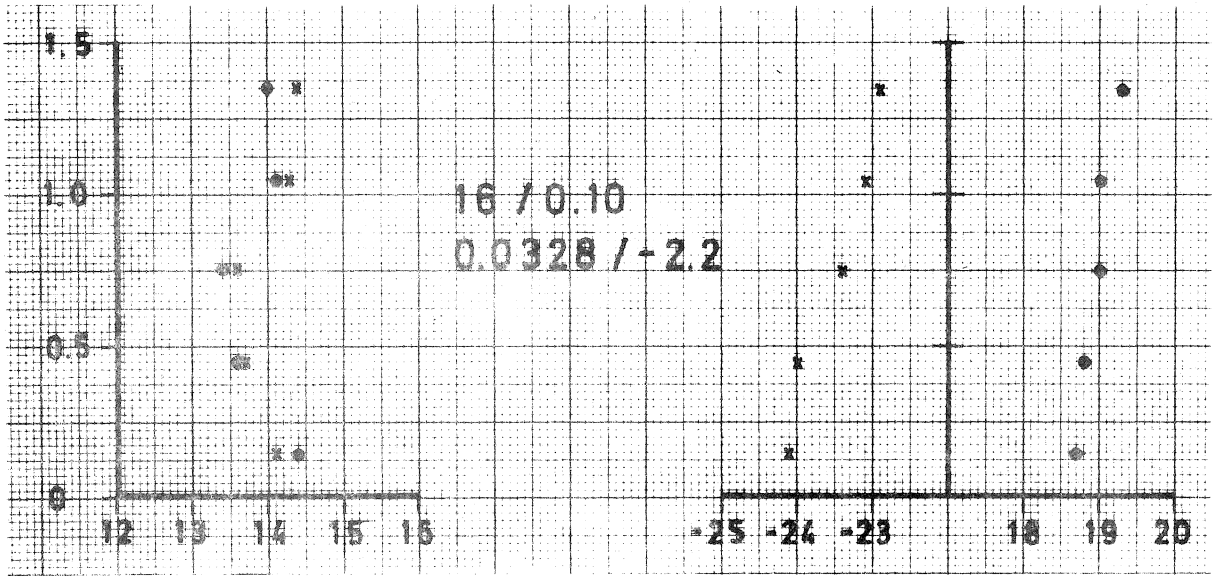
1.5
1.0
0.5
0
12
13
14
15
16
16 / 0.10
0.0328 / -2.2
-25
-24
-23
18
19
20

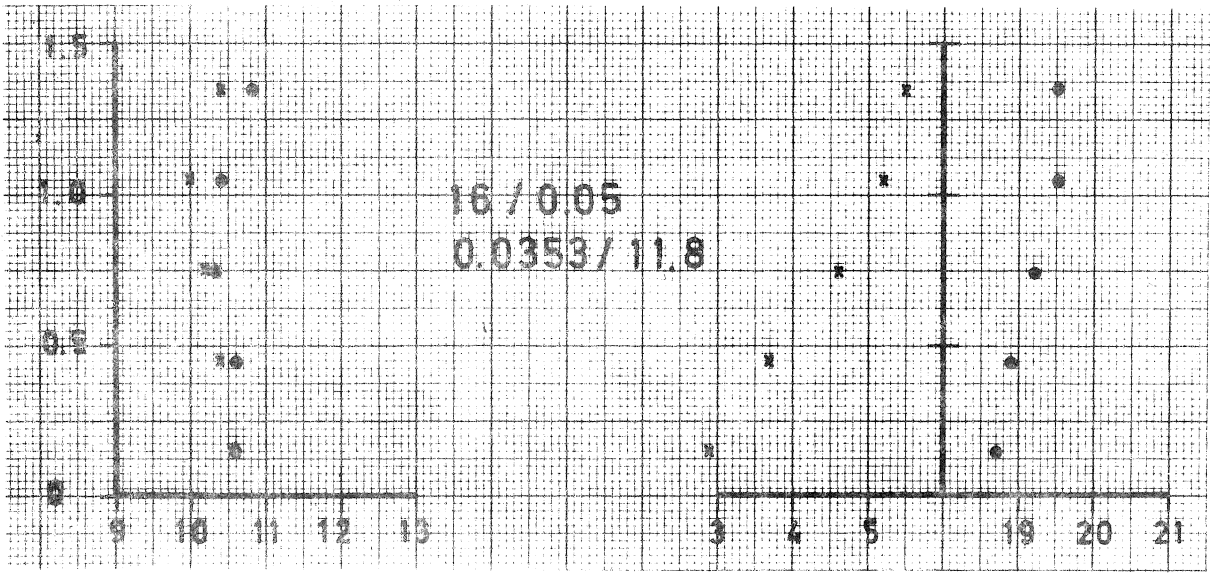
1.5
1.0
0.5
0
9
10
11
12
16 / 0.05
0.0353 / 11.8
3
4
5
19
20
21

GLASS FIBER

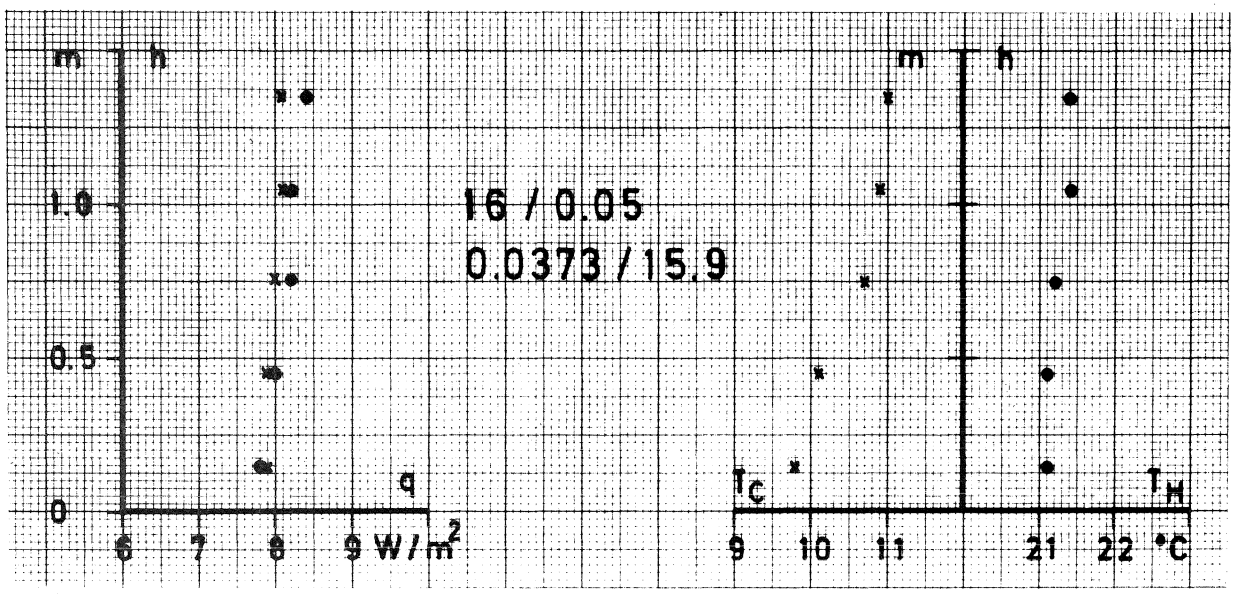
m
h
1.0
0.5
0
q
6 7 8 9 W/m²
16 / 0.05
0.0373 / 15.9
m
h
T_C
T_H
9 10 11 21 22 °C

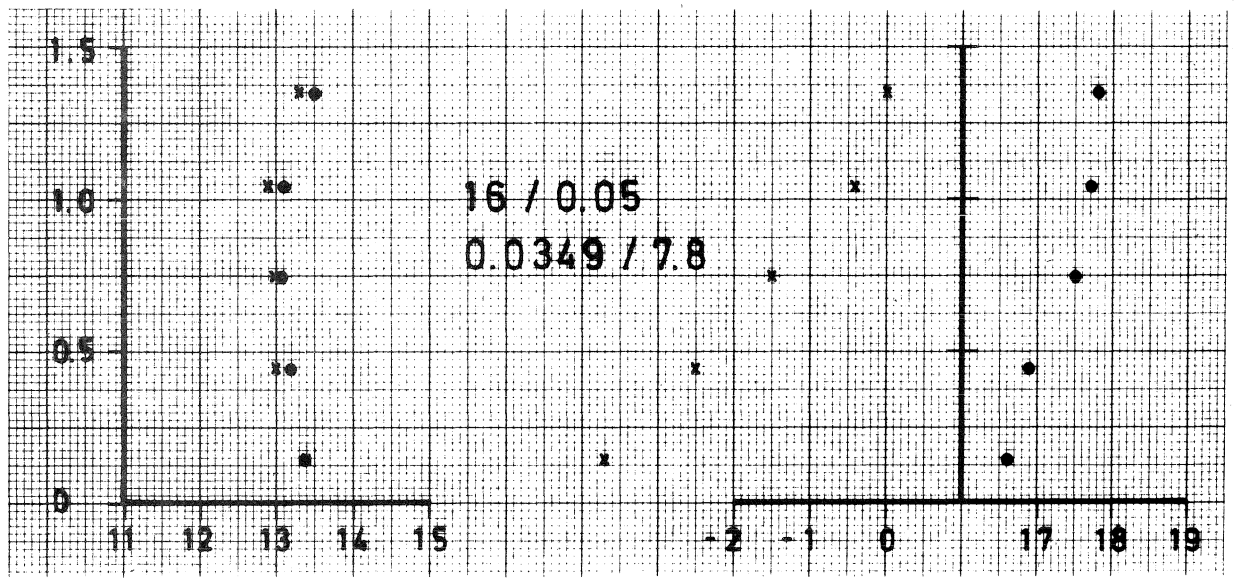
1.5
1.0
0.5
0
11 12 13 14 15
16 / 0.05
0.0349 / 7.8
-2 -1 0 17 18 19

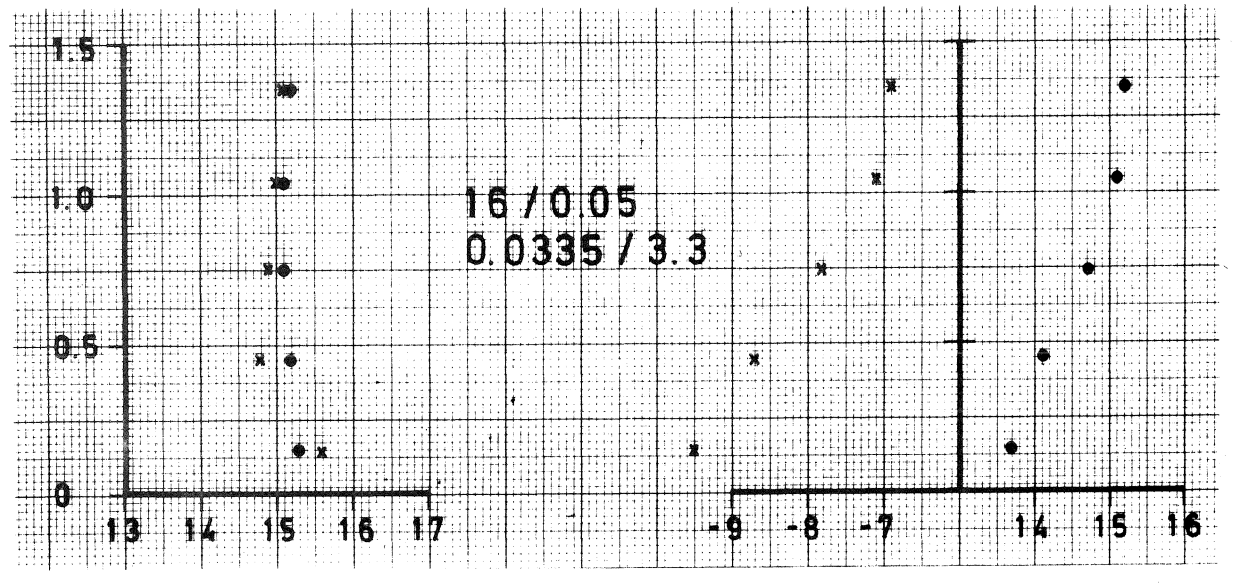
1.5
1.0
0.5
0
13 14 15 16 17
16 / 0.05
0.0335 / 3.3
-9 -8 -7 14 15 16

GLASS FIBER

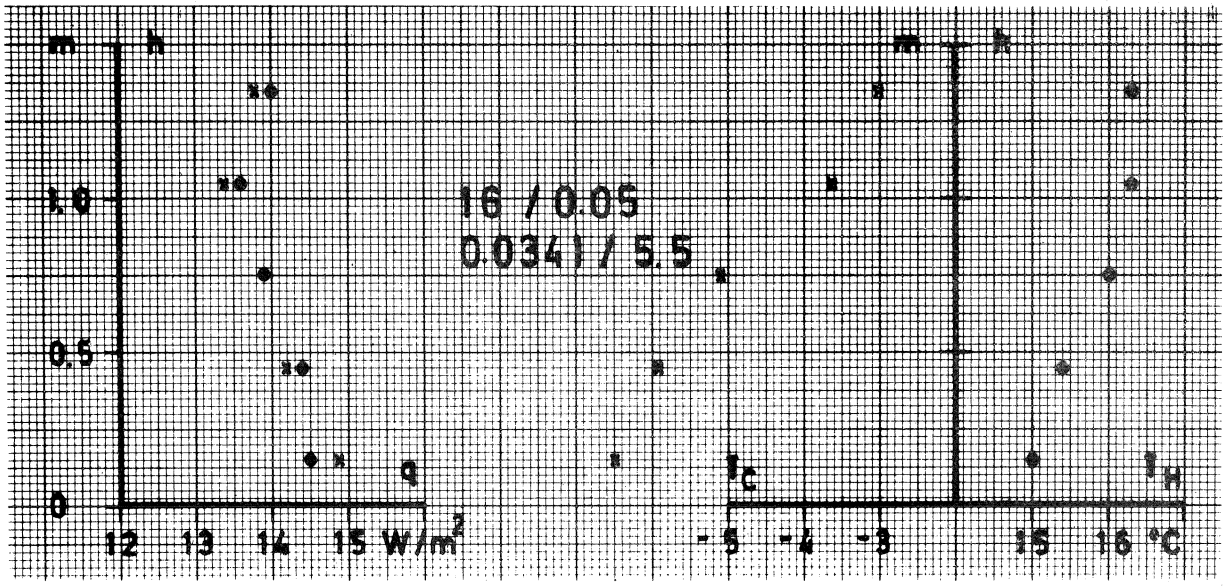
m
h
1.0
0.5
0
16 / 0.05
0.0341 / 5.5
q
12 13 14 15 W/m²
t_C
t_H
-5 -4 -3
15 16 °C

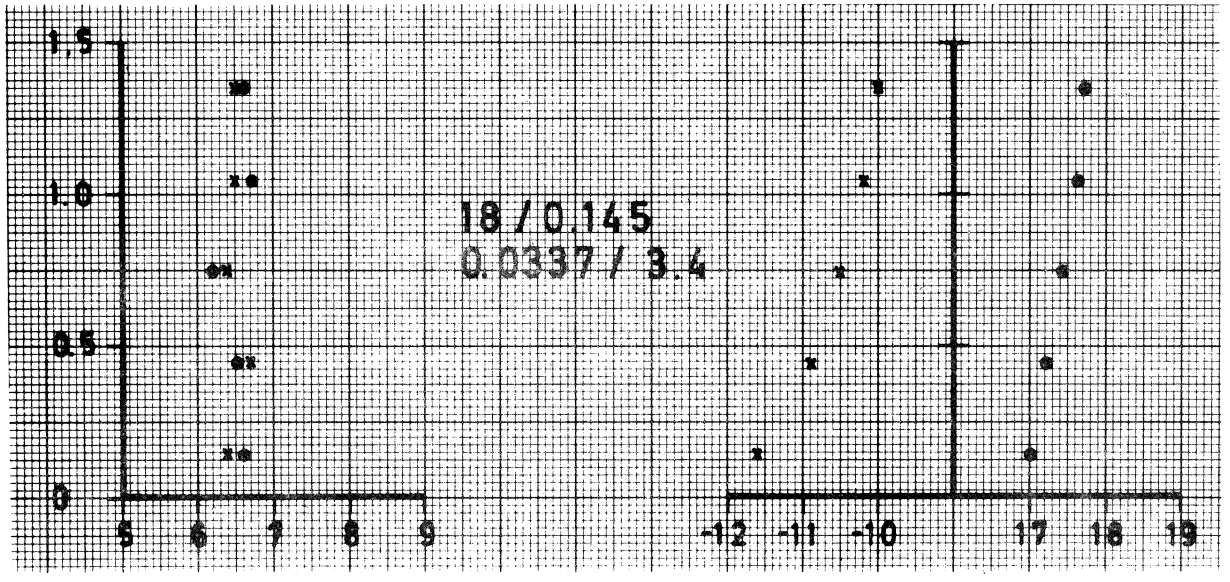
1.5
1.0
0.5
0
18 / 0.145
0.0337 / 3.4
5 6 7 8 9
-12 -11 -10
17 18 19

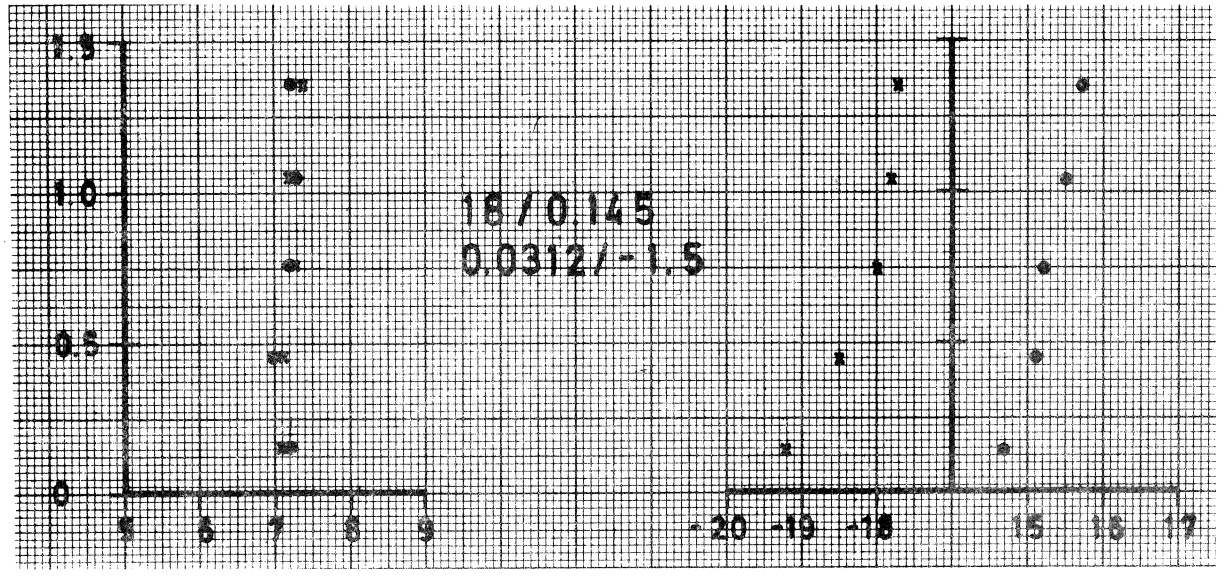
1.5
1.0
0.5
0
18 / 0.145
0.0312 / -1.5
5 6 7 8 9
-20 -19 -18
15 16 17

GLASS FIBER

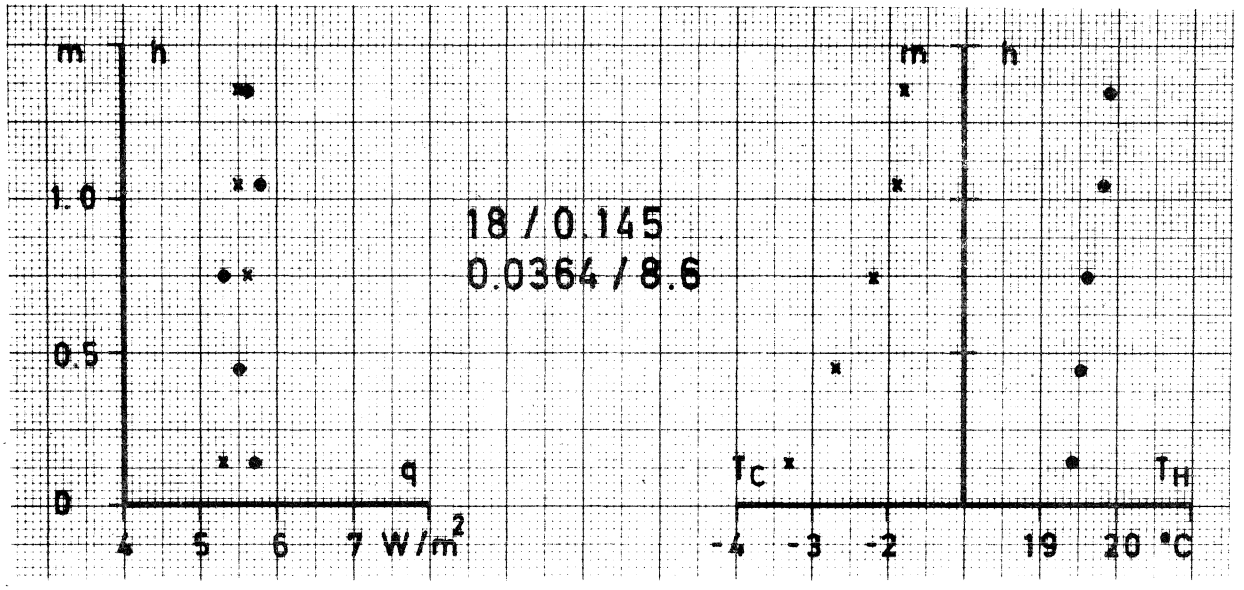
m
h
1.0
0.5
0
q
4 5 6 7 W/m²
18 / 0.145
0.0364 / 8.6
m
h
Tc
TH
-4 -3 -2 19 20 °C

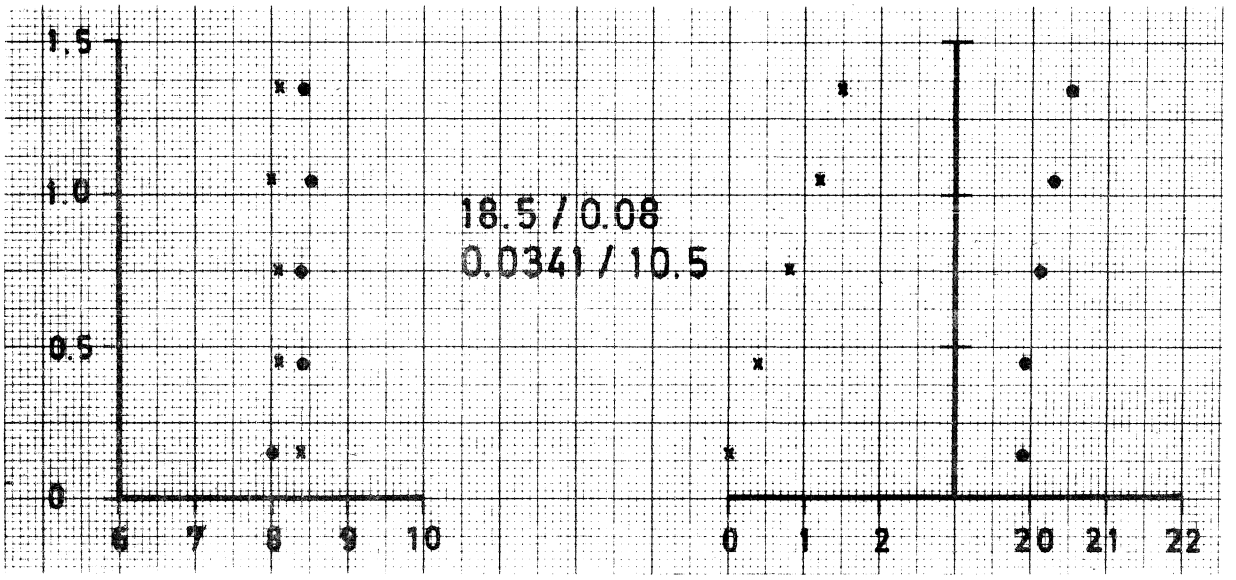
1.5
1.0
0.5
0
6 7 8 9 10
18.5 / 0.08
0.0341 / 10.5
0 1 2 20 21 22

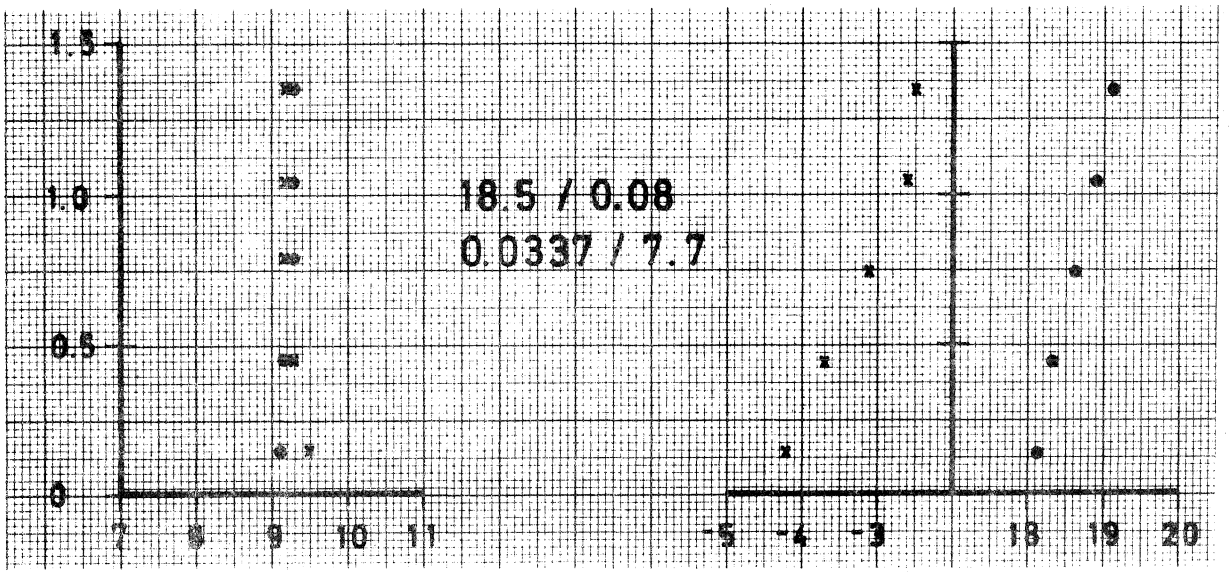
1.5
1.0
0.5
0
7 8 9 10 11
18.5 / 0.08
0.0337 / 7.7
-5 -4 -3 18 19 20

GLASS FIBER

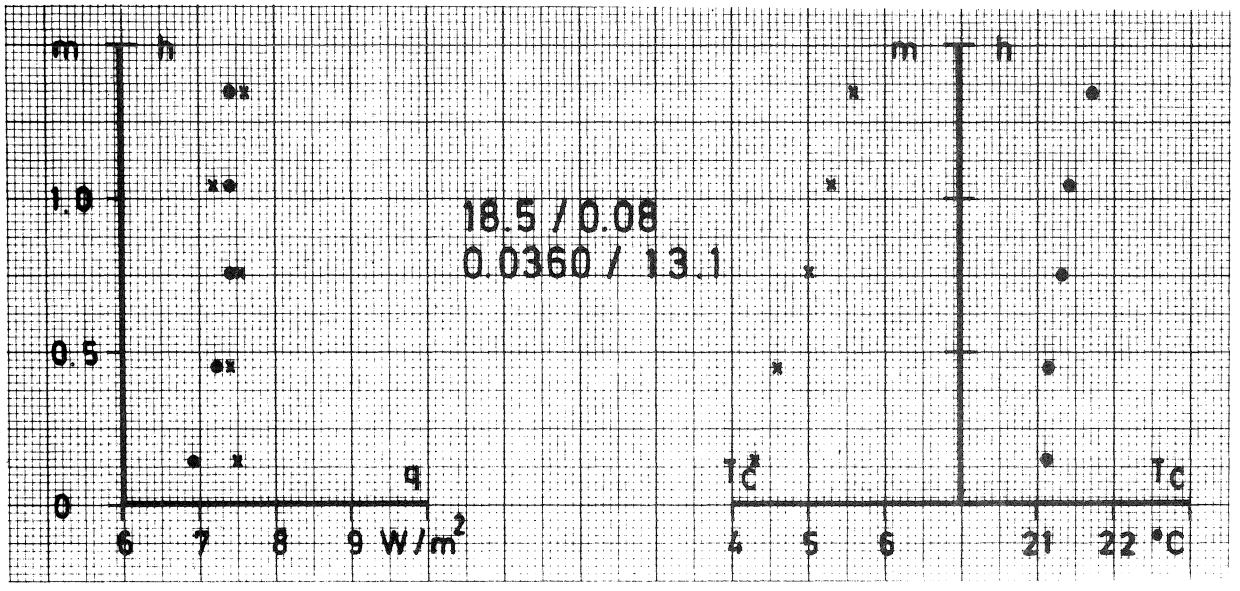
m
h
1.0
0.5
0
q
6
7
8
9 W/m²
18.5 / 0.08
0.0360 / 13.1
m
h
Tc²
Tc
4
5
6
21
22 °C

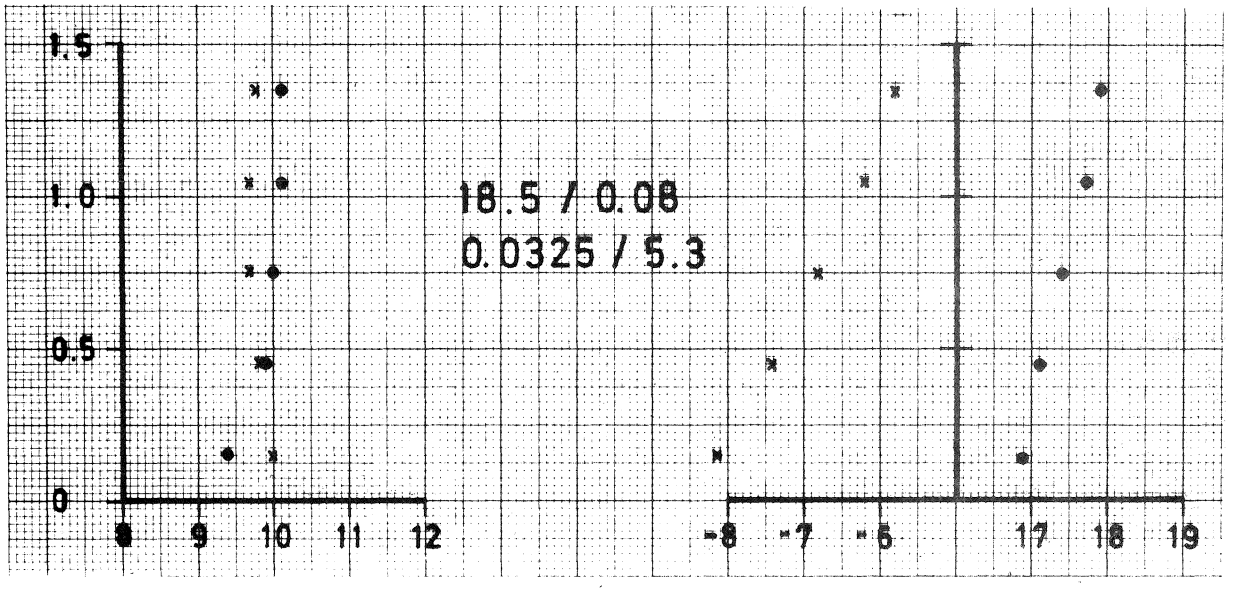
1.5
1.0
0.5
0
9
10
11
12
18.5 / 0.08
0.0325 / 5.3
-8
-7
-6
17
18
19

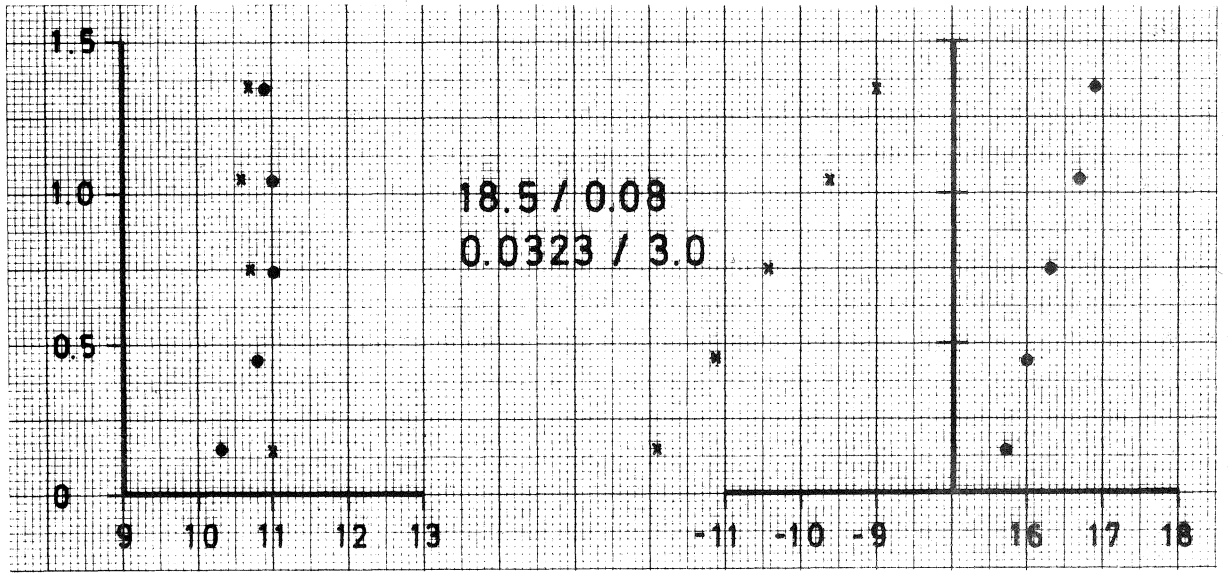
1.5
1.0
0.5
0
9
10
11
12
13
18.5 / 0.08
0.0323 / 3.0
-11
-10
-9
16
17
18

GLASS FIBER

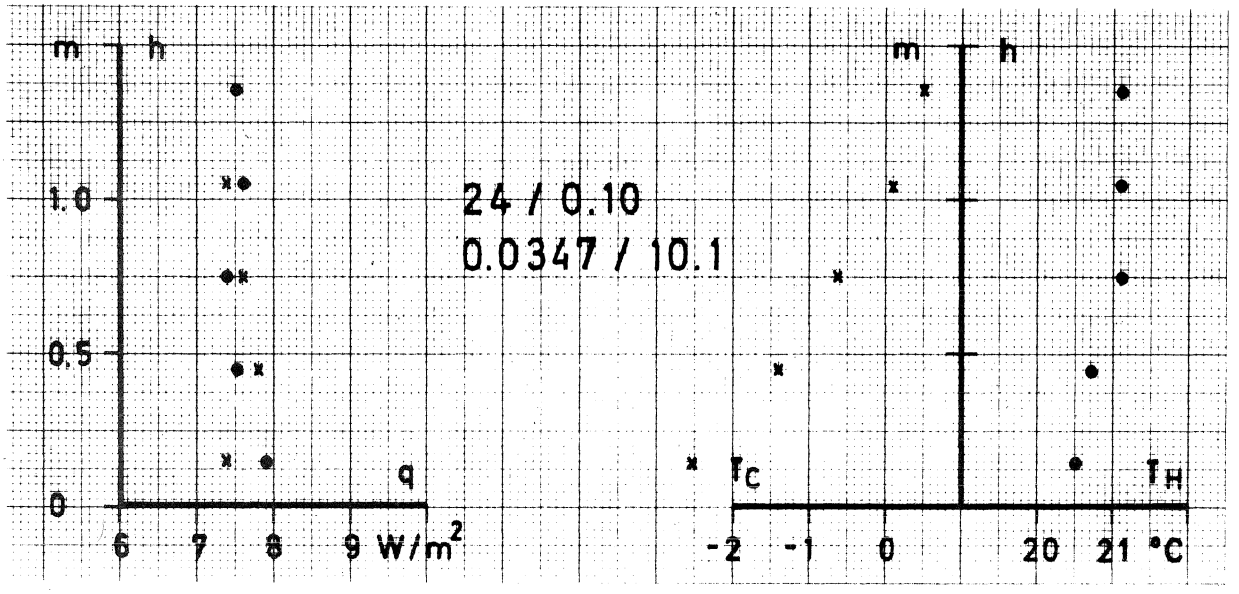
m
h
1.0
0.5
0
q
6
7
8
9 W/m²
24 / 0.10
0.0347 / 10.1
m
h
T_C
T_H
-2
-1
0
20
21 °C

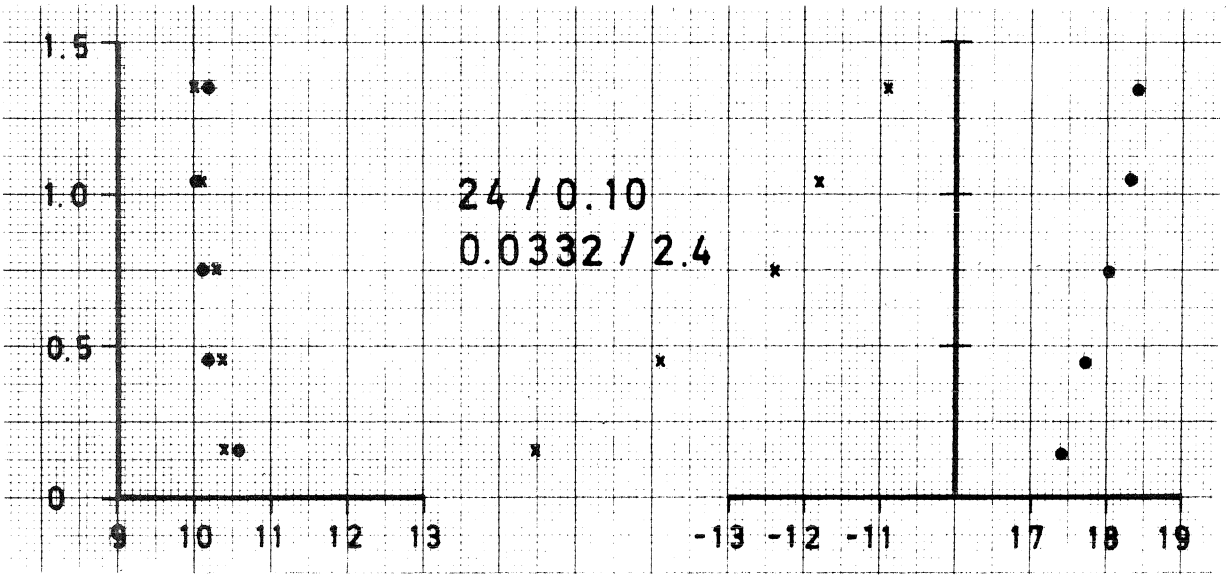
1.5
1.0
0.5
0
9
10
11
12
13
24 / 0.10
0.0332 / 2.4
-13
-12
-11
17
18
19

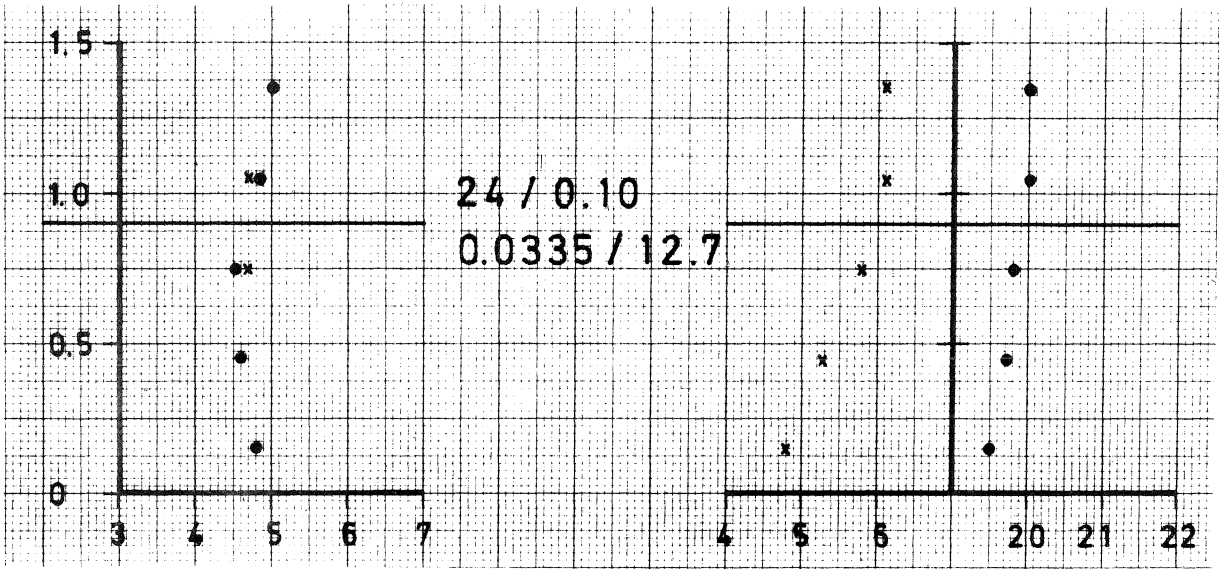
1.5
1.0
0.5
0
3
4
5
6
7
24 / 0.10
0.0335 / 12.7
4
5
6
20
21
22

GLASS FIBER

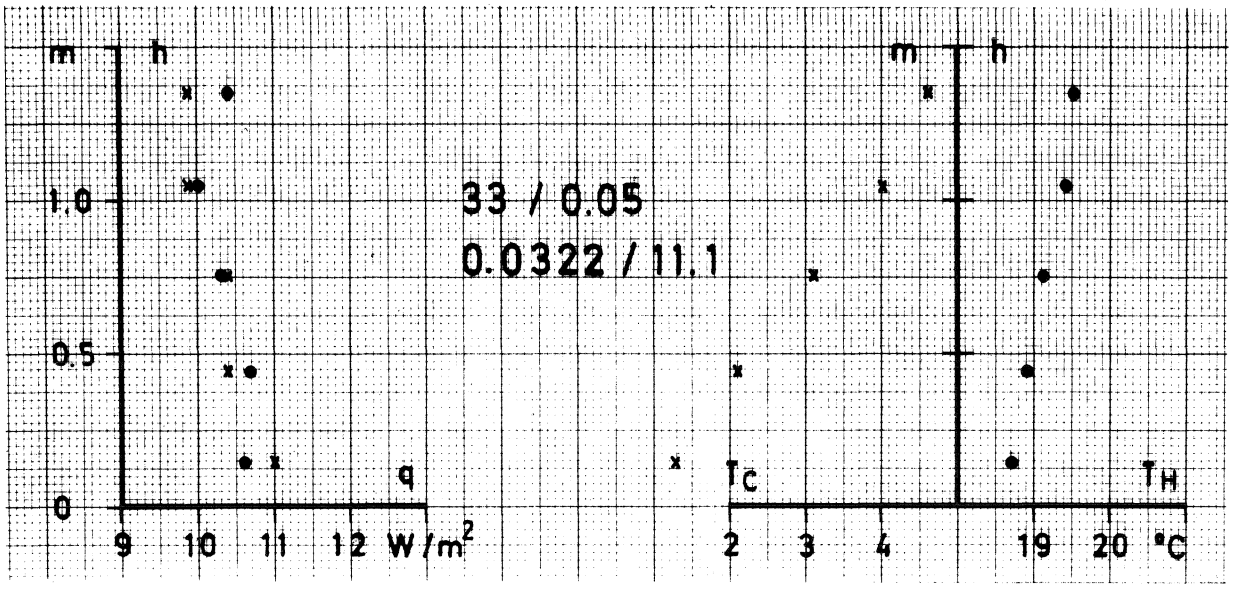
m
h
1.0
0.5
0
33 / 0.05
0.0322 / 11.1
q
9
10
11
12
W/m²
m
h
Tc
2
3
4
TH
19
20
°C

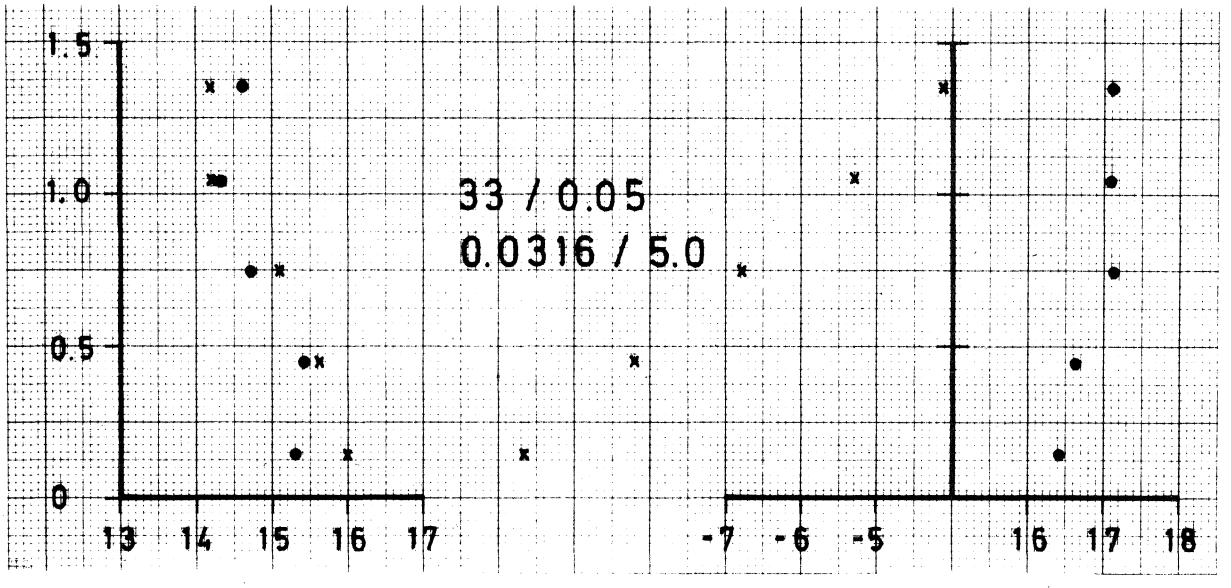
1.5
1.0
0.5
0
33 / 0.05
0.0316 / 5.0
13
14
15
16
17
-7
-6
-5
16
17
18

DIABASE FIBER

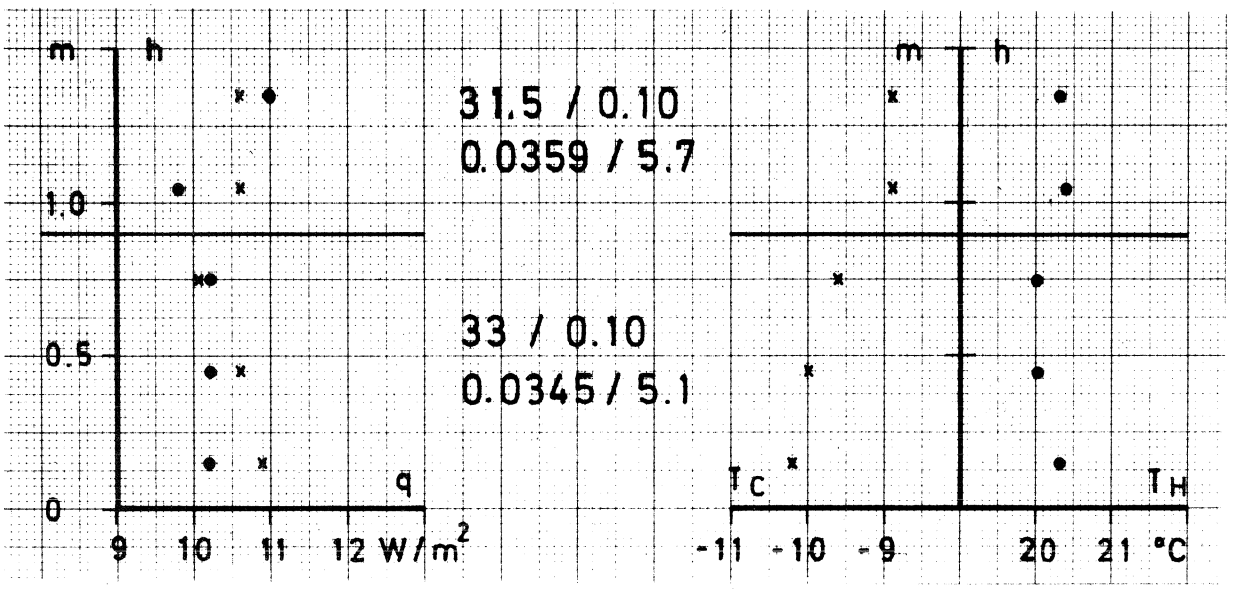

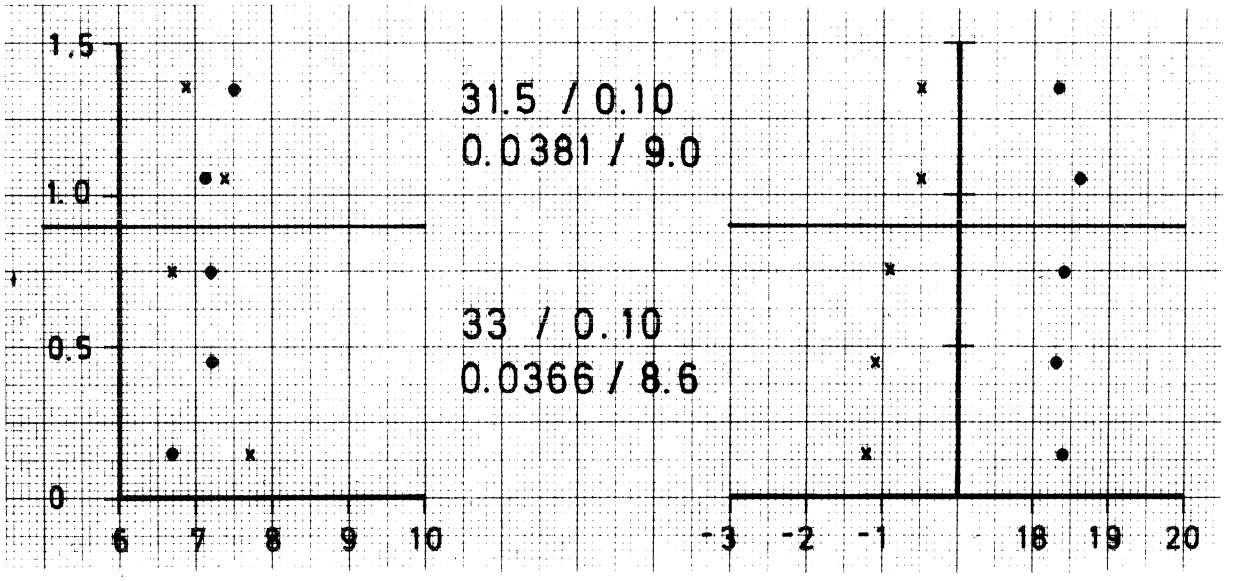

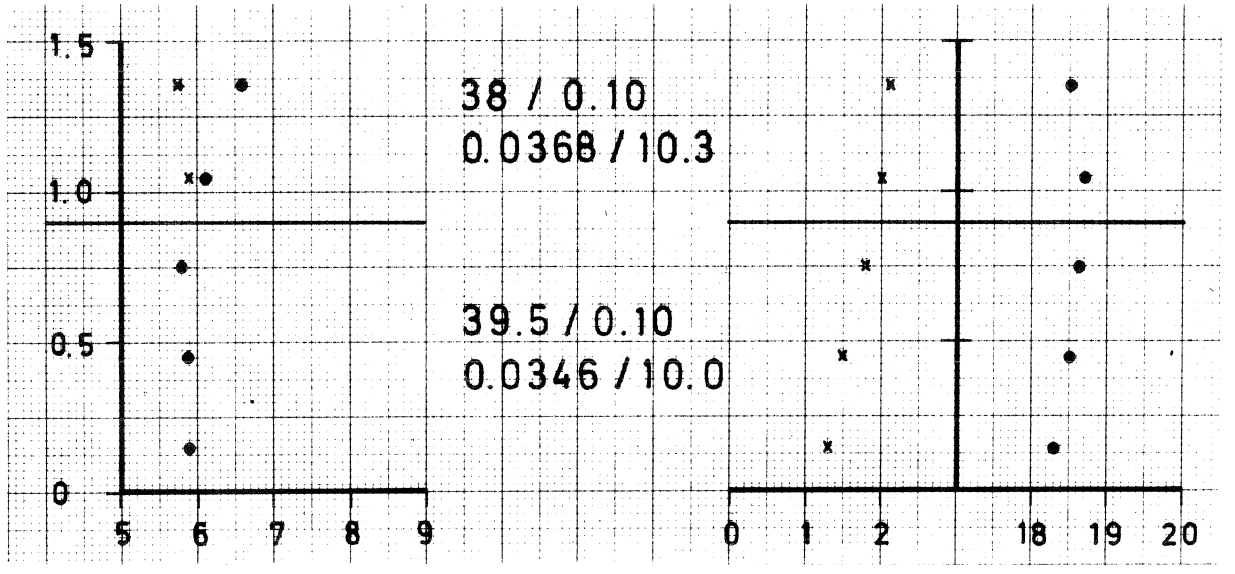

DIABASE FIBER

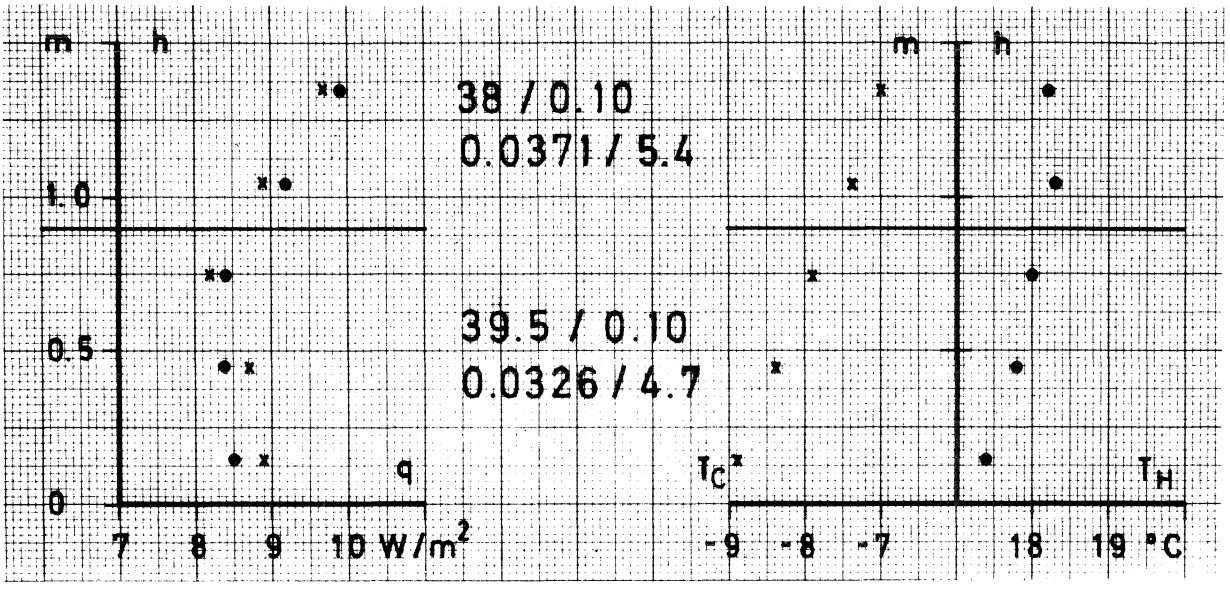

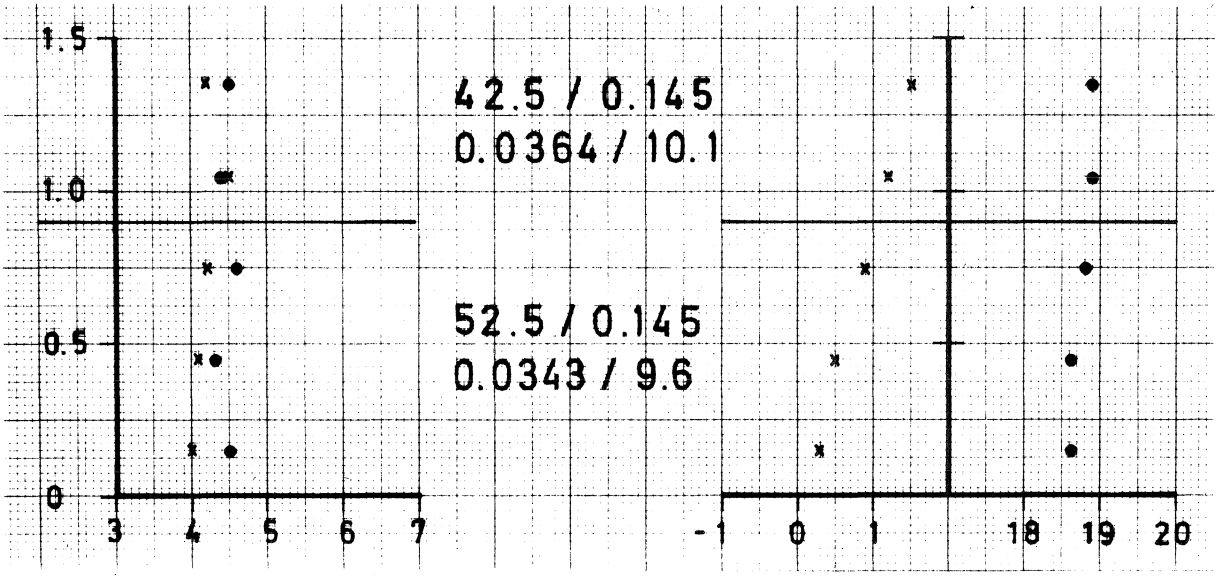

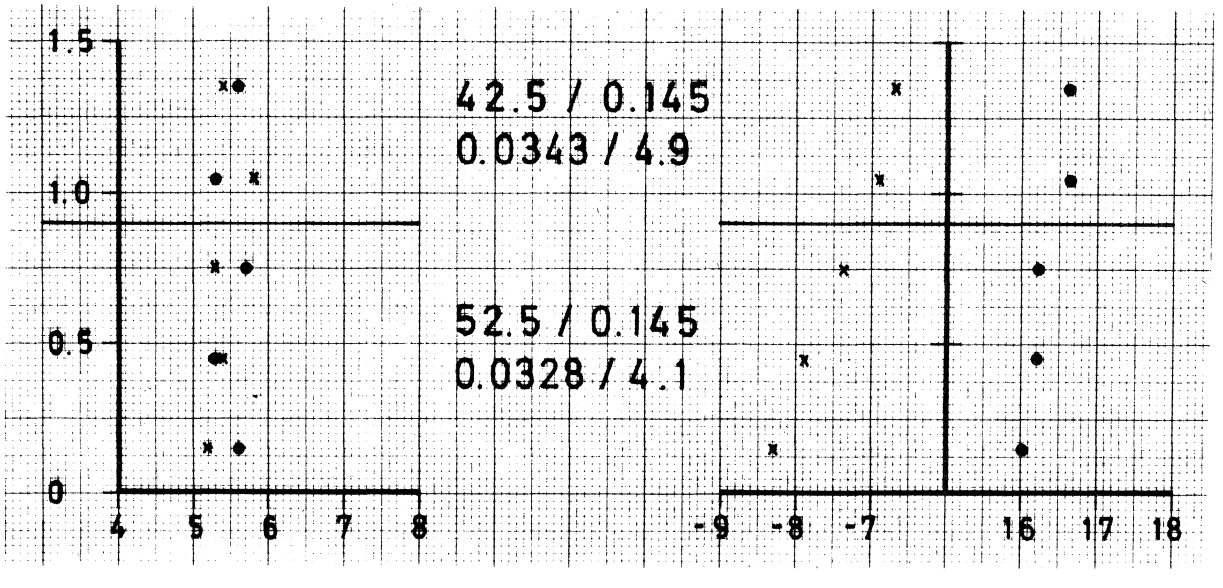

DIABASE FIBER

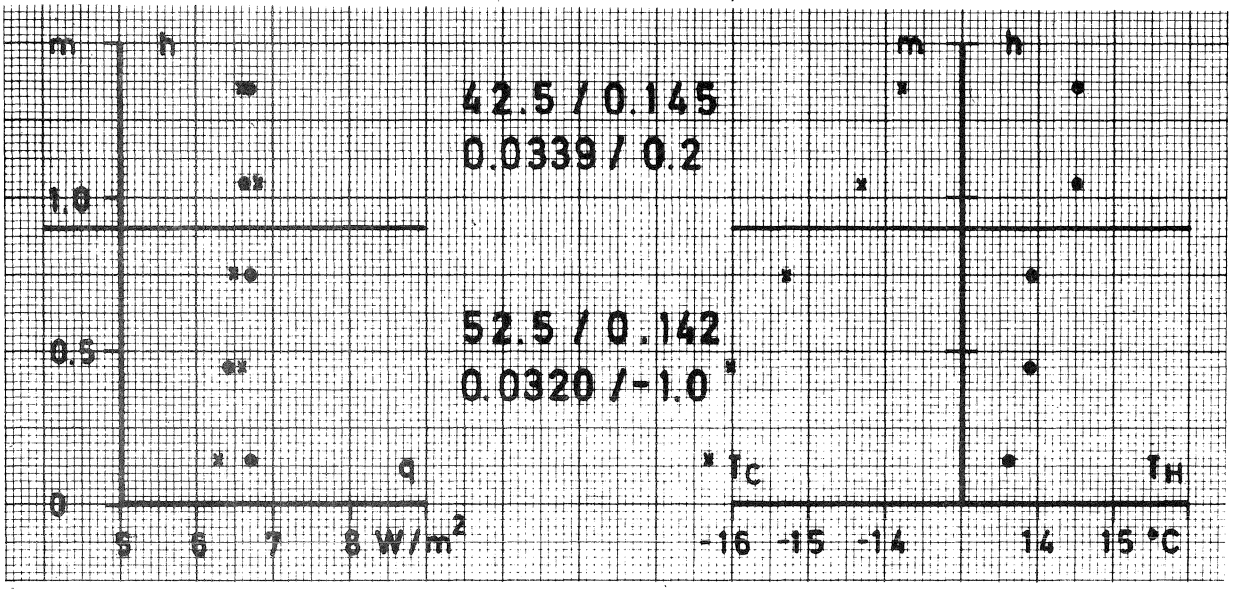

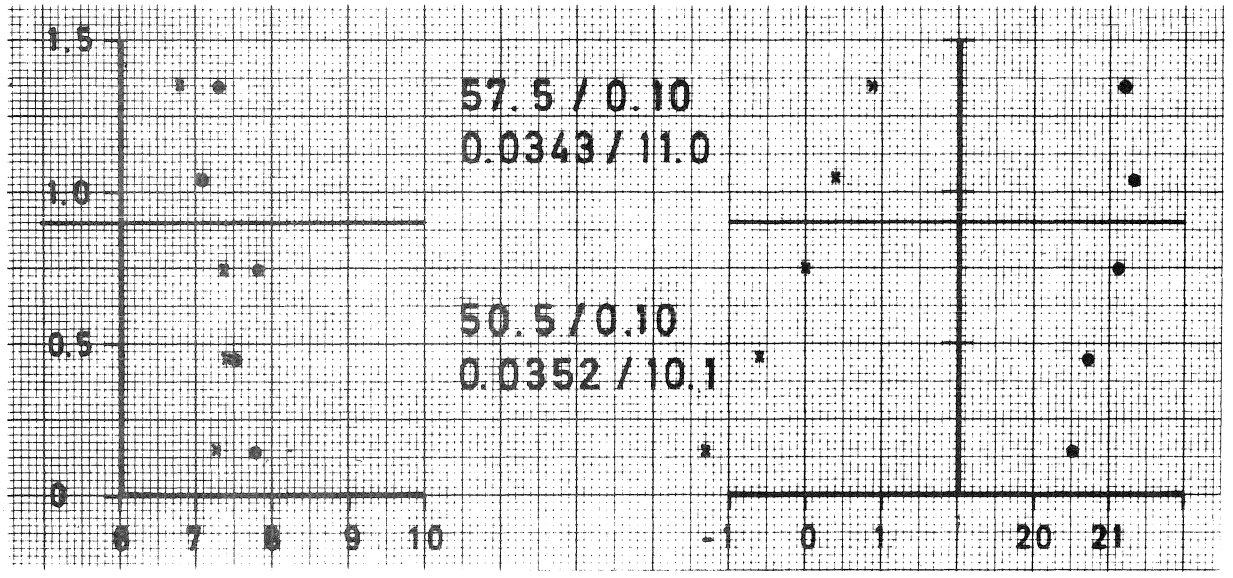

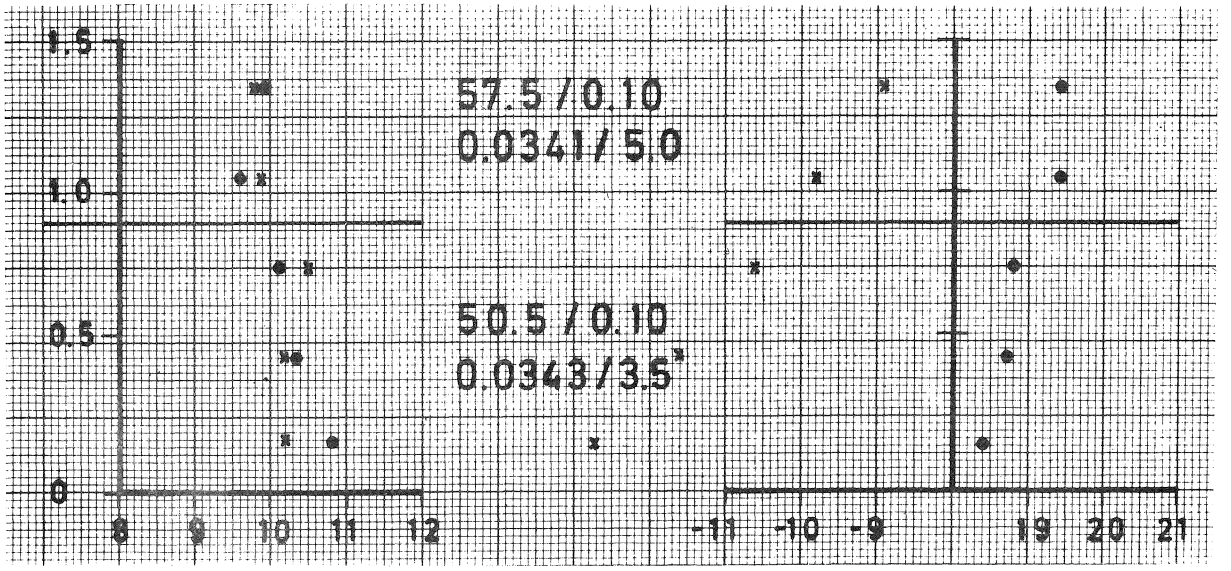

DIABASE FIBER

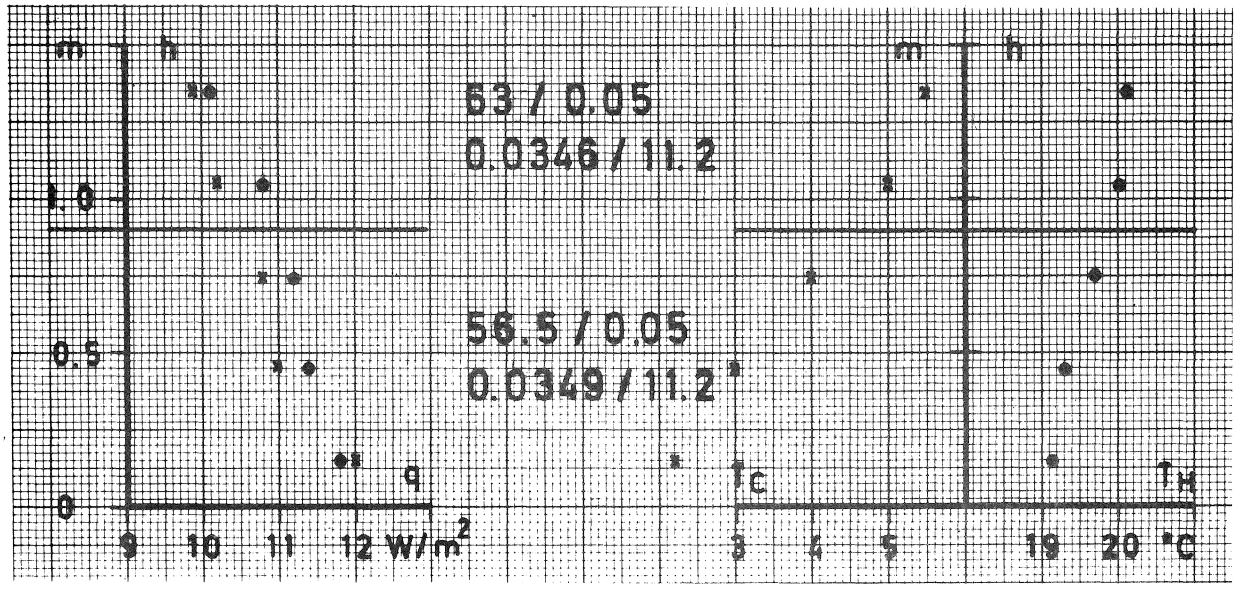

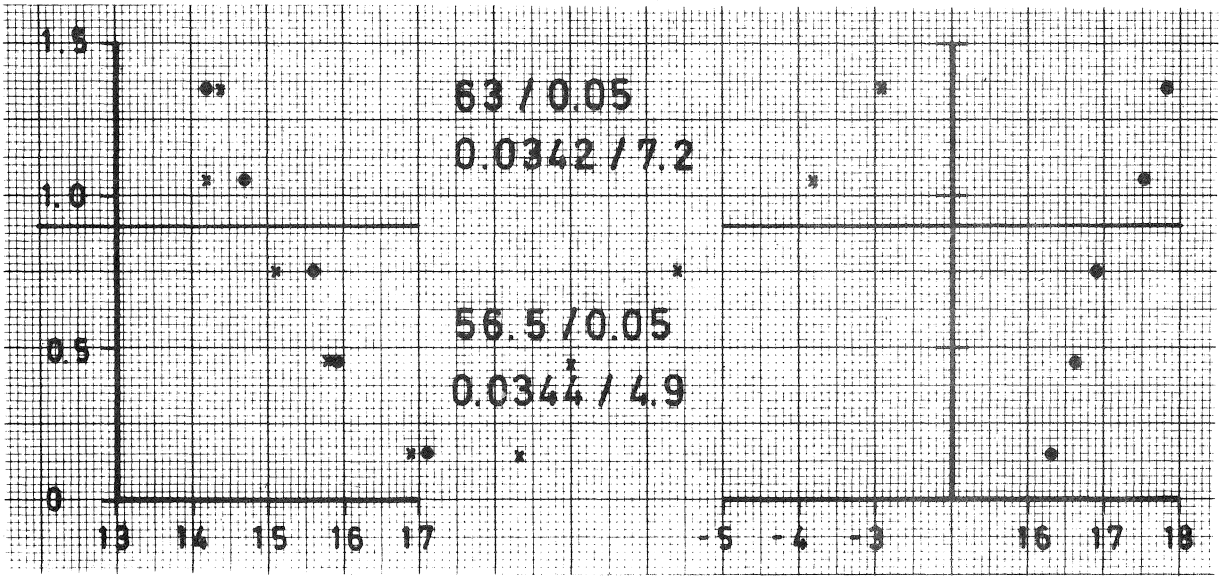

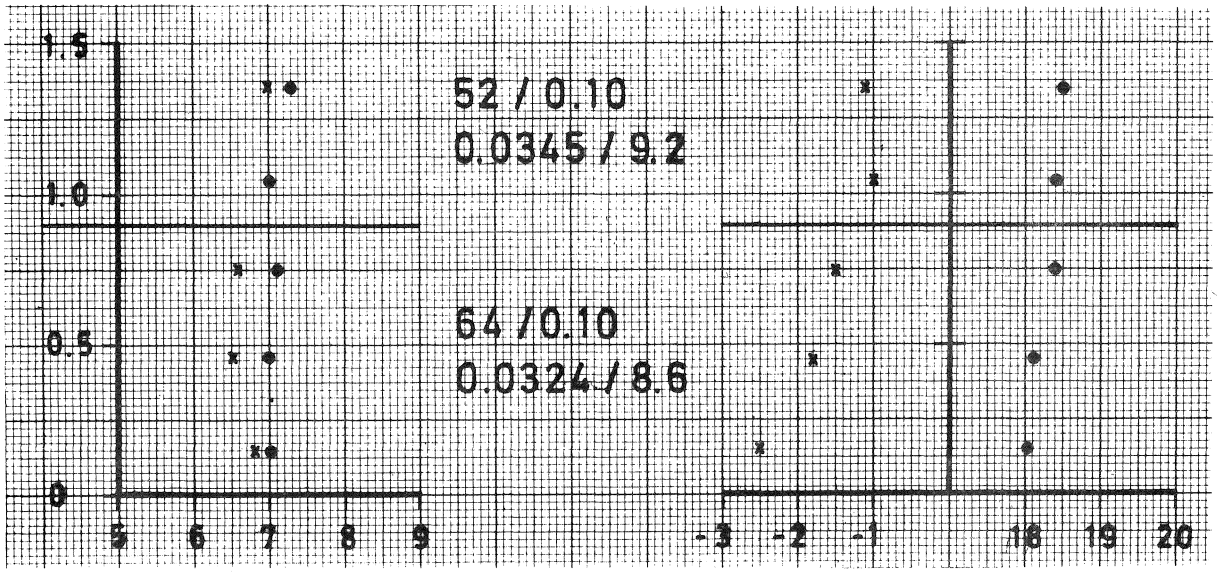

DIABASE FIBER

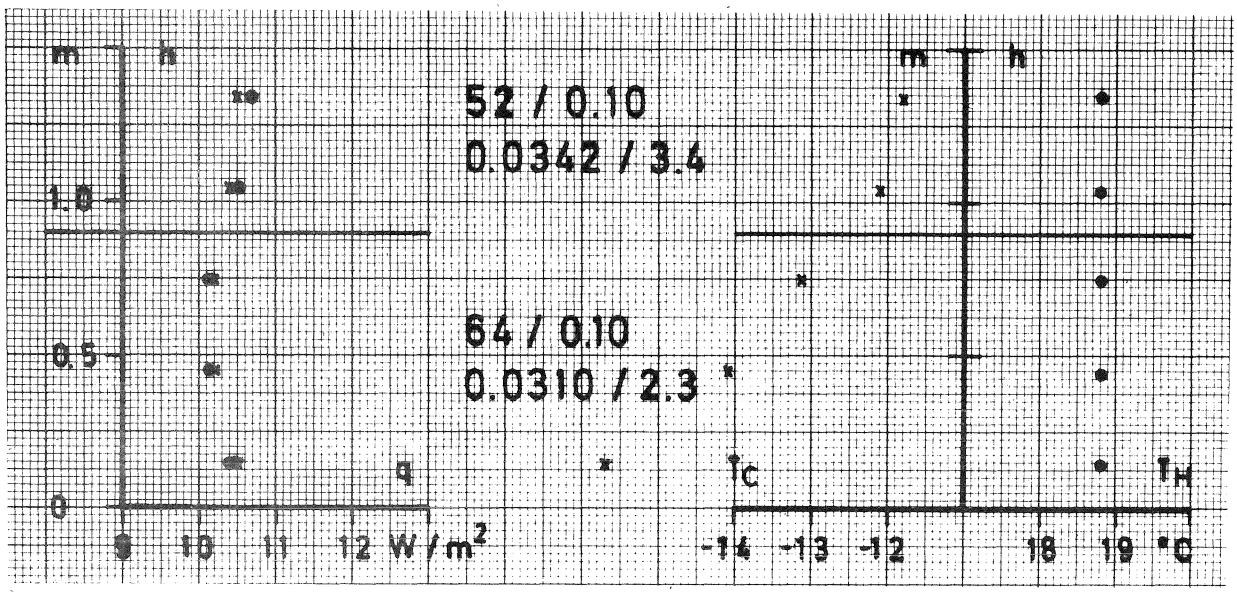

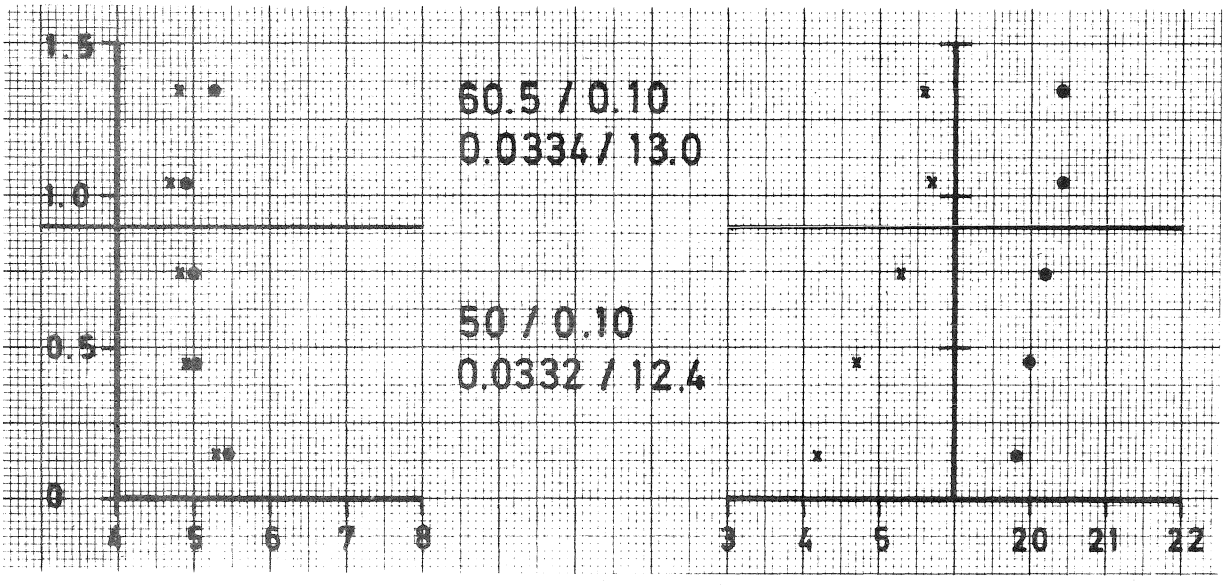

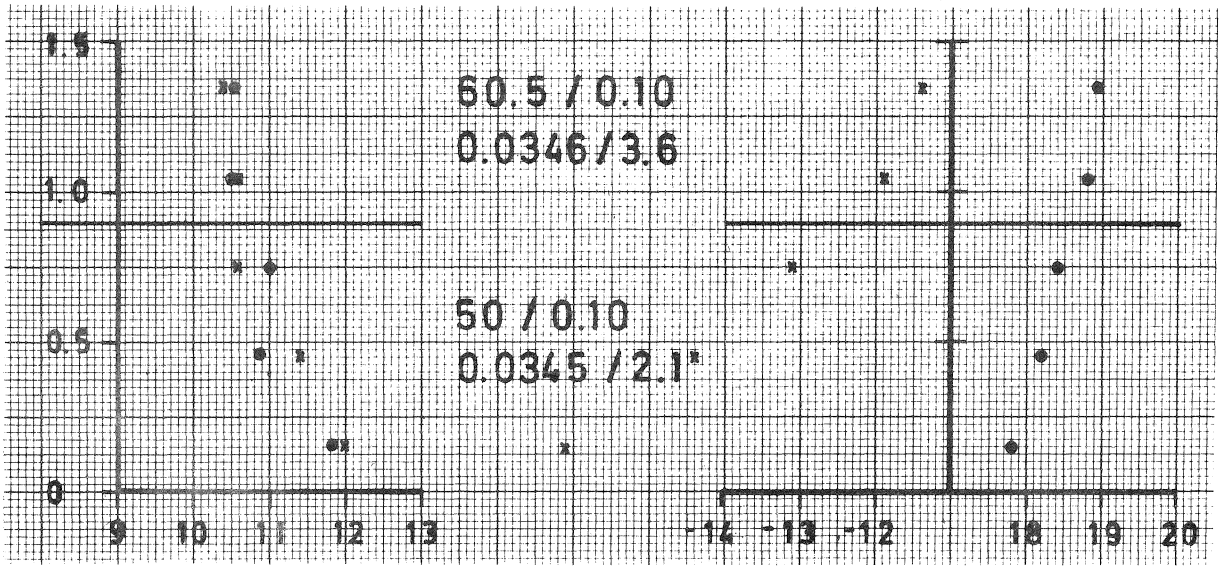

Glassfiber, ρ = 17 kg/m^3, "0".

Thermal resistance (m^2 K/W)			Mean temperature (^{o}C)		
2.62	2.68	2.49	7.0	7.0	7.1
2.49	2.57	2.47	6.1	6.2	5.9
2.56	2.64	2.47	4.9	5.1	4.6

Glassfiber, "ρ = 17 kg/m^3", vertical slits.

Thermal resistance (m^2 K/W)			Mean temperature (^{o}C)		
2.45	2.13	1.20	7.6	8.3	8.4
2.23	1.69	0.83	6.2	6.4	5.9
2.47	2.09	1.37	4.6	4.4	4.2

Glassfiber, ρ = 17.5 kg/m^3, "0".

Thermal resistance (m^2 K/W)			Mean temperature (^{o}C)		
2.52	2.68	2.49	6.7	6.8	6.9
2.49	2.67	2.44	5.7	5.9	5.6
2.59	2.63	2.46	4.7	4.9	4.5

Glassfiber, "ρ = 17.5 kg/m^3", horizontal slits.

Thermal resistance (m^2 K/W)			Mean temperature (^{o}C)		
1.10	0.65	0.93	7.6	9.1	9.5
2.17	2.03	2.12	6.5	6.6	6.6
2.36	2.27	2.26	5.4	5.8	5.1

Glassfiber, ρ = 15 kg/m^3, "0".

Thermal resistance (m^2 K/W)			Mean temperature (^{o}C)		
2.41	2.57	2.38	5.6	5.6	5.8
2.43	2.46	2.33	4.6	4.9	4.5
2.46	2.50	2.32	3.5	3.8	3.5

Glassfiber, ρ = 15 kg/m^3, d - 10 mm.

Thermal resistance (m^2 K/W)			Mean temperature ($^\circ$C)		
2.42	2.54	2.30	4.1	4.2	4.3
2.45	2.43	2.32	3.0	3.4	3.2
2.45	2.52	2.36	2.3	2.6	2.2

Glassfiber, ρ = 15 kg/m^3, d - 25 mm.

Thermal resistance (m^2 K/W)			Mean temperature ($^\circ$C)		
1.96	2.13	1.96	4.3	4.4	4.4
1.98	2.07	1.95	3.2	3.6	3.2
2.06	2.12	1.95	2.3	2.6	2.2

Glassfiber, ρ = 15.5 kg/m^3, d - 50 mm.

Thermal resistance (m^2 K/W)			Mean temperature ($^\circ$C)		
1.35	1.43	1.32	6.0	6.2	6.2
1.36	1.40	1.33	5.0	5.2	4.9
1.35	1.40	1.30	3.8	4.0	3.6

Diabase fiber,ρ = 46 kg/m^3, "0".

Thermal resistance (m^2 K/W)			Mean temperature ($^\circ$C)		
2.70	2.83	2.53	7.9	7.9	7.8
2.62	2.71	2.59	6.9	7.2	6.9
2.58	2.71	2.64	6.0	6.3	6.0

Diabase fiber, "ρ = 46 kg/m^3", vertical slits.

Thermal resistance (m^2 K/W)			Mean temperature ($^\circ$C)		
2.46	1.95	1.42	7.6	8.3	8.4
2.20	1.25	0.73	6.0	6.1	5.9
2.30	1.63	1.37	4.3	4.0	4.3

Diabase fiber, ρ = 45.5 kg/m^3, "0".

Thermal resistance (m^2 K/W)			Mean temperature (°C)		
2.68	2.78	2.61	7.4	7.3	7.2
2.58	2.70	2.63	6.4	6.5	6.2
2.65	2.72	2.64	5.4	5.5	5.2

Diabase fiber, "ρ = 45.5 kg/m^3", horizontal slits.

Thermal resistance (m^2 K/W)			Mean temperature (°C)		
1.29	0.69	1.12	4.7	6.6	6.1
2.54	2.18	2.33	3.3	3.5	3.6
2.78	2.65	2.55	2.2	2.4	2.1

Diabase fiber, ρ = 49 kg/m^3, "0".

Thermal resistance (m^2 K/W)			Mean temperature (°C)		
2.66	2.81	2.55	6.8	6.8	6.8
2.61	2.72	2.61	5.8	6.0	5.7
2.64	2.76	2.62	4.9	4.9	4.7

Diabase fiber, ρ = 49 kg/m^3, d - 10 mm.

Thermal resistance (m^2 K/W)			Mean temperature (°C)		
2.62	2.64	2.44	6.7	7.0	6.9
2.51	2.54	2.44	5.7	5.9	5.6
2.49	2.56	2.44	4.9	4.9	4.7

Diabase fiber, ρ = 49 kg/m^3, d - 25 mm.

Thermal resistance (m^2 K/W)			Mean temperature (°C)		
2.18	2.26	2.03	7.0	7.0	6.9
2.16	2.18	2.06	5.7	5.9	5.5
2.25	2.22	2.13	4.3	4.6	4.3

Diabase fiber, ρ = 49.5 kg/m^3, d - 50 mm.

Thermal resistance (m^2 K/W)			Mean temperature ($^\circ$C)		
1.45	1.52	1.37	8.4	8.5	8.4
1.47	1.50	1.41	6.9	7.1	6.7
1.50	1.50	1.45	5.3	5.4	5.2

Cellular plastics, ρ = 15 kg/m^3, "0".

Thermal resistance (m^2 K/W)			Mean temperature ($^\circ$C)		
2.29	2.33	2.24	7.7	7.7	7.6
2.23	2.31	2.26	6.7	6.8	6.5
2.26	2.38	2.26	5.6	5.7	5.3

Cellular plastics, "ρ = 15 kg/m^3", vertical slits.

Thermal resistance (m^2 K/W)			Mean temperature ($^\circ$C)		
1.89	1.58	1.22	8.8	9.3	9.2
1.87	1.25	0.68	6.8	7.2	6.6
1.88	1.35	1.16	4.5	4.2	4.7

Cellular plastic , ρ = 15 kg/m^3, "0".

Thermal resistance (m^2 K/W)			Mean temperature ($^\circ$C)		
2.34	2.38	2.25	6.6	6.7	6.6
2.32	2.36	2.22	5.3	5.6	5.3
2.38	2.40	2.27	4.1	4.3	4.3

Cellular plastic , ρ = 15 kg/m^3, d - 10 mm.

Thermal resistance (m^2 K/W)			Mean temperature ($^\circ$C)		
2.28	2.28	2.16	5.0	5.1	5.1
2.31	2.26	2.15	3.8	4.2	3.8
2.39	2.28	2.20	2.6	3.0	2.9

Cellular plastic , ρ = 15.5 kg/m^3, d - 25 mm.

Thermal resistance (m^2 K/W)			Mean temperature ($^\circ$C)		
1.95	1.99	1.89	5.7	5.9	5.9
1.96	2.00	1.90	4.6	4.8	4.6
2.05	2.04	1.92	3.4	3.7	3.4

Cellular plastic , ρ = 16 kg/m^3, d - 50 mm.

Thermal resistance (m^2 K/W)			Mean temperature ($^\circ$C)		
1.33	1.32	1.26	7.0	7.1	7.1
1.35	1.37	1.29	5.4	5.7	5.4
1.36	1.34	1.31	3.8	4.0	3.7

9 BIBLIOGRAPHY

9.1 Natural convection, fluid (air) space.

For the convienience of the reader, the following key is used to indicate references in the article and the contents of these references as well as the other literature listed here

* Reference used in text.
G Of general interest.
H Treats horizontal space.
V Treats vertical space
A Contains analytical discussions.
N Contains numerical calculations.
E Contains experimental investigations.

Aziz, K. & Hellums, J.D., Numerical solution of the three-dimensional equations of motion for laminar natural convection. Physics of fluids, Vol. 10, No. 2, 1967, p. 314-324. (*,H,N)

Bansal, T.D., Steady state free convection phenomenon. J. Sci. Industr. Res., Vol. 24, June 1965, p. 271-281. (V,H)

Batchelor, G.K., Heat transfer by free convection across a closed cavity between vertical boundaries at different temperatures. Quarterly J. of Applied Mathematics, Vol. XII, No. 3, October 1954, p. 209-233. (*,V,A)

Bénard, H., Les tourbillons cellulaires dans une nappe liquide. Revue General des Sciences Pures et Appliquees, Vol. 11, 1900, p. 1261-1271. (*,H,E)

Catton, I., Natural convection in horizontal liquid layers. Physics of Fluids, Vol. 9, 1966, p. 2521-2522. (*,H,N)

Catton, I. & Edwards, D.K., Effect of side walls on natural convection between horizontal plates heated from below. J. Heat Transfer, Nov. 1967, p. 295-299. (*,H,A,E)

Catton, I., The effect of insulating vertical walls on the onset of motion in a fluid heated from below. Int. J. Heat Mass Transfer, Vol. 15, 1972, p. 665-672. (H,A,E)

Chandra, K., Instability of fluids heated from below. Proc. Roy. Soc. A., Vol. 164, 1938, p. 231-242 (H,E)

Chandrasekhar, S., Hydrodynamic and hydromagnetic stability. Oxford Univ. Press, London, 1961. (*,G)

Christensen, G., Brown, W.P. & Wilson, A.G., Thermal performance of idealized double windows, unvented. ASHRAE Transactions, 1964, p. 408-418. (V,E)

Crawford, L. & Lemlich, R., Natural convection in horizontal concentric cylindrical annuli. I. & E.C. Fundamentals, Vol. 1, No. 4, 1962, p. 260-264. (V,N,E)

Davis, S.H., Convection in a box linear theory. J. Fluid Mech., Vol. 30, 1967, p. 465-478. (H,A,N)

Deardorff, J.W., A numerical study of two-dimensional parallel-plate convection. J. Atmospheric Sciences, Vol. 21, July 1964, p. 419-438. (H,N)

Dropkin, D. & Somerscales, E., Heat transfer by natural convection in liquids confined by two parallel plates which are inclined at various angles with respect to the horizontal. J. Heat Transfer, Feb. 1965, p. 77-84 (H,V,E)

Eckert, E.R.G. & Carlson, W.O., Natural convection in an air layer enclosed between two vertical plates with different temperatures. Inst. J. Heat Mass Transfer, Vol. 2, 1961, p. 106-120. (*,V,A,E)

Eckert, E.R.G. & Drake, R.M., Heat and mass transfer. McGraw-Hill, London, 1959. (G)

Edwards, D.K., Suppression of cellular convection by lateral walls. Journal of Heat Transfer, Feb. 1969, p. 145-150. (H,A,E)

Edwards, D.K. & Catton, I., Prediction of heat transfer by natural convection in closed cylinders heated from below. Int. J. Heat Mass Transfer, Vol. 12, 1969, p. 23-30. (*,H,A,E)

Elder, J.W., Laminar free convection in a vertical slot. J. Fluid Mech., Vol. 23, 1965, p. 77-98. (V,A,E)

Elder, J.W., Turbulent free convection in a vertical slot. J. Fluid Mech., Vol. 23, 1965, p. 99-111. (V,E)

Elder, J.W., Numerical experiments with free convection in a vertical slot. J. Fluid Mech., Vol. 24, 1966, p. 823-843. (*,V,N)

Emery, A. & Chu, N.C., Heat transfer across vertical layers. J. Heat Transfer, Feb. 1965, p. 110-114. (*,V,A,E)

Fromm, J.E., Numerical solutions of the nonlinear equations for a heated fluid layer. Physics of Fluids, Vol. 8, No. 10, 1965, p. 1757-1769. (*,H,N)

Gill, A.E., The boundary-layer regime for convection in a rectangular cavity. J. Fluid Mech., Vol. 26, 1966, p. 515-536. (*,V,A)

Gill, A.E. & Davey, A., Instabilities of a buoyancy-driven system. J. Fluid Mech., Vol. 35, 1969, p. 775-798. (V,A)

Globe, S. & Dropkin, D., Natural-convection heat transfer in liquids confined by two horizontal plates and heated from below. J. Heat Transfer, Feb. 1959, p. 24-28. (H,E)

Gotoh, K. & Satoh, M., The stability of a natural convection between two parallel vertical plates. J. Physical Society of Japan, Vol. 21, No. 3, March 1966, p. 542-548. (V,A)

de Graaf, J.G.A. & van der Held, E.F.M., The relation between the heat transfer and the convection phenomena in enclosed plane air layers. Appl. Sci Res. A3, 1953, p. 393-409. (*,H,V,E)

Heitz, W.L. & Westwater, J.W., Critical Rayleigh numbers for natural convection of water confined in square cells with L/D from 0.5 to 8. J. Heat Transfer, May 1971, p. 188-196. (H,E)

Hellums, J.D. & Churchill, S.W., Transient and steady state, free and natural convection, numerical solutions. A.I.Ch.E. Journal, Vol. 8, No. 5, 1962, p. 690-695. (V,N)

Jakob, M., Free heat convection through enclosed plane gas layers. Transactions of the A.S.M.E., April 1946, p. 189-194. (H,V,E)

Jannot, J. & Mordchelles-Regnier, G., Convection naturelle en espaces confines. EUR 4280 d/f/i/n/e, Vol. II, Euratom, 1969, p. 431-474. (H,V,E)

Jeffreys, H., The stability of a layer of fluid heated below. Phil. Mag., Vol. 2, 1926, p. 833-844. (*,H,A)

Jeffreys, H., Some cases of instability in fluid motion. Proc. Roy. Soc. A., Vol. 118, 1928, p. 195-208. (*,H,A)

Kays, W.M., Convective heat and mass transfer. McGraw-Hill, London, 1966. (*,G)

Krings, A. & Olink, J.T., Wärmeübertragung durch Doppel- und Mehrfachscheiben mit dicht eingeschlossener Gasschicht. Glastechn. Ber., Mai 1957, p. 175-182. (V,E)

Kroutil, J.C. & Sauer, Jr., H.J., Convective heat transfer in small enclosed air spaces. ASJRAE Transactions, 1964, p. 242-247. (H,E)

Kuo, H.L., Solution of the non-linear equations of cellular convection and heat transport. J. Fluid Mech., Vol. 10, 1961, p. 611-634. (H,A)

Linke, W., Die Wärmeübertragung durch Thermopane-Fenster. Kältetechnik, Heft 12, 1956, p. 378-384. (V)

Low, A.R., On the criterion for stability of a layer of viscous fluid heated from below. Proc. Roy. Soc. A., Vol. 125, 1929, p. 180-195. (H,A)

MacGregor, R.K. & Emery, A.F., Free convection through vertical plane layers - moderate and high Prandtl number fluids. J. Heat Transfer, August 1969, p. 391-403. (*,V,N,E)

MacGregor, R.K. & Emery, A.F., Prandtl number effects on natural convection in an enclosed vertical layer. J. Heat Transfer, May 1971, p. 253-254. (V,E)

Malkus, W.V.R. & Veronis, G., Finite amplitude cellular convection. J. Fluid Mech., Vol. 4, 1958, p. 225-260. (*,H,A)

Mitchell, W.T. & Quinn, J.A., Thermal convection in a completely confined fluid layer. A.I.Ch.E. Journal, Vol. 12, No. 6, 1966, p. 1116-1124. (H,E)

Mordchelles-Regnier, G. & Kaplan, C., Visualization of natural convection on a plane wall and in a vertical gap by differential interferometry. Proc. 1963 Heat Transfer and Fluid Mech. Inst., p. 94-111. (V,E)

Morrison, H.L., Preliminary measurements relative to the onset of thermal convection currents in unconsolidated sands. Applied Physics, Vol. 18, 1947, p. 849-850. (H,E)

Mull, W. & Reiher, H, Der Wärmeschutz von Luftschichten, seine experimentelle Bestimmung und graphische Berechnung. Beiheft z. Gesundh.-ing.,Reihe 1, Heft 28, 1930, p. 1-26. (*,H,V,E)

Nagendra, H.R., Tirunarayanan, M.A. & Ramachandran, A., Free convection heat transfer in vertical annuli. Chemical Engineering Science, Vol. 25, 1970, p. 605-610. (V,A,E)

Nagendra, H.R. & Tirunarayanan, M.A., Free convection heat transfer between vertical parallel plates. Nuclear Engineering and Design, 1971, p. 17-28. (*,V,A)

Nakagawa, Y., Heat transport by convection. Physics of Fluids, Vol. 3, No. 1, 1960, p. 82-86. (H,A)

Newell, M.E. & Schmidt, F.W., Heat transfer by laminar natural convection within rectangular enclosures. J. Heat Transfer, 1970, p. 159-168. (V,N)

Oshima, Y., Experimental studies of free convection in a rectangular cavity. J. Physical Society of Japan, Vol. 30, No. 3, 1971, p. 872-882. (*,V,E)

Ostrach, S. & Pneuli, D., The thermal instability of completely confined fluids inside some particular configurations. J. Heat Transfer, Vol. 85, No. 4, 1963, p. 346-354. (H,A,E)

Pellew, A. & Southwell, R.V., On maintained convective motion in a fluid heated from below. Proc. Royal Soc., Sci. A., Vol. 176, 1940, p. 312-343. (*,H,A)

Pillow, A.F., The free convection cell in two dimensions. Aeronautical Research Lab., Report A 79, Melbourne, 1952, (H,A)

Poots, G., Heat transfer by laminar free convection in enclosed plane gas layers. Quarterly Journal of Mechanics and Applied Mathematics, Vol. 11, 1958, p. 257-273. (*,V,A)

Pratt, A.W. & Ball, E.F., The thermal resistance of airspaces in building structures. J. Institution of Heating and Ventilating Engineers, Vol. 34, 1966, p. 133-145. (H,V,E)

Quon, C., High Rayleigh number convection in an enclosure - A numerical study. Physics of Fluids, Vol. 15, No. 1, 1972, p. 12-19. (V,N)

Rayleigh, J.W.S., On convection currents in a horizontal layer of fluid, when the higher temperature is on the under side. Phil. Mag., Dec. 1916, p. 529-546. (*,H,A)

Robinson, J.L., The failure of a boundary layer model to describe certain cases of cellular convection. Int. J. Heat Mass Tranfer, Vol. 12, 1969, p. 1257-1265. (H,A)

Robinson, H.E. & Powlitch, F.J., The thermal insulating value of airspaces. Housing Research paper 32, April 1954, p. 1-32. (H,V,E)

Rohsenow, W.M. & Choi, H.Y., Heat,mass and momentum transfer. Prentice-Hall, New Jersey, 1961. (G)

Rubel, A. & Landis, F., Numerical study of natural convection in a vertical rectangular enclosure. High-speed computing in fluid dynamics, The Physics of Fluids Supplement II, 1969, p. 208-213. (*,V,N)

Samuels, M.R. & Churchill, S.W., Stability of a fluid in a rectangular region heated from below. A.I.Ch.E. Journal, Vol. 13, No. 1, 1967, p. 77-85. (H,N)

Schlichting, H, Boundary-layer theory. McGraw-Hill, London, 1968. (G)

Schmidt, R.J. & Milverton, S.W., On the instability of a fluid when heated from below. Proc. Roy. Soc., Series A., Vol. 152, 1935, p. 586-594. (H,E)

Schmidt, R.J. & Saunders, O.A., On the motion of a fluid heated from below. Proc. Roy. Soc., A165, 1938, p. 216-228. (H,E)

Schmidt, E & Silveston, P.L., Natural convection in horizontal liquid layers. Chemical Engineering Progress Symposium Series, Vol. 55, No. 29, 1959, p. 163-169. (H,E)

Sherman, M. & Ostrach, S., Lower bounds to the critical Rayleigh number in completely confined regions. J. Applied Mechanics, Vol. 34, Vol. 89, No. 2, 1967, p. 308-312. (H,A)

Silveston, P.L., Wärmedurchgang in waagerechten Flüssigkeits-schichten. Forsk. Ing.-wes., Bd. 24, 1958, p. 29-32, 59-69. (*,H,E)

Soberman, R.K., Effects of lateral boundaries on natural convection. J. Applied Physics, Vol. 29, 1958, p. 872-873. (H,E)

Sokolov, M. & Tanner, R.I., Convective stability of a general viscoelastic fluid heated from below. The Physics of Fluids, Vol. 15, No. 4, 1972, p. 534-539. (H,A)

Sutton, O.G., On the stability of a fluid heated from below. Proc. Roy. Soc. A., Vol. 204, 1951, p. 297-309. (H,A,E)

Szekely, J. & Todd, M.R., Natural convection in a rectangular cavity transient behavior and two phase systems in laminar flow. Int. J. Heat Mass Transfer, Vol. 14, 1971, p. 467-482. (*,V,N,E)

Thompson, H.A. & Sogin, H.H., Experiments on the onset of thermal convection in horizontal layers of gases. J. Fluid Mechanics, Vol. 24, 1966, p. 451-479. (H,E)

de Vahl Davis, G., Laminar natural convection in a rectangular cavity. New York University, March 1967. (V,N)

de Vahl Davis, G., Laminar natural convection in an enclosed rectangular cavity. Int. J. Heat Mass Transfer, Vol. 11, 1968, p. 1675-1693. (*,V,N)

de Vahl Davis, G. & Kettleborough, C.F., Natural convection in an enclosed rectangular cavity. Mechanical and Chemical Engineering Transactions, May 1965, p. 43-49. (V,N)

Vest, C.M. & Arpaci, V.S., Stability of natural convection in a vertical slot. J. Fluid Mech., Vol. 36, 1969, p. 1-15. (V,A,E)

Wilkes, J.O. & Churchill, S.W., The finite-difference computation of natural convection in a rectangular enclosure. A.I.Ch.E. Journal, Vol. 12, No. 1, 1966, p. 161-166. (*,V,N)

Yih, C.S., Thermal stability of viscous fluids. Quarterly J. of Applied Mathematics, Vol. 17, 1959, p. 25-42. (H,A)

9.2 Flow in porous material

ASTM, Air flow resistance of accustical materials, ASTM, C522-63T, 1968, p. 231-237.

Carman, P.C., Flow of gases through porous media. Butterworths Sci. Publ., 1956.

Collins, R.E., Flow of fluids through porous materials. Reinhold Publ. Col. 1961.

Darcy, H., Les fontaines publiques de la ville de Dijon. Libraire des corps impériaux des ponts et chaussées et des mines, Paris, 1856.

DIN, Statische Bestimmung des Stömungswiderstandes, DIN 52213, 1958.

Emersleben, O., Das Darcysche Filtergesatz. Physik. Zeitschr., XXVI, 1925, p. 601-610.

Ferrandon, J., Les lois de l'écoulement de filtration. Le Génie Civil, Vol. 75, No. 2, 1948, p. 24-28.

Fournier, D., Andre, G. & Klarsfeld, S., Nouvelles recherches sur les relations existant entre la structure des isolants fibreux et leur conductibilite thermique. International Institute of Refrigeration, Proceedings,1967, p. 117-125.

Fowler, J.L. & Hertel, K.L., Flow of a gas through porous media. J. Applied Physics, Vol. 11, 1940, p. 496-502.

Fulks, W.B., Guenther, R.B. & Roetman, E.L., Equations of motion and continuity for fluid flow in a porous medium. Acta Mechanica 12, 1971, p. 121-129.

Hubbert, M.K., Darcy's law and the field equations of the flow of underground fluids. Petroleum Transactions, AIME, Vol. 207, 1956, p. 222-239.

Houpeurt, A., Sur l´ecoulement des gaz dans les milieux poreux. Revue de l´Institut Français du Pétrole, XIV, No. 11, p. 1468-1684.

Höglund, I., Högisolerande ytterväggars värmemotstånd. Byggnadsteknik, KTH, Nr 30, Stockholm, 1963, p. 43-48.

Iberall, A.S., Permeability of glass wool and other highly porous media. J. Research of the NBS, Vol. 45, No. 5, 1950, p. 398-406.

Kozeny, J., Über kapillare Leitung des Wassers in Boden. Akad. Wiss. Wien, 1927, p. 271-306.

Kyan, C.P., Wasan, D.T. & Kintner, R.C., Flow of single-phase fluids through fibrous beds. Ind. Eng. Chem. Fundam., Vol. 9, No. 4, 1970, p. 596-603.

Liao, K.H. & Scheidegger, A.E., Statistical models of flow through porous media. Pure and appl. geophysics, Vol. 83, No. 6, 1970, p. 74-81.

Lord, E., Air flow through plugs of textile fibres. J. Textile Institute, Vol. 46, 1955, p. T191-T213.

Scheidegger, A.E., Directional permeability of pourus media to homogeneous fluids. Geofis. Pura Appl., Vol. 28, 1954, p. 75-90.

Scheidegger, A.E., The physics of flow through porous media. University of Toronto Press, 1963.

Torelli, L. & Scheidegger, A.E., Random maze models of flow through porous media. Pure and applied geophysics, Vol. 89, 1971, p. 32-44.

Whitaker, S., The equations of motion in porous media. Chemical Engineering Science, Vol. 21, 1966, p. 291-300.

9.3 Natural convection in permeable space.

Achtziger, J., Wärmeleitfähigkeitsmessungen an Isolierstoffen mit dem Plattengerät bei tiefen Temperaturen. Kältetechnik, Heft 12, 1960, p. 372-375.

Allcut, E.A., An analysis of heat transfer through thermal insulating materials. Gen. disc. on Heat Transfer, London, 1951, p. 232-235.

Aziz, K. & Combarnous, N., Transfert de chaleur par convection naturelle dans une couche poreuse horizontale. C. R. Acad. Sc., Paris, t. 271, Série B 1970, p. 813-815

Baker, C.K. & Haselden, G.G., The effect of natural convection on the apparent thermal conductivity of porous insulants. International Institute of Refrigeration Proceedings, 1970, p. 49-61.

Bech, J.L., Convection in a box of porous material saturated with fluid. Physics of Fluids, Vol. 15, No. 8, 1972, p. 1377-1383.

Betbeder, J. & Jolas, P., Influence de la convection libre sur la conductivite d´une couche verticale d´isolant poreux. Int. J. Heat Mass Transfer, Vol. 15, 1972, p. 721-732.

Bories, S., Sur les mécanismes fondamentaux de la convection naturelle en milieu poreux. Revue Générale de Thermique, No. 108, 1970, p. 1377-1401.

Boires, S. & Monferran, L., Condition de stabilité et échange thermique par convection naturelle dans une couche poreuse incliné de grande extension. C.R. Acad. Sc., Paris, t. 274, Série B, 1972, p. 4-7.

Chan, B.K.G., Ivey, C.M. & Barry, J.M., Natural convection in enclosed porous media with rectangular boundaries. J. Heat Transfer, Feb. 1970, p. 21-27.

Combarnons, M., Convection naturelle et convection mixte dans une couche poreuse horizontale. Revue Générale de Thermique, No. 108, 1970, p. 1355-1375.

Combarnous, M. & Aziz, K., Influence de la convection naturelle dans les réservoirs d'huile ou de gaz. Revue de l'Institut Français du Pétrole, XXV, No. 12, 1970, p. 1335-1353

Combarnous, M.A. & Bia, P., Combined free and forced convection in porous media. Soc. of Petroleum Eng. Journal, Dec. 1971., p. 399-405.

Combarnous, M. & Le Fur, B., Transfert de chaleur par convection naturelle dans une couche horizontale. C.R. Acad. Sc. , Paris, t. 269, Série B, 1969, p. 1009-1012.

Elder, J.W., Steady free convection in a porous medium heated from below. J. Fluid Mech., Vol. 27, 1967, p. 29-48.

Holst, P.H. & Aziz, K., Transient three-dimensional natural convection in confined porous media. Int. J. Heat Mass Transfer, Vol. 15, 1972, p. 73-90.

Horton, C.W. & Rogers, F.T., Convection currents in a porous medium. J. Applied Physics, Vol. 16, 1945, p. 367-370.

Katto, Y. & Masuoka, T., Criterion for the onset of convective flow in a fluid in a porous medium. Int. J. Heat Mass Transfer, Vol. 10, 1967, p. 297-309.

Klarsfeld, S., Champs de température associés aux mouvements de convection naturelle dans un milieu poreux limité. Revue Générale de Thermique, No. 108, 1970, p. 1403-1423.

Lapwood, E.R., Convection of a fluid in a porous medium. Proc. Cambr. Phil. Soc., 1948, p. 508-521.

Martin, G. & Haselden, G.G., Heat transfer by natural convection in porous insulants. International Institute of Refrigeration Proceedings, 1963, p. 241-243.

Mordchelles-Regnier, G., Micheau, P., Pirovano, A., Jumentier, C., Terpstra, J.S., Lecourt, Y., Cave, P. & Breuille, M., Recherches recentes effectuees en France sur l'isolation thermique des reacteures nucleaires. International Atomic Energy Agency, Vienna, 1969, p. 529-544.

Morrison, H.L., Rogers, F.T. & Horton, C.W., Convection currents in porous media II. Observations of conditions at onset of convection. J. Applied Physics, Vol. 20, 1949, p. 1027-1029.

Palm, E., Weber, J.E. & Kernvold, O., On the steady convection in a porous medium. J. Fluid Mech., Vol. 54, 1972, p. 153-161.

Rogers, F.T., Convection currents in porous media V. Variational form of the theory. J. Applied Physics, Vol. 24, No. 7, 1953, p. 877-880.

Rogers, F.T. & Morrison, H.L., Convection currents in porous media III. Extended theory of the critical gradient. J. Applied Physics, Vol. 21, 1950, p. 1177-1180.

Rogers, F.T. & Schilberg, L.E., Convection currents in porous media IV. Remarks on theory. J. Applied Physics, Vol. 22, No 12, 1951, p. 1476-1479.

Schneider, K.J., Investigation of the influence of free thermal convection on heat transfer through granular material. International Institute of Refrigeration, Proceedings, 1963, p. 247-253.

Westbrook, D.R., Stability of convective flow in a porous medium. The Physics of Fluids, Vol. 12, No. 8, 1969, p. 1547-1551.

Wooding, R.A., Steady state free thermal convection of liquid in a saturated permeable medium. J. Fluid Mech., Vol. 2, 1957, p. 273-285.

Wooding, R.A., An experiment on free thermal convection of water in saturated permeable material. J. Fluid Mech., Vol. 3, 1958, p. 582-600.

Wooding, R.A., Instability of a viscous liquid of variable density in a vertical Hele-Shaw cell. J. Fluid Mech., Vol. 7, 1960, p. 501-515.

Wooding, R.A., Free convection of fluid in a vertical tube filled with porous material. J. Fluid Mech., Vol. 13, 1962, p. 129-144.

Wooding, R.A., Convection in a saturated porous medium at large Rayleigh number or Peclet number. J. Fluid Mech., Vol. 15, 1963, p. 527-544.

Zehendner, H., Einfluss der freien Konvection auf die Wärmeleitfähigkeit einer leichten Mineralfasermatte bei tiefen Temperaturen. Kältetechnik, Band 16, Heft 10, 1964, p. 308-311.

9.4 Miscellaneous references.

Bankvall, C.G., Principer för teoretisk behandling av konvektionsförloppet i en sluten värmeisolerad konstruktion. Byggnadsteknik, Rapport nr 1, LTH, Lund, 1966.

Bankvall, C.G., Guarded hot plate apparatus for the investigation of thermal insulations. Document D5, National Swedish Building Research, 1972a.

Bankvall, C.G., Heat transfer in fibrous materials. Document D4, National Swedish Building Research, 1972b.

Cammerer, W.F., Der Konvektionseinfluss auf die Wärmeleitfähigkeit von Wandisolierungen aus Mineralfaserstoffen. Allg. Wärmetechnik, Bd. 11, H. 6, 1962, p. 95-101.

Draper, N.R. & Smith, H., Applied regression analysis. Wiley & Sons, London, 1966.

Fournier, D. & Klarsfeld, S., Mesures de conductivité thermique des matériaux isolants par un appareil orientable à plaque chaude bi-gardée. International Institute of Refrigeration, Proceedings, 1969, p. 321-332.

Fournier, D. & Klarsfeld, S., Utilisation d´un appareil orientable à plaque chaude gardée pour la mise en évidence de transfert de chaleur par convection naturelle en milieu poreux dans des conditions simulées. International Institute of Refrigeration, Proceedings, 1971, p. 1-9.

Handegord, G.O. & Hutcheon, N.B., Thermal performance of frame walls. Heating, Piping & Air Conditioning, March 1952, p. 113-118.

Handegord, G.O. & Hutcheon, N.B., Thermal performance of frame walls. Air spaces blocked at mid-height. Heating, Piping & Air Conditioning, Aug. 1953, p. 117-122.

Höglund, I., Högisolerande ytterväggars värmemotstånd. Handlingar nr 41, Statens råd för byggnadsforskning, Stockholm, 1963.

Höglund, I. & Hansson, T., Inre konvektion i byggnadskonstruktioner. Byggnadsteknik, Meddelande nr 37, KTH, Stockholm, 1964.

Lorentzen, G. & Brendeng, E., The influence of free convection in insulated, vertical walls. Insulation Review, No. 4, 1960, p. 17-23.

Lorentzen, G. & Nesje, R., Experimental and theoretical investigation of the influence of natural convection in walls with slab type insulation. International Institute of Refrigeration, Proceedings, 1966, p. 115-125.

Lotz, W.A., Heat and air transfer in cold storage insulation. ASHRAE Semiannual Meeting, 1964.

Lund, C.E. & Lander, R.M., Heat transfer through mineral wool insulation in combination with reflective surfaces. ASHRAE Journal, March 1961, p. 47-54, 98-104.

Ogston, W.M., Influence of natural convection on temperature distribution and heat transfer in a wall of granular material. International Institute of Refrigeration, Proceedings, 1970, p. 65-76.

Paljak, I., Examination of convective heat transport in an air-proof cased plate of mineral wool. International Institute of Refrigeration, Proceedings, 1969, p. 231-240.

Robinson, H.E., Cosgrove, L.A. & Rowell, F.J., Thermal resistance of airspaces and fibrous insulations bounded by reflective surfaces. NBS, Building Materials and Structures Report 151, 1957.

Wilkes, G.B. & Vianey, L.R., The effect of convection in ceiling insulation. Transactions ASHVE, Vol. 49, 1943, p. 196-210.

Wolf, S., A theory for the effects of convective air flow through fibrous thermal insulation. ASHRAE Transactions, 1966.

Wolf, S., Solvason, K.R. & Wilson, A.G., Convective air flow effects with mineral wool insulation in wood-frame walls. ASHRAE Transactions, 1966.

Zehendner, H., Einfluss der freien Konvection auf die Wärmeleiffähigkeit einer leichten Mineralfasermatte bei tiefen Temperaturen. Kältetechnik, Bd 16, Heft 10, 1964, p. 308-311.